Dilemmas in the pathological diagnosis of rare soft tissue tumors

classical and novel diagnostic biomarkers and emerging concepts

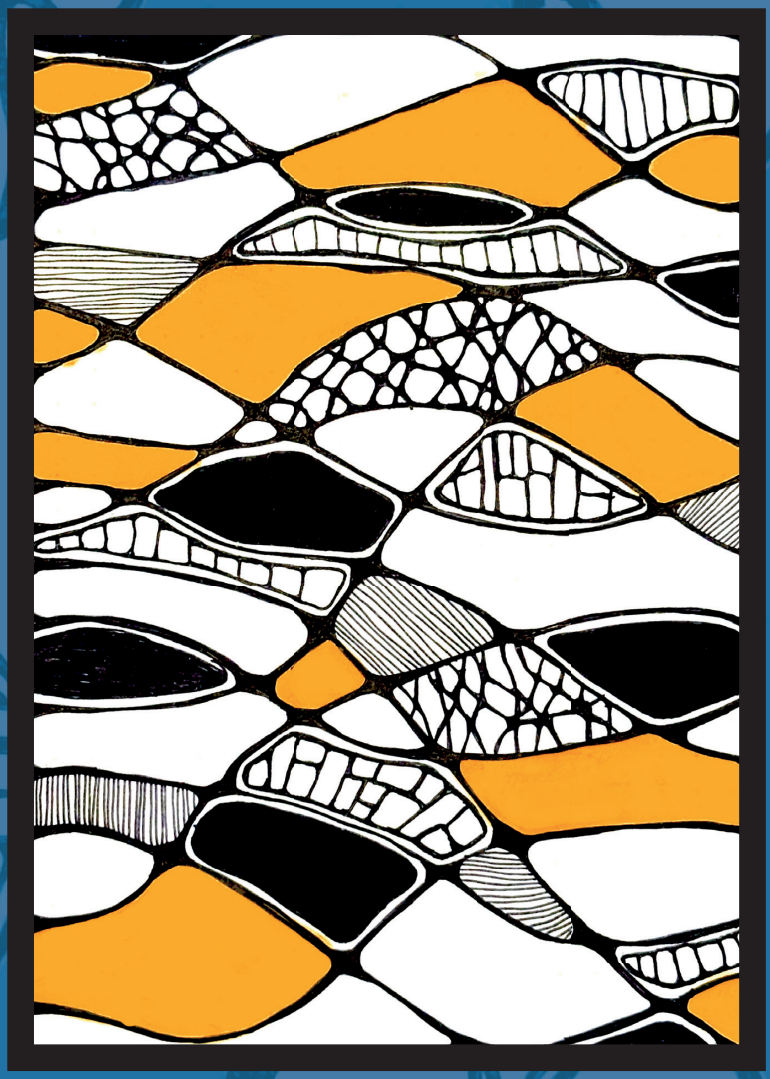

Elise Bekers

RADBOUD UNIVERSITY PRESS

Radboud Dissertation Series

Dilemmas in the pathological diagnosis of rare soft tissue tumors

Classical and novel diagnostic biomarkers and emerging concepts

Elise Bekers

Dilemmas in the pathological diagnosis of rare soft tissue tumors: Classical and novel diagnostic biomarkers and emerging concepts
Elise Bekers

Radboud Dissertation Series
ISSN: 2950-2772 (Online); 2950-2780 (Print)

Published by RADBOUD UNIVERSITY PRESS
Postbus 9100, 6500 HA Nijmegen, The Netherlands
www.radbouduniversitypress.nl

Design: Proefschrift AIO | Annelies Lips
Cover: Kim Trum & Guntra Laivacuma
Printing: DPN Rikken/Pumbo

ISBN: 9789465151403
DOI: 10.54195/9789465151403
Free download at: https://doi.org/10.54195/9789465151403

RADBOUD
UNIVERSITY
PRESS

Dilemmas in the pathological diagnosis of rare soft tissue tumors

Classical and novel diagnostic biomarkers and emerging concepts

Proefschrift ter verkrijging van de graad van doctor

aan de Radboud Universiteit Nijmegen

op gezag van de rector magnificus prof. dr. J.M. Sanders,

volgens besluit van het college voor promoties

in het openbaar te verdedigen op

vrijdag 21 november 2025

om 10.30 uur precies

door

Elisabeth Maria Bekers

geboren op 15 april 1985

te Tilburg

Promotor:
Prof. dr. J.H.J.M. van Krieken

Copromotoren:
Dr. U.E. Flucke
Dr. G.P.H. Scheijen

Manuscriptcommissie:
Prof. dr. H.W.B. Schreuder
Dr. F.C.M. van den Hout (Maastricht UMC+)
Prof. dr. W.T.A. van der Graaf (Erasmus MC)

Table of contents

Chapter 1

Introduction: Overview of emerging concepts in soft tissue tumor pathology and outline of thesis

Introduction

Soft tissue tumors originate from mesenchymal precursor cells and are associated with muscle, fat, connective tissue, endothelium (vessels), peripheral nerves and other supporting tissue of the body. These represent a highly heterogeneous group of tumors that comprises multiple entities. Traditionally soft tissue tumors are classified by their line of differentiation according to the normal counterpart they most closely resemble [1].

These tumors are subdivided into benign and malignant, but there are also two intermediate groups; intermediate (locally aggressive) and intermediate (rarely metastasizing). Benign tumors most closely resemble normal tissue and have limited capacity for autonomous growth. They show little tendency for infiltration into adjacent structures and local recurrence following local excision, and never metastasize. Tumors in the intermediate group (locally aggressive) are associated with an infiltrative and locally destructive growth pattern and show a substantial rate of local recurrence but very rarely metastasize. Tumors in the intermediate group (rarely metastasizing) are also often locally aggressive but in addition show the ability to give distant metastasis. Malignant tumors, called sarcomas, represent aggressive tumors that are capable of invasive and destructive growth and have a high tendency for recurrence and metastasis [1, 2]. These sarcomas are graded into low, intermediate and high grade based on morphological features and in combination with the histologic diagnosis, grade is the best predictor of distant metastasis and outcome [3, 4].

Soft tissue tumors are relatively rare in the general population. The vast majority of soft tissue tumors is benign and outnumbers the malignant tumors by a factor estimated of at least 100 [5]. The annual clinical incidence of new patients consulting a doctor for a benign soft tissue tumors is estimated at 3000 per million people. There is also a group of patients that will never consult a doctor, so the actual incidence of benign soft tissue tumors will be even higher. In contrast, the annual incidence of sarcomas is around 50 per million people and constitute less than 1% of all malignancies [2, 6, 7].

Classification of soft tissue tumors

Soft tissue tumors are classified based on the widely used 'WHO Classification of Tumours of Soft Tissue and Bone'. The first edition was published in 1969 by Enzinger [8]. This classification is revised thoroughly about every 10 years and provides an overview of soft tissue tumors divided into groups according to their

possible cell lineage based on a combination of histologic, immunohistochemical and sometimes, molecular findings. Based on the described criteria these tumors can be uniformly and reproducibly diagnosed [9, 10].

In the current WHO classification there are ~70 different soft tissue tumor entities defined in histogenetic groups comprising adipocytic, (myo)fibroblastic, fibrohistiocytic, vascular, pericytic (perivascular), smooth-muscle, skeletal muscle, gastrointestinal stromal tumors, chondro-osseous and peripheral nerve sheath tumors. Although the majority of neoplasms can be assigned to their respective lineage/group there is a growing subset of lesions, which seem to have no normal cell counterpart such as e.g. synovial sarcoma, epithelioid sarcoma and undifferentiated sarcoma. They are grouped as tumors of uncertain differentiation. The last separate category are undifferentiated small round cell sarcomas of soft tissue including for example Ewing sarcoma [2, 6].

Classifying soft tissue tumors in a consistent manner provides a uniform and reproducible diagnostic process and advancing molecular techniques will help to distinguish entities based on specific and defined genetic alterations that will lead to more knowledge of intrinsic tumor biology and further reshape the current classification.

Tumorigenesis

Soft tissue tumors originate from mesenchymal stem- or precursor cells by acquiring genetic alterations. Stem cells are immature tissue precursor cells that have the capability to self-renew and differentiate into multiple cell lineages and can be classified in four main groups; embryonic stem cells, induced pluripotent stem cells, cancer stem cells and tissue/organ-specific stem cells [11]. Mesenchymal multipotent stem cells (MSC) are defined as tissue-specific stem cells that are able to differentiate into many different mesenchymal cell types including lipoblasts/adipocytes (fat), fibroblasts (fibrous tissue), myoblasts/myocytes (muscle), osteoblasts/osteocytes (bone) and chondroblasts/chondrocytes (cartilage) [12, 13]. MSC are rare non-hematopoietic stromal cells present in bone marrow and other, sometimes organ-specific connective tissues in the body [11]. The process of MSC differentiation and transformation towards more defined and differentiated cell types is influenced by many different signaling pathways (Figure 1). During this process genetic changes may occur, causing them to acquire or lose certain abilities usually leading to aberrant morphology, growth kinetics, cell surface markers, genetic composition and tumorigenicity [11, 12].

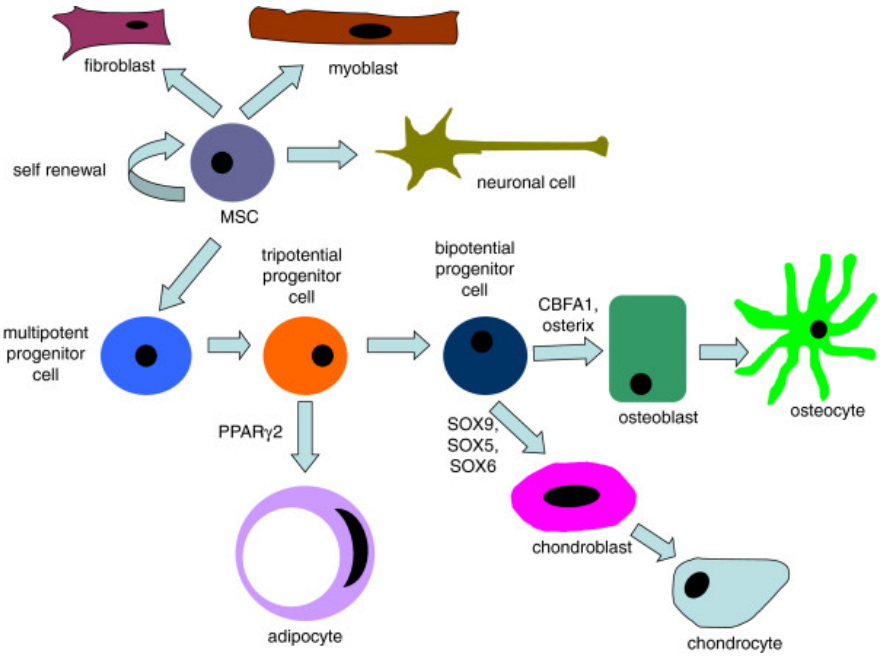

Figure 1. Mesenchymal multipotent stem cell differentiation.

Under the influence of different signaling pathways (arrows), multipotent stem cells (MSCs) can differentiate into different cell types. This process involves sequential signaling regulation with subsequent differentiation stages [12].

Soft tissue tumors are clonal outgrowths of neoplastic cells caused by gene mutations that play a role in signaling pathways that are involved in lineage differentiation, cell survival and proliferation. They can originate in any stem cell, regardless of its differentiation stage by acquiring a mutation in a crucial, usually 'gatekeeping' pathway ensuring a growth advantage [13].

The exact cell of origin for soft tissue tumors has not been conclusively identified yet and the current understanding is that they originate from MSC transformation. MSC can be in different developmental stages of differentiation and it is assumed that these preprogrammed stages are responsible for the phenotype of soft tissue tumors [14, 15]. This explains why some tumors closely resemble their normal mesenchymal counterpart (eg. atypical lipomatous tumor, leiomyoma and well-differentiated leiomyosarcoma) and others show a more primitive undifferentiated phenotype like Ewing sarcoma and alveolar rhabdomyosarcoma.

The most recent hypothesis is that soft tissue tumors originate from a mutated MSC, which is vulnerable for subsequent genetic and epigenetic changes. Depending on the impact of the initial and/or subsequent genetic changes, various differentiation pathways are deregulated leading to a specific subtype of soft tissue tumor (Figure 2) [14, 16].

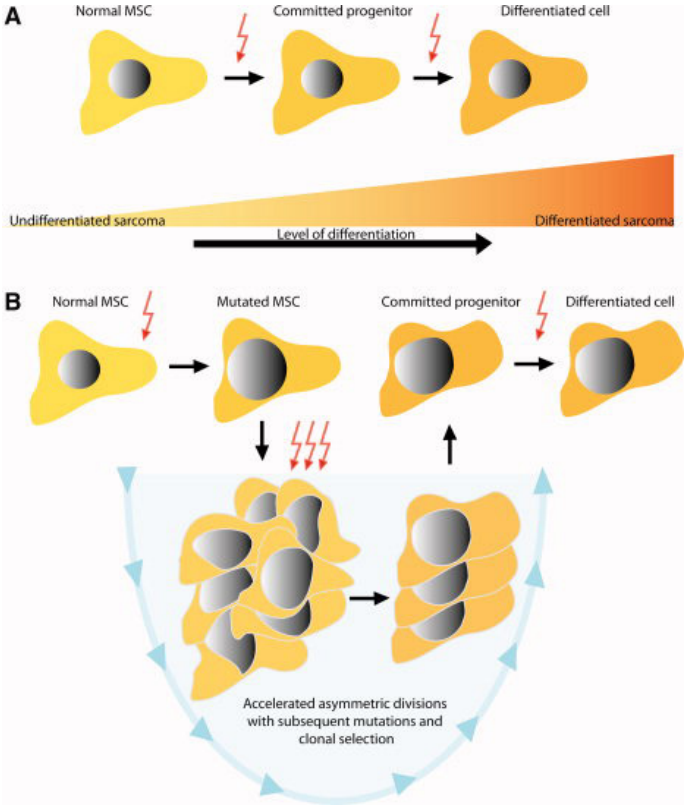

Figure 2. Mesenchymal differentiation and sarcomagenesis.

Impaired differentiation starting from a mutated "vulnerable" stem cell instead of a normal mesenchymal multipotent stem cell (MSC). Because of this early mutation, the stem cell undergoes asymmetric divisions giving rise to a mixture of cells with all additional mutations. Subsequently, immortalized clones with partially or fully impaired differentiation capacity (based on the mutations) generate soft tissue tumors with a certain degree of differentiation [14].

In contrast, sequential accumulation of carcinogenic hits in precursor lesions leading to carcinomas is rarely seen in soft tissue tumors. This can indicate that several mutational factors are required in the same MSC to create tumor outgrowth, which in itself might explain the relative rarity of soft tissue tumors in comparison to epithelial tumors [17].

Genetic changes in tumors often occur in oncogenes or tumor suppressor genes. Oncogenes are defined as genes that encode for proteins that promote cell growth and differentiation and are often involved in signal transduction. Activation of oncogenes result in gain of function and may be quantitative (an increase in the production of an unaltered protein) or qualitative (the production of a modified protein). As a result of these alterations, activated oncogenes induce abnormal cell proliferation and therefore favor tumor development. These changes are generally dominant and only occur in one allele. Quantitative oncogene activation occurs either by amplification or by translocation of the oncogene to an active chromatin domain (promotor) of another gene leading to increased protein expression. Qualitative forms of activation occur either by point mutation or by the production of a novel protein from a chimeric gene known as fusion gene, which are described in up to one-third of all soft tissue tumors [18, 19].

In contrast, tumor suppressor genes encode for proteins that suppress cell division and growth and sometimes promote apoptosis. Genetic alterations in these genes are loss-of-function alterations and often occur in both alleles. Once tumor suppressor genes are inactivated, the cell escapes stringent cell cycle control leading to uncontrolled growth and division. Multiple mechanisms of inactivation are observed including deletions, nonsense mutations, frame-shift mutations, insertions, or missense mutations that result in inactivation of the functional activity of a protein or production of a dominant negative protein that interferes with the function of the normal protein, replacement of the remaining unmutated copy by an inactive gene copy (loss of heterozygosity), reduced expression by hypermethylation of regulatory sequences of the gene or gene interruption due to non-recurrent translocations [18].

Molecular diagnostics of soft tissue tumors

Soft tissue tumors are well known for showing considerable morphologic and sometimes immunohistochemical overlap between distinct benign and malignant entities. This is further complicated by the fact that there can be considerable morphological heterogeneity within one single tumor entity. For example nodular fasciitis can mimic a wide range of sarcomas including myxofibrosarcoma and leiomyosarcoma, while intramuscular myxoma can mimic myxofibrosarcoma and low-grade fibromyxoid sarcoma [20]. Therefore detecting specific recurrent genetic alterations in distinct tumor entities can be extremely helpful in the diagnostic work-up.

To date, approximately 50% of soft tissue tumor types harbor recurrent genetic alterations and can be divided into three groups: those that contain specific translocations or amplifications, those that harbor specific mutations and those that contain complex genetic changes in various chromosomal regions [19, 21]. For all these different alterations many molecular techniques are currently available (for examples of the first two groups see Table 1). Each technique has their own suitable applicability, sensitivity and specificity for identifying specific genetic alterations [22].

For over the past two decades the single-gene sequencing technology known as Sanger sequencing has been used to detect single nucleotide changes (point mutations) and small deletions or insertions (*indels)*.

More recently high-throughput genome-wide methods have been developed allowing massively parallel sequencing (MPS) of cancer genomes, also known as next-generation sequencing (NGS) [22-24]. This technique can detect a wide range of genetic alterations including mutations, copy number alterations, insertions, deletions and chromosomal rearrangements. Within the spectrum of NGS there are several different platforms each with their own performance characteristics in terms of accuracy, sensitivity, read length, run time, throughput, coverage, error mode and costs.

Table 1. Examples of genetic alterations of specific genes with their possible corresponding diagnosis and most used molecular techniques.

Genetic change	Diagnosis	Molecular technique
Gene fusion		
AHRR-NCOA2 *GTF2I-NCOA2*	Soft tissue angiofibroma	RT-PCR NGS (Archer) FISH
NAB2-STAT6	Solitary fibrous tumor	RT-PCR NGS (Archer)
USP6	Nodular fasciitis Myositis ossificans Fibro-osseos pseudotumor of digits Aneurysmal bone cyst Cellular fibroma of tendon sheath	RT-PCR NGS (Archer) FISH
SS18-SSX1 *SS18-SSX2* *SS18-SSX4*	Synovial sarcoma	RT-PCR NGS (Archer) FISH

Table 1. Continued

Genetic change	Diagnosis	Molecular technique
EWSR1	Ewing sarcoma Desmoplastic round cell tumor Myxoid liposarcoma Extraskeletal myxoid chondrosarcoma Clear cell sarcoma Myoepithelioma of soft tissue Angiomatoid fibrous histiocytoma Sclerosing epithelioid fibrosarcoma	RT-PCR NGS (Archer) FISH
FUS-DDIT3 *FUS-CREB*	Myxoid liposarcoma Low-grade fibromyxoid sarcoma Sclerosing epithelioid fibrosarcoma	RT-PCR NGS (Archer) FISH
COL6A3-CSF1	Tenosynovial giant cell tumor	RT-PCR NGS (Archer)
Amplification		
MDM2	Liposarcoma	FISH NGS
Mutation		
GNAS	Intramuscular myxoma	NGS
CTNNB1	Desmoid fibromatosis	NGS
PRKAR1A	Cardiac myxoma	NGS
KIT	Gastro-intestinal stroma cell tumor	NGS

**not complete*

Different NGS techniques can extract information from the genome (DNA), transcriptome (RNA), epigenome (methyl-Seq) or chromatin (ChIP-Seq). These techniques are all widely used in the research setting but are at different levels of implementation in clinical diagnostic processes [23, 25, 26].

The big advantage of these new NGS techniques is that they require remarkably low amount of input material for successful analysis, which is very beneficial considering the demanding precision diagnostics on often limited biopsy material. Most platforms and applications need input in the range of 0,1-1 µg DNA or RNA and this can be obtained from only a few formalin-fixed paraffin-embedded (FFPE) tissue sections (one 20-50 µm thick tissue section, with >20% tumor cells) [22].

One of the techniques that has been developed for extracting information from DNA that has been isolated from FFPE tissues is the NGS-based approach employing single-molecule molecular inversion probes (smMIP) that combines multiplex analysis with single-molecule tagging, also named Unique Molecule Identifiers (UMI). By using this method, duplicate reads from both strands can be identified

and merged into a single consensus, reducing false-positive calls originated during PCR or related to fixation artefacts and allowing a technical sensitivity of 1% mutant allele. In addition, the actual number of sequenced genomic DNA (gDNA) molecules can be determined, which is especially relevant when analyzing limited amounts of gDNA [27].

Challenges for soft tissue tumor diagnostics

In soft tissue pathology, molecular analysis plays an increasing role in the diagnostic process. Integration of clinical, pathological and genetic information is critical and recent publications have shown that molecular testing was necessary to diagnose and guide management in more than 20% of soft tissue tumors [28-30].

The recently developed and emerging genome-wide molecular techniques have already led and will continue to lead to new discoveries and this fast growing amount of data is reshaping our current understanding of soft tissue tumors. Novel entities arise and previously established entities are being reclassified according to their genotype and a more nuanced classification is emerging [26, 30-34]. Ongoing thorough evaluation and validation of newly detected genetic alterations and correlation with clinical and pathological data is necessary for improved insight in soft tissue tumor biology.

The aim of this thesis is to analyze genetic alterations especially in benign soft tissue tumors to help to improve the diagnostic work-up and contribute to reshaping the current classification.

Outline of thesis

Intramuscular myxoma (IM) is a hypocellular benign soft tissue neoplasm and, especially on biopsy material, can be difficult to distinguish from low-grade fibromyxoid sarcoma or low-grade myxofibrosarcoma. *GNAS* mutations are frequently involved in IM, in contrast to these other malignant tumors. Therefore, sensitive molecular techniques for detection of *GNAS* aberrations in IM, which frequently yield low amounts of DNA due to poor cellularity, will be beneficial for differential diagnosis. In **chapter 2** we investigated *GNAS* mutations in intramuscular myxoma using two different molecular techniques; real-time PCR technique, called TaqMan assay, and the NGS smMIP assay in order to compare results in reliable mutation detection and report on the wider range of *GNAS* mutations using the NGS technique.

Cardiac myxoma is the most common primary cardiac benign soft tissue tumor and 10% arise as a component of the Carney complex of which the majority is caused

by mutations in the *PRKAR1A* gene. Several attempts have been made to identify *PRKAR1A* mutations in sporadic non-syndromic cardiac myxoma with only limited success. In **chapter 3** we analyzed *PRKAR1A*, the regulatory subunit of cAMP-dependent protein kinase A (PKA) using custom Ion AmpliSeq and smMIP assays in sporadic cardiac myxomas to examine new insights in tumor biology.

In **chapter 4** we examined the incidence of *USP6* rearrangements in myositis ossificans, a soft tissue tumor defined as a self-limiting pseudotumor composed of fibrous tissue and bone using FISH. Therefore we evaluated its relationship to nodular fasciitis and aneurysmal bone cyst, two lesions also known to harbor *USP6* rearrangements. Testing of these genetic aberrations in the diagnostic workup of (myo)fibroblastic lesions of soft tissue and bone is important for discriminating these lesions from malignant tumors. **Chapter 5** further explores *USP6* rearrangements in fibro-osseous pseudotumor of digits, another bone forming (myo)fibroblastic lesion and expand the spectrum of clonal transient neoplasms harboring this rearrangement leading to possible reclassification.

Desmoid fibromatosis is a locally aggressive myofibroblastic neoplasm that usually arises in deep soft tissue. It is characterized by mutations in the *CTNNB1* gene coding for β-catenin or alternatively, in the *APC* tumor suppressor gene. **Chapter 6** reports the multifocal occurrence of mainly sporadic extra-abdominal desmoid fibromatosis. This rare multifocality is mostly described in patients with germline *APC* mutations. The biological background in multifocal cases remains poorly understood with often aggressive clinical behavior and challenging therapeutical management.

Soft tissue angiofibroma (STAF) is a rare benign soft tissue tumor with recurrent chromosomal translocations resulting in rearrangement of *NCOA2,*in most cases. In **chapter 7** we investigated the diagnostic value of fusion genes *AHRR-NCOA2* and *GTF2I-NCOA2* described in STAF using RT-PCR. In addition, we used a RNA sequence technique to detect a novel alternative fusion gene. We also examined the potential use of *NCOA2* immunohistochemistry as a diagnostic marker.

Chapter 8 reports on myxoid liposarcoma (MLS), the only translocation-associated liposarcoma subtype, in distal extremities using RT-PCR and/or FISH. This tumor is extremely rare in this location and atypical presentation of MLS is important to recognize because of its ability to widespread metastasize while normally being known as a radiotherapy- and chemotherapy-sensitive tumor.

References

1. Hornick, J.L., Practical Surgical Soft Tissue Pathology: a Diagnostic Approach, 2nd Edition. Elsevier, ed. J.L. Hornick. 2019.
2. WHO Classification of Tumours Editorial Board. Soft tissue and bone tumours. Lyon (France): International Agency for Research on Cancer; 2020. (WHO classification of tumours series, 5th ed.; vol. 3). https://publications.iarc.fr/588. 2020.
3. Coindre, J.M., Grading of soft tissue sarcomas: review and update. Arch Pathol Lab Med, 2006. 130(10): p. 1448-53.
4. Deyrup, A.T. and S.W. Weiss, Grading of soft tissue sarcomas: the challenge of providing precise information in an imprecise world. Histopathology, 2006. 48(1): p. 42-50.
5. Myhre-Jensen, O., A consecutive 7-year series of 1331 benign soft tissue tumours. Clinicopathologic data. Comparison with sarcomas. Acta Orthop Scand, 1981. 52(3): p. 287-93.
6. Fletcher CDM, B.J., Hogendoorn PCW, Mertens F, eds, World Health Organization Classification of Soft Tissue and Bone. 4th Edition, ed. B.J. Fletcher CDM, Hogendoorn PCW, Mertens F. 2013, Lyon: IARC Press.
7. Gatta, G., et al., Burden and centralised treatment in Europe of rare tumours: results of RARECAREnet-a population-based study. Lancet Oncol, 2017. 18(8): p. 1022-1039.
8. Enzinger, F.M., et al., Histological typing of soft tissue tumours. 1969.
9. Heslin, M.J., et al., Core needle biopsy for diagnosis of extremity soft tissue sarcoma. Ann Surg Oncol, 1997. 4(5): p. 425-31.
10. Kasraeian, S., et al., A comparison of fine-needle aspiration, core biopsy, and surgical biopsy in the diagnosis of extremity soft tissue masses. Clin Orthop Relat Res, 2010. 468(11): p. 2992-3002.
11. Lye, K.L., et al., Mesenchymal stem cells: From stem cells to sarcomas. Cell Biol Int, 2016. 40(6): p. 610-8.
12. Xiao, W., et al., Mesenchymal stem cell transformation and sarcoma genesis. Clin Sarcoma Res, 2013. 3(1): p. 10.
13. Greaves, M. and C.C. Maley, Clonal evolution in cancer. Nature, 2012. 481(7381): p. 306-13.
14. Mohseny, A.B. and P.C. Hogendoorn, Concise review: mesenchymal tumors: when stem cells go mad. Stem Cells, 2011. 29(3): p. 397-403.
15. Yang, J., et al., The role of mesenchymal stem/progenitor cells in sarcoma: update and dispute. Stem Cell Investig, 2014. 1: p. 18.
16. Franceschini, N., et al., Transformed Canine and Murine Mesenchymal Stem Cells as a Model for Sarcoma with Complex Genomics. Cancers (Basel), 2021. 13(5).
17. Helman, L.J. and P. Meltzer, Mechanisms of sarcoma development. Nat Rev Cancer, 2003. 3(9): p. 685-94.
18. Rédei, G.P., Encyclopedia of genetics, genomics, proteomics, and informatics. 2008: Springer Science & Business Media.
19. Taylor, B.S., et al., Advances in sarcoma genomics and new therapeutic targets. Nat Rev Cancer, 2011. 11(8): p. 541-57.
20. Weiss, S.W., J.R. Goldblum, and A.L. Folpe, Enzinger and Weiss's soft tissue tumors. 2007: Elsevier Health Sciences.
21. Soini, Y., Epigenetic and genetic changes in soft tissue sarcomas: a review. APMIS, 2016. 124(11): p. 925-934.

22. Marino-Enriquez, A., Advances in the Molecular Analysis of Soft Tissue Tumors and Clinical Implications. Surg Pathol Clin, 2015. 8(3): p. 525-37.
23. Ross, J.S. and M. Cronin, Whole cancer genome sequencing by next-generation methods. Am J Clin Pathol, 2011. 136(4): p. 527-39.
24. Szurian, K., K. Kashofer, and B. Liegl-Atzwanger, Role of Next-Generation Sequencing as a Diagnostic Tool for the Evaluation of Bone and Soft-Tissue Tumors. Pathobiology, 2017. 84(6): p. 323-338.
25. Schaefer, I.M. and C.D.M. Fletcher, Recent advances in the diagnosis of soft tissue tumours. Pathology, 2018. 50(1): p. 37-48.
26. Wang, X.Q., et al., Advances in sarcoma molecular diagnostics. Genes Chromosomes Cancer, 2022. 61(6): p. 332-345.
27. Eijkelenboom, A., et al., Reliable Next-Generation Sequencing of Formalin-Fixed, Paraffin-Embedded Tissue Using Single Molecule Tags. J Mol Diagn, 2016. 18(6): p. 851-863.
28. Blay, J.Y., M. Brahmi, and I. Ray-Coquard, European Journal of Cancer's Biennial report on soft tissue and visceral sarcomas or the rapid evolution of treatment concepts in sarcomas. Eur J Cancer, 2017. 70: p. 83-86.
29. Italiano, A., et al., Clinical effect of molecular methods in sarcoma diagnosis (GENSARC): a prospective, multicentre, observational study. Lancet Oncol, 2016. 17(4): p. 532-538.
30. Rottmann, D., E. Abdulfatah, and L. Pantanowitz, Molecular testing of soft tissue tumors. Diagn Cytopathol, 2023. 51(1): p. 12-25.
31. Oda, Y., et al., Soft tissue sarcomas: From a morphological to a molecular biological approach. Pathol Int, 2017. 67(9): p. 435-446.
32. Schaefer, I.M., G.M. Cote, and J.L. Hornick, Contemporary Sarcoma Diagnosis, Genetics, and Genomics. J Clin Oncol, 2018. 36(2): p. 101-110.
33. Vroobel, K., et al., Ancillary molecular analysis in the diagnosis of soft tissue tumours: reassessment of its utility at a specialist centre. J Clin Pathol, 2016. 69(6): p. 505-10.
34. Obeidin, F., What's new in bone and soft tissue pathology 2023: guidelines for molecular testing. J Pathol Transl Med, 2023. 57(3): p. 184-187.

Chapter 2

Identification of novel GNAS mutations in intramuscular myxoma using next-generation sequencing with single-molecule tagged molecular inversion probes

Elise M. Bekers, Astrid Eijkelenboom, Paul Rombout, Peter van Zwam, Suzanne Mol, Emiel Ruijter, Blanca Scheijen, Uta Flucke

Diagn. Pathol 2019 Feb 8; 14(1):15.

Abstract

Background: Intramuscular myxoma (IM) is a hypocellular benign soft tissue neoplasm characterized by abundant myxoid stroma and occasional hypercellular areas. These tumors can, especially on biopsy material, be difficult to distinguish from low-grade fibromyxoid sarcoma or low-grade myxofibrosarcoma. *GNAS* mutations are frequently involved in IM, in contrast to these other malignant tumors. Therefore, sensitive molecular techniques for detection of *GNAS* aberrations in IM, which frequently yield low amounts of DNA due to poor cellularity, will be beneficial for differential diagnosis.

Methods: In our study, a total of 34 IM samples from 33 patients were analyzed for the presence of *GNAS* mutations, of which 29 samples were analyzed using a gene-specific TaqMan genotyping assay for the detection of *GNAS* hotspot mutations c.601C>T and c602G>A in IM, and 32 samples using a novel next generation sequencing (NGS)-based approach employing single-molecule tagged molecular inversion probes (smMIP) to identify mutations in exon 8 and 9 of *GNAS*. Results between the two assays were compared for their ability to detect *GNAS* mutations with high confidence.

Results: In total, 23 of 34 samples were successfully analyzed with both techniques showing *GNAS* mutations in 12 out of 23 (52%) samples. The remaining 11 samples were analyzed with either TaqMan assay or smMIP assay only. The TaqMan assay revealed *GNAS* mutations in 16 out of 29 samples (55%), with six samples c.601C>T (p.R201C; 38%) and ten samples c.602G>A (p.R201H; 62%) missense mutations. The smMIP assay identified mutations in 16 out of 28 samples (57%), with five samples c.601C>T (p.R201C; 31%) and seven samples c.602G>A (p.R201H; 44%) missense mutations. In addition, four samples (25%) revealed novel IM-associated mutations, including c.601C>A (p.R201S), c.602G>T (p.R201L), c.602G>C (p.R201P) and c.680A>G (p.Q227R). Combining the results of both tests, 23 out of 34 sporadic IM samples (68%) showed a *GNAS* mutation.

Conclusions: Both the TaqMan and the smMIP assay a show a high degree of concordance in detecting *GNAS* hotspot mutations in IM with comparable sensitivity. However, since the NGS-based smMIP assay permits mutation detection in whole exons of *GNAS*, a broader range of *GNAS* mutations can be identified by the smMIP approach.

Keywords: next generation sequencing, TaqMan genotyping, smMIP assay, *GNAS* mutation, intramuscular myxoma

Background

Intramuscular myxoma (IM) is a benign soft tissue neoplasm that belongs to the group of myxoid tumors characterized by a marked abundance of extracellular myxoid matrix. These tumors share several histological features, and depending on their clinical presentation and place of origin, can be subdivided into intramuscular, superficial-cutaneous, odontogenic and juxta-articular myxoma [1, 2]. These myxomas all represent distinct entities with different characteristic gene lesions involved in their pathogenesis. Therefore, gene mutation analysis can be very helpful in differential diagnosis to support the histopathology of these tumors [3, 4].

IM is characterized by bland spindle- and/or stellate-shaped cells embedded in a hypovascular, abundant myxoid stroma. The nuclei are small showing no or minimal nuclear atypia. Often areas with increased cellularity can be observed and when hypercellular areas predominate it is designated as cellular myxoma [2, 5, 6], which can easily be confused with low-grade fibromyxoid sarcoma or low-grade myxofibrosarcoma, especially in very small biopsies. IM is a somatic mosaic disorder generally occurring as a sporadic solitary neoplasm, although it can be part of Mazabraud's syndrome characterized by a combination of polyostotic fibrous dysplasia with multiple IM's [7, 8]. Mazabraud's syndrome and the closely related McCune-Albright syndrome, which is associated with fibrous dysplasia, café au lait macules and endocrine disorders, are caused by activating missense mutations in codon 201 of the *GNAS* gene [8-12].

GNAS encodes the stimulatory G-alpha subunit of the heterotrimeric G-protein complex, which regulates activation of adenylyl cyclase that converts adenosine triphosphate (ATP) into cyclic adenosine monophosphate (cAMP). Overproduction of second messenger cAMP and activation of downstream signaling pathways has been observed in cells harboring *GNAS* mutations [13, 14]. In 2000, Okamoto *et al*. first described somatic post-zygotic *GNAS* mutations in IM with and without fibrous dysplasia [8]. Thereafter, three more studies showed that *GNAS* lesions occur frequently in sporadic IM, which were detected in 36%-61% of the cases, and exclusively involved c.601C>T (p.R201C) and c.602G>A (p.R201H) mutations [8, 15, 16]. On the other hand, *GNAS* mutations are absent in low-grade myxofibrosarcoma, which can be useful in the differential diagnosis with (cellular) IM [17, 18]. Notably, juxta-articular myxoma and cardiac myxoma also lack *GNAS* driver mutations [4, 16].

A complicating factor for mutation detection in IM is the mosaicism of *GNAS* mutations combined with hypocellularity of the tumor, where low concentrations

of genomic DNA are isolated from these tissue specimens, especially in the case of biopsy material. In the past decades, several techniques for *GNAS* mutation detection have been developed and used [8, 19-21]. In 2009, Delaney *et al*. tested 28 IM's for *GNAS* mutations by using conventional PCR followed by mutation-specific restriction enzyme digestion (PCR-MSRED) and COLD-PCR/MSRED and showed that COLD-PCR/MSRED was more sensitive than the conventional PCR (61% vs. 29% mutations) [15]. Thus, this tumor type may benefit from the development of more robust and sensitive techniques for mutation detection, such as next generation sequencing (NGS). Recently, our molecular diagnostic laboratory has developed a novel NGS-based approach employing single-molecule molecular inversion probes (smMIP) that combines multiplex analysis with single-molecule tagging, also named Unique Molecule Identifiers (UMI) [22, 23]. By using this method, duplicate reads can be identified and merged into a single consensus, reducing false-positive calls originated during PCR and sequencing and allowing a technical sensitivity of 1% mutant allele. In addition, the actual number of sequenced genomic DNA (gDNA) molecules can be determined, which is especially relevant when analyzing limited amounts of gDNA. Furthermore, the strand-specific amplifications allows the distinction between genuine C>T and G>A mutations from deamination artifacts frequently observed when sequencing gDNA in older formalin-fixed paraffin-embedded (FFPE) tissue specimens. [22, 23].

In this study, we applied both TaqMan-based assays and the smMIP technique for *GNAS* mutation detection in IM, and compared both methods for reliable mutation detection in a diagnostic setting.

Methods

Patient sample

This study included 34 samples of sporadic intramuscular myxoma from 33 patients that were collected retrospectively (from 1998 till 2018) from archives of the Pathology Departments in the Netherlands of the Radboud University Medical Centre, Jeroen Bosch Hospital (Den Bosch), PAMM institute (Eindhoven) and Rijnstate Hospital (Arnhem). None of the patients were prior diagnosed with fibrous dysplasia or developed this during follow-up. From one patient, two samples (sample 28 and 29) were analyzed, which yielded identical data for mutation analyses. For each case, a 4 µm thick section of FFPE material was stained with haematotoxylin and eosin (H&E). The histological diagnoses were revised (UF, EB) and classified according to the 2013 World Health Organization criteria [2]. The

samples included in this study complied with the standards of the Committee for Human Research Ethics (CMO).

DNA isolation

Three 20 µm thick sections were cut from each specimen of FFPE tissue and were digested at 56°C for at least 1 hour in the presence of TET-lysis buffer (10 mmol/L Tris/HCl pH8.5, 1 mmol/L EDTA pH8.0, 0.01% Tween-20) with 5% Chelex-100 (143 to 2832; Bio-Rad, Hercules, CA), 15 µg/mL GlycoBlue (AM9516; Thermo Fisher, Waltham, MA), and 400 µg proteinase K (19133; Qiagen, Valencia, CA), followed by inactivation at 95°C for 10 minutes. DNA concentration for TaqMan assay was assessed with the NanoDrop Microvolume Spectrophotometer (Peqlab Biotechnologies, Erlangen, Germany) and for smMIP assay with the Qubit Broad Range Kit (Q32853; Thermo Fisher). To concentrate the DNA samples for the robotized protocol of the smMIP procedure, supernatant was cooled on ice and precipitated in the presence of 70% EtOH and 1/10 volume 3M NaAc (pH 5.2). Pellets were washed with cold 70% EtOH and dissolved in 80 µL Tris-EDTA. DNA quality of the samples was tested using a size ladder control PCR, in which gene segments of house-keeping genes were amplified, yielding different fragment sizes (100, 200, 300 and 400 bp), depending on the extent of fragmentation of the DNA.

TaqMan genotyping assay

Pre-designed and validated gene-specific TaqMan Genotyping Assays from Thermo Fisher Scientific was used for quantitative real-time RT-PCR. Every set contained gene specific forward 5'-CTTTGGTGAGATCCATTGACCTCAA-3' and reverse primers 3'-CACCTGGAACTTGGTCTCAAAGATT-5' and fluorescence labeled probes (Table 1). Probes are spanning an exon junction to detect genomic DNA. The PCR reaction volume was 20 µl and contained 1 µl DNA (10 ng/µl), 10 µl TaqMan Universal PCR Mastermix NoAmpErase UNG (Applied Biosystems, Foster City, CA), 0,5 µl predesigned and validated gene-specific TaqMan Gene Expression Assay mix (Applied Biosystems), 0,5 µl TE buffer (Promega) and 8 µl water. ABI Prism 7500 Real-Time PCR system (Applied Biosystem) was used to amplify codon 201 of exon 8 of the *GNAS* gene from each sample on a 96-well reaction plate with the following protocol: 10 min denaturation at 95°C, 40 cycles of 15 sec denaturation at 95°C, 1 min annealing and extension at 60°C. Dilution studies were performed using fibrous dysplasia samples harboring the two previously described *GNAS* mutations. The limit of detection was reliable at a variant allele frequency (VAF) of 5%.

Table 1. Fluorescent reporter probes for TaqMan assay

TaqMan assay	Reporter probe wild-type	Reporter probe mutant
GNAS c.601C>T	5'-CAGGACACGGCAGCGA-3'	5'-CAGGACACAGCAGCGA-3'
GNAS c.602G>A	5'-TTCGCTGCCGTGTCCT-3'	5'-CGCTGCCATGTCCT-3'

Underscored nucleotides are hot-spot mutation position

Next generation sequencing with single-molecule molecular inversion probes

The single-molecule molecular inversion probe (smMIP) procedure was performed as described elsewhere [22]. In short, a pool of smMIPs covering 41 mutational hotspot regions of 23 distinct genes, including *GNAS*, was phopshorylated with T4 polynucleotide kinase. A total of 100 ng genomic DNA was used as input in the capture reaction with the diluted phosphorylated smMIP pool. After extension, ligation and exonuclease treatment, PCR reactions were performed with barcoded reverse primers and iProof high-fidelity master-mix (Biorad). PCR reactions of the different samples were pooled, and purified with 0.8 x volume of Agencourt Ampure XP Beads (Beckman Coulter, Brea, CA). The purified libraries were prepared for sequencing on a NextSeq 500 instrument (Illumina, San Diego, CA) according to the manufacturer's protocol (300 cycles Mid Output sequencing kit, v2), resulting in 2 x 150 bp paired-end reads. Data analyses were performed as previously described [22]. Variants were called at a VAF of >1% and ≥3 mutant gDNA molecules and a minimum of 20 gDNA molecules analyzed at that position. Samples that did not fulfil the standard settings with respect to gene coverage in combination with tumor load were marked as inconclusive [22].

Results

Histopathology and clinical information of intramuscular myxoma cases

Histopathology of H&E-stained slides confirmed that a selected set of 34 samples from 33 patients showed the classical features of IM, which were composed of uniform, sparsely distributed cytological bland spindle- or stellate-shaped cells with tapering eosinophilic cytoplasm and small nuclei embedded in an abundant myxoid stroma. One case showed prominent hypercellular areas with more collagenous stroma and was diagnosed as cellular myxoma according to the criteria defined by Nielsen *et al* (Figure 1) [5, 6]. Of the 34 myxoid tumors, 31 samples were obtained by local excision and 3 samples by needle biopsy (Table 2). From one patient (sample 28 and 29), a biopsy and the following excision were analyzed for *GNAS*

mutational status. No recurrences were reported in any of the cases and no additional treatment was given. Follow up time ranged between 2 months and 21 years.

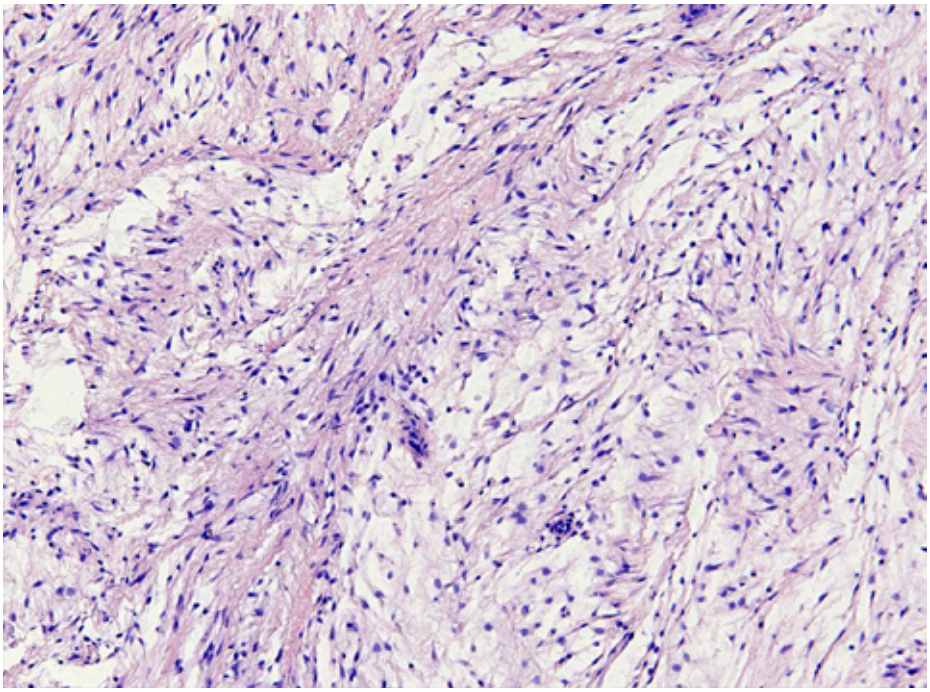

Figure 1. Representative photomicrograph of heamatoxylin and eosine (H&E)-stained section of a cellular intramuscular myxoma showing its characteristic histological morphology.

Table 2. Patient characteristics

Patient	Age at presentation (years)	Gender	Tumor Localization	Tumor size (cm) excision	Follow-up (months)
1	74	M	Lower leg	14	207
2	42	F	Thigh	5	201
3	51	F	Upper arm	0.8	128
4	45	M	Upper leg	5.5	126
5	40	F	Thigh	Bx	99
6	47	F	Lower leg	10	93
7	51	M	Shoulder	3	85
8	64	M	Thigh	5.2	83
9*	53	M	Upper arm	2	83
10	45	M	Thigh	5.8	82

Table 2. Continued

Patient	Age at presentation (years)	Gender	Tumor Localization	Tumor size (cm) excision	Follow-up (months)
11	57	F	Thigh	9	67
12	72	M	Thigh	3.5	63
13	71	M	Back	3	210
14	55	M	Thigh	4	182
15	55	M	Thigh	4	157
16	53	F	Upper arm	3	156
17	47	F	Upper arm	5.5	100
18	38	F	Upper arm	2	108
19	57	M	Thigh	3.2	126
20	39	F	Upper arm	7	191
21	69	F	Chest	2	63
22	46	F	Shoulder	3.5	200
23	64	F	Thigh	3	194
24	46	M	Thigh	5	181
25	67	F	Lower arm	1.7	127
26	49	F	Thigh	3	73
27	58	F	Thigh	3	244
28#	33	F	Thigh	7.5	224
29	65	M	Thigh	5.5	31
30	59	F	Thigh	7	12
31	40	F	Upper arm	Bx	260
32	71	F	Thigh	1	6
33	54	M	Thigh	Bx	2

Bx: biopsy, *cellular myxoma, # patient with two intramuscular myxoma samples

GNAS mutation detection in intramuscular myxoma

All samples (n=34) were tested for the presence of *GNAS* mutations, 32 samples using the smMIP assay and 29 samples with the TaqMan genotyping assay. First, *GNAS* mutation detection was performed for 29 DNA samples with the TaqMan assay, where specific fluorescently labeled probes were used for the detection of c.601C>T (p.R201C) and c.602G>A (p.R201H) hotspot mutations (Figure 2). Each sample was analyzed in two independent assays together with both negative and positive control samples. *GNAS* genetic alterations were identified in 16 out of 29 samples (55%), with six samples c.601C>T (38%) and ten samples c.602G>A (62%) mutations (Table 3). From one patient both samples (biopsy and excision) were positive for c.601C>T mutation (Table 3; sample 28 and 29).

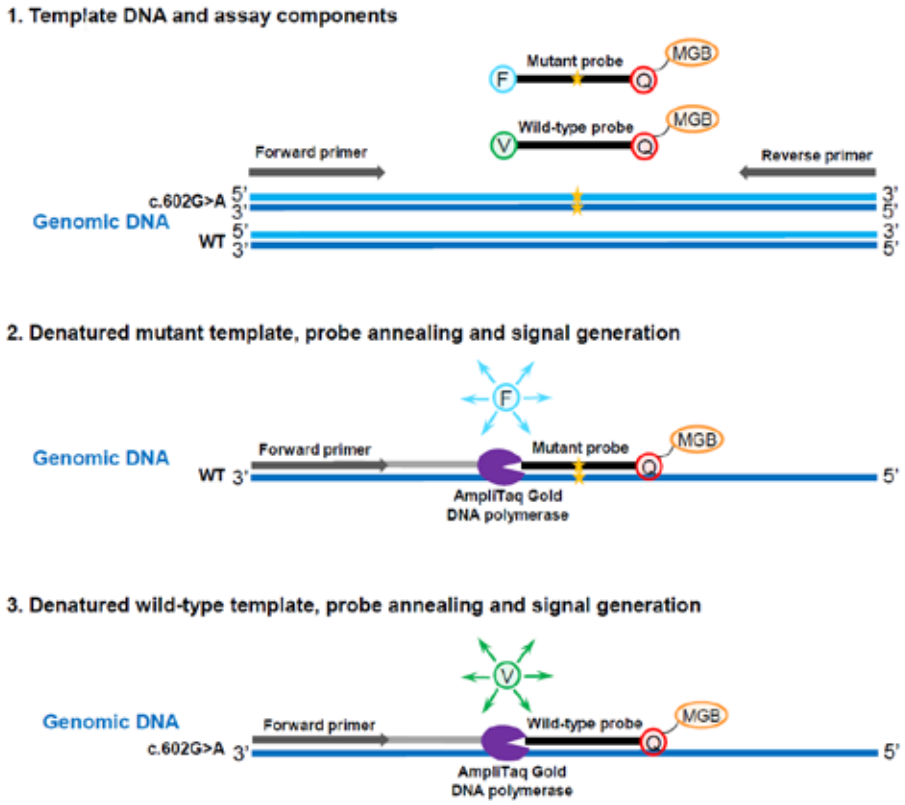

Figure 2. Schematic overview of the Taqman assay. In addition to the genomic DNA template, four additional oligonucleotide components are required to detect the mutation. These include an unlabeled PCR primer pair and two TaqMan probes with a FAM (F) or a VIC (V) dye label on the 5'end, in combination with a minor groove binder (MGB) and a nonfluorescent quencher (Q) on the 3'end (1). The TaqMan probes hybridize to the target DNA after denaturation between the unlabeled PCR primers. The signal from the fluorescent dye on the 5'end of a TaqMan probe is quenched by the quencher on its 3'end through fluorescence resonance energy transfer (FRET) (2). During PCR, the AmpliTaq Gold DNA polymerase extends the unlabeled primers using the genomic DNA template strand. When the DNA polymerase reaches the TaqMan probe, it cleaves the molecule, separating the fluorescent dye from the quencher. The qPCR instrument detects fluorescence from the unquenched FAM or VIC dye in one reaction (3).

Next, we determined the presence of *GNAS* mutations in exon 8 and exon 9 by the smMIP assay. Within the smMIP Cancer Hotspot Panel, two smMIPs covered *GNAS* exon 8 (providing sequencing analysis of both DNA strands for a total 74 bp) and two smMIPs *GNAS* exon 9 (sequencing analysis of 59 bp), respectively (Figure 3). Other mutational hotspot regions that were covered by smMIPs included *BRAF, CTNNB1, EGFR, HRAS, KRAS, NRAS, IDH1, IDH2* and *KIT* (for the complete list see [22]).

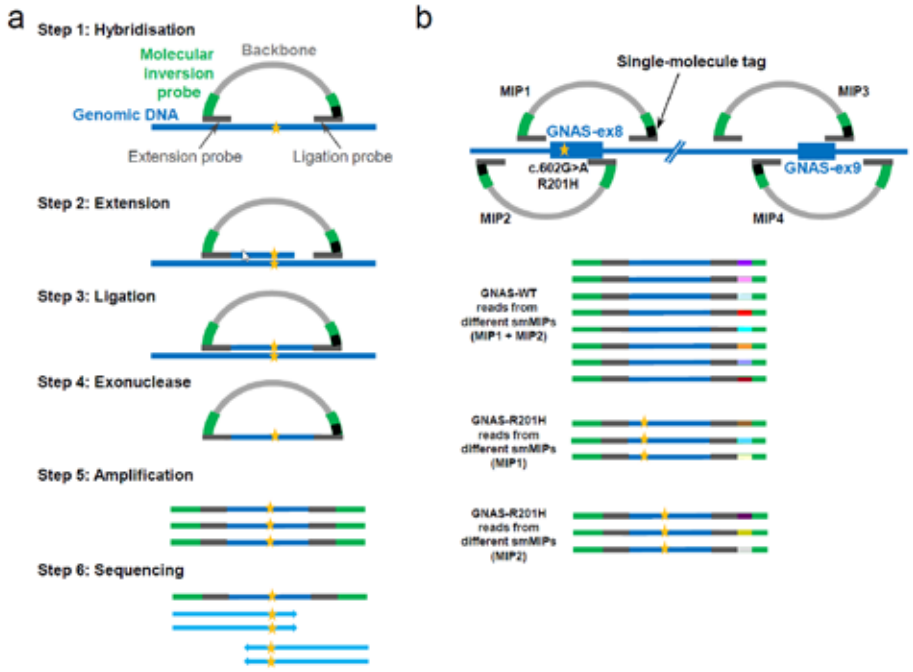

Figure 3. Schematic overview of the smMIP assay. (**a**) First, the single molecule molecular inversion probe (smMIP) capture procedure is performed. smMIPs are long oligonucleotides consisting of two targeting arms (extension probe and ligation probe), joined by a backbone. The probe sequences are complementary to genomic DNA sequences surrounding the target region that covers a hotspot location (indicated by the yellow asterisk). During the capture reaction, smMIPs are hybridized to genomic DNA (gDNA), followed by an extension and ligation reaction, which results in circular smMIPs. Subsequent exonuclease treatment will remove all linear gDNA and unused smMIPs. Between the backbone and probe sequences are primer sequences (green bars) that are used to amplify the target region, followed by library preparation and next-generation sequencing (NGS). (**b**) By including a single-molecule tag of 8 random nucleotides (N_8) at the end of the ligation probe, duplicate reads can be identified and merged into a consensus thereby removing PCR and sequencing artifacts. Genuine C>T and G>A mutations can be distinguished from deamination artifacts by strand specific amplification of the smMIPs. In our smMIP design, exon 8 and exon 9 of the GNAS gene are each covered by two independent smMIPs targeting both strands (smMIP1-2 and smMIP3-4, respectively).

The smMIP assay was performed on 32 samples in total, including the 27 samples that also showed a successful TaqMan assay and an additional set of 5 IM samples. From these 32 samples, the NGS data of 5 samples (for which a successful TaqMan assay was available) was based on a very limited number of gDNA molecules, and therefore could not reliably be interpreted, most likely because of very low cellularity of the IM sample and/or inferior DNA quality (Table 3; inconclusive, Inc). In total, 16 out of 28 samples (57%) showed a *GNAS* mutation, with five samples c.601C>T (31%) and seven samples c.602G>A (44%) mutations. In addition, four

samples (25%) revealed novel IM-associated mutations, including c.601C>A (p.R201S), c.602G>T (p.R201L), c.602G>C (p.R201P) and c.680A>G (p.Q227R).

Combining the above, 23 samples were successfully analyzed with both techniques showing *GNAS* mutations in 12 out of 23 (52%) samples. Collectively, our data demonstrate that in 23 out of 34 IM samples (68%) a *GNAS* mutation was detected using either TaqMan and/or smMIP assay. All samples that were successfully analyzed with both approaches and harbored the classical c.601C>T or c.602G>T mutations were identified with both methods.

In total, eight samples showed the classical c.601C>T mutation (35%) and eleven samples harbored the c.602G>T mutation (48%). All hotspot mutations detected by smMIP were also identified by the TaqMan assay, including samples with a VAF of 5% (sample 2). On the other hand, due to the more stringent settings of the smMIP assay, five cases with hotspot mutations identified by TaqMan assay did not yield sufficient data by the smMIP approach for reliable interpretation. In contrast, the smMIP assay allowed the detection of four novel (potential) pathogenic *GNAS* mutations (17% of the 23 mutated samples) beyond the c.601C>T and c.602G>A mutations, not previously described for IM. Thus, both assays provide merits in the molecular diagnostics of IM.

Table 3. Mutation analysis intramuscular myxoma

Sample	Taqman assay (WT/ Mut/Inc)	smMIP assay (WT/ Mut/Inc)	Mutation	Amino acid substitution	Mutant allele frequency (smMIP)	Concordance between Taqman and smMIP assay
1	WT	WT				Concordant
2	Mut	Mut	c.601C>T	p.R201C	5%	Concordant
3	WT	WT				Concordant
4	WT	WT				Concordant
5*	WT	Mut	c.680A>G	p.Q227R	27%	Mutation not included in TaqMan assay
6	WT	WT				Concordant
7	Mut	Mut	c.602G>A	p.R201H	13%	Concordant
8	Mut	Mut	c.602G>A	p.R201H	14%	Concordant
9	WT	WT				Concordant
10	Mut	Mut	c.602G>A	p.R201H	26%	Concordant
11	Mut	NA	c.601C>T	p.R201C		Not analyzed by smMIP

Table 3. Continued

Sample	Taqman assay (WT/ Mut/Inc)	smMIP assay (WT/ Mut/Inc)	Mutation	Amino acid substitution	Mutant allele frequency (smMIP)	Concordance between Taqman and smMIP assay
12	WT	WT				Concordant
13	WT	WT				Concordant
14	Mut	Mut	c.601C>T	p.R201C	13%	Concordant
15	Mut	Inc	c.602G>A	p.R201H		Insufficient quality for smMIP assay
16	WT	WT				Concordant
17	WT	WT				Concordant
18	Mut	Inc	c.602G>A	p.R201H		Insufficient quality for smMIP assay
19	Mut	Mut	c.602G>A	p.R201H	10%	Concordant
20	Mut	Mut	c.602G>A	p.R201H	9%	Concordant
21	Mut	NA	c.602G>A	p.R201H		Not analyzed by smMIP
22	Mut	Mut	c.601C>T	p.R201C	15%	Concordant
23	Mut	Mut	c.602G>A	p.R201H	19%	Concordant
24	WT	WT				Concordant
25	WT	WT				Concordant
26*	WT	Mut	c.602G>T	p.R201L	15%	Mutation not included in TaqMan assay
27	Mut	Mut	c.602G>A	p.R201H	14%	Concordant
28**	Mut	Inc	c.601C>T	p.R201C		Insufficient quality for smMIP assay
29**	Mut	Inc	c.601C>T	p.R201C		Insufficient quality for smMIP assay
30*	NA	Mut	c.602G>C	p.R201P	12%	Not analyzed by Taqman
31	NA	Mut	c.601C>T	p.R201C	13%	Not analyzed by Taqman
32*	NA	Mut	c.601C>A	p.R201S	14%	Not analyzed by Taqman
33	NA	Mut	c.601C>T	p.R201C	17%	Not analyzed by Taqman
34	NA	Mut	c.602G>A	p.R201H	7%	Not analyzed by Taqman

WT: wild-type; Mut: mutation identified; Inc: inconclusive; NA: not analyzed

*Samples with novel mutations in smMIP assay which are not included in the TaqMan assay

**Two samples tested from the same patient (biopsy and excision)

Discussion

Intramuscular myxoma (IM) mostly occurs sporadically in the skeletal muscle of the thigh. These lesions affect mainly middle-aged adults, women more often than man [1, 24]. The prevailing view is that driver mutations of this neoplasm are exclusively located in codon 201 of the *GNAS* gene, encoding the stimulatory G-protein alpha subunit that activates the enzyme adenylate cyclase. Due to the low cellularity and somatic mosaicism in most of these lesions, mutation detection can be quite challenging and the presence of a mutation can be easily missed.

In our study we used two different techniques (TaqMan and smMIP assay) to compare the detection sensitivity of *GNAS* mutations in these lesions. In our series, 23 out of 34 sporadic IM cases (68%) showed a *GNAS* mutation, 16 out of 29 samples (55%) in the TaqMan assay and 16 out of 28 samples (57%) in the smMIP assay of which 23 samples were successfully analyzed with both techniques showing *GNAS* mutations in 12 out of 23 (52%) samples. The test-specific detection rate was 55% with the TaqMan assay and 57% for the smMIP approach. The VAF for the TaqMan assay was determined at >5% in this study and the required input was only 10 ng gDNA. The VAF for smMIP was set at >1% and a minimum of 3 mutant gDNA molecules, and a coverage of 20 gDNA molecules. This demonstrates that both tests are sensitive methods and useful for molecular diagnostics of tumor samples harboring mutations with a low mutant allele frequency.

In comparison, Walther *et al* found *GNAS* mutations in 37% (23/63) of IMs with direct Sanger sequencing and Delaney *et al* detected mutations in 61% (17/28) using COLD-PCR/MSRED [15, 16]. However, the smMIP technique, because of the whole exon sequencing nature of this test, allowed detection of four additional mutations that previously have not been described in IM. By using smMIP we identified one c.680A>G mutation in exon 9, and three novel mutations in exon 8, one mutation at position c.601, namely c.601C>A, and two mutations at position c.602, which included c.602G>C and c.602G>T. The c.601C>A mutation has previously been reported in fibrous dysplasia, while the c.602G>C and c.602G>T mutations were only reported in sporadic endocrine tumors so far [9, 10, 19, 25]. These mutations were not detected by TaqMan, since this assay was designed to report only the two classical hotspot mutations c.601C>T and c.602G>T.

The smMIP approach allows the distinction between genuine C>T and G>A mutations from deamination artifacts frequently observed when sequencing gDNA from FFPE tissue specimens [22]. All cases harboring a C>T or G>A mutation in

GNAS, mutant reads originating from both DNA strands were observed, showing that these represent genuine mutations. Since the TaqMan approach does not allow this distinction, deamination artifact could potentially cause false positive results. In our study, all hotspot mutations detected with the Taqman assay were confirmed with the smMIP technique, indicating no false-positive results with Taqman. Even samples with a VAF of around 5% could be detected by both TaqMan assay and smMIP. The four samples with a hotspot mutation that were detected by TaqMan, but did not yield a reliable smMIP assay result, all had a mutated VAF of approximately 10-30% as judged by Taqman assay, and were therefore interpreted as true mutations.

Significant benefits of the TaqMan assay include low cost and short turn-around time (≤2 working days). A limitation of Taqman is that within one assay only one or two hotspot mutations can be detected. For smMIP analysis the turn-around time in our laboratory is ≤7 working days. A large initial investment was needed and high numbers of samples are required for parallel analyses to have a cost-efficient test. Because multiple genes can be tested at once with the smMIP assay, large amounts of samples are relatively easy obtained in routine clinical setting with the current demand of molecular diagnostics [22]. Because of the sensitive characteristics of the smMIP technique and its accuracy of mutation detection on FFPE material as well as the broader coverage of the *GNAS* gene, this technique to our opinion is preferable.

The most important differential diagnoses of IM, especially the cellular variant, are low-grade fibromyxoid sarcoma and low-grade myxofibrosarcoma. In biopsy material the distinction can be challenging and in those cases molecular diagnostics can be beneficial. A specific immunohistochemical and molecular signature is well known for low-grade fibromyxoid sarcomas with expression of MUC4 and the presence of *FUS/EWSR1-CREB 3L2/1* fusions making a distinction from IM easily possible [17, 18]. In contrast, for low-grade myxofibrosarcoma, specific immunohistochemical or molecular characteristics are lacking. Sensitive molecular tests, like smMIP and TaqMan assays for *GNAS* mutation analysis, might be very helpful in assessing the diagnosis, which has therapeutic consequences when considering malignancy [21]. Nevertheless there are also cases in which no *GNAS* mutation could be detected, suggesting that there are still other aberrations to be identified in IM.

Panagopoulos *et al* recently found abnormal karyotypes in 21 out of 68 cases, with nine cases showing nonrandom involvement of chromosome 8 (which harbors the

GNAS gene) with seven cases showing trisomy 8, one with a deletion and one with a translocation. Only one case in their series showed a c.601C>T *GNAS* mutation [26]. Thus, chromosomal aberrations could be an alternative explanation for at least a subset of the non-mutated cases.

The smMIP-NGS cancer hotspot panel that was employed to check for *GNAS* mutations, also contained smMIPs that covered mutational hotspots in the genes *AKT1, BRAF, CTNNB1, EGFR, ERBB2, GNA11, GNAQ, H3F3A, H3F3B, HRAS, IDH1, IDH2, JAK2, KRAS, MPL, MYD88, NRAS, PDGFRA* and *PIK3CA*. In none of the 32 samples that could be reliably analyzed by smMIPs, additional mutations were detected in these regions. Thus, *GNAS* mutations represent a unique driver mutation for this benign tumor type.

Conclusion

In conclusion, both TaqMan and smMIP assay are comparably sensitive molecular methods with valuable applicability in diagnostic pathology for IM. Furthermore, due to a broader coverage of the *GNAS* gene by the smMIP approach, four novel IM-associated missense mutations of *GNAS* could be identified (17% of all mutated samples), which previously have only been reported in McCune-Albright syndrome and sporadic endocrine tumors.

References

1. Goldblum JR, Folpe AL, Weiss SW, Enzinger FM, Weiss SW. Enzinger and Weiss's soft tissue tumors. 6th ed. Philadelphia, PA: Saunders/Elsevier; 2014. xiv, 1155 p.
2. Fletcher CDM, World Health Organization., International Agency for Research on Cancer. WHO classification of tumours of soft tissue and bone. 4th ed. Lyon: IARC Press; 2013. 468 p.
3. Boson WL, Gomez RS, Araujo L, Kalapothakis E, Friedman E, De Marco L. Odontogenic myxomas are not associated with activating mutations of the Gs alpha gene. Anticancer Res. 1998;18(6A):4415-7.
4. Okamoto S, Hisaoka M, Meis-Kindblom JM, Kindblom LG, Hashimoto H. Juxta-articular myxoma and intramuscular myxoma are two distinct entities. Activating Gs alpha mutation at Arg 201 codon does not occur in juxta-articular myxoma. Virchows Arch. 2002;440(1):12-5.
5. Nielsen GP, O'Connell JX, Rosenberg AE. Intramuscular myxoma: a clinicopathologic study of 51 cases with emphasis on hypercellular and hypervascular variants. Am J Surg Pathol. 1998;22(10):1222-7.
6. van Roggen JF, McMenamin ME, Fletcher CD. Cellular myxoma of soft tissue: a clinicopathological study of 38 cases confirming indolent clinical behaviour. Histopathology. 2001;39(3):287-97.
7. Cabral CE, Guedes P, Fonseca T, Rezende JF, Cruz Junior LC, Smith J. Polyostotic fibrous dysplasia associated with intramuscular myxomas: Mazabraud's syndrome. Skeletal Radiol. 1998;27(5):278-82.
8. Okamoto S, Hisaoka M, Ushijima M, Nakahara S, Toyoshima S, Hashimoto H. Activating Gs(alpha) mutation in intramuscular myxomas with and without fibrous dysplasia of bone. Virchows Arch. 2000;437(2):133-7.
9. Schwindinger WF, Francomano CA, Levine MA. Identification of a mutation in the gene encoding the alpha subunit of the stimulatory G protein of adenylyl cyclase in McCune-Albright syndrome. Proc Natl Acad Sci U S A. 1992;89(11):5152-6.
10. Shenker A, Weinstein LS, Moran A, Pescovitz OH, Charest NJ, Boney CM, et al. Severe endocrine and nonendocrine manifestations of the McCune-Albright syndrome associated with activating mutations of stimulatory G protein GS. J Pediatr. 1993;123(4):509-18.
11. Shenker A, Weinstein LS, Sweet DE, Spiegel AM. An activating Gs alpha mutation is present in fibrous dysplasia of bone in the McCune-Albright syndrome. J Clin Endocrinol Metab. 1994;79(3):750-5.
12. Weinstein LS, Shenker A, Gejman PV, Merino MJ, Friedman E, Spiegel AM. Activating mutations of the stimulatory G protein in the McCune-Albright syndrome. N Engl J Med. 1991;325(24):1688-95.
13. O'Hayre M, Vazquez-Prado J, Kufareva I, Stawiski EW, Handel TM, Seshagiri S, et al. The emerging mutational landscape of G proteins and G-protein-coupled receptors in cancer. Nat Rev Cancer. 2013;13(6):412-24.
14. Weinstein LS, Chen M, Xie T, Liu J. Genetic diseases associated with heterotrimeric G proteins. Trends Pharmacol Sci. 2006;27(5):260-6.
15. Delaney D, Diss TC, Presneau N, Hing S, Berisha F, Idowu BD, et al. GNAS1 mutations occur more commonly than previously thought in intramuscular myxoma. Mod Pathol. 2009;22(5):718-24.
16. Walther I, Walther BM, Chen Y, Petersen I. Analysis of GNAS1 mutations in myxoid soft tissue and bone tumors. Pathol Res Pract. 2014;210(1):1-4.
17. Bartuma H, Moller E, Collin A, Domanski HA, Von Steyern FV, Mandahl N, et al. Fusion of the FUS and CREB3L2 genes in a supernumerary ring chromosome in low-grade fibromyxoid sarcoma. Cancer Genet Cytogenet. 2010;199(2):143-6.

18. Mertens F, Fletcher CD, Antonescu CR, Coindre JM, Colecchia M, Domanski HA, et al. Clinicopathologic and molecular genetic characterization of low-grade fibromyxoid sarcoma, and cloning of a novel FUS/CREB3L1 fusion gene. Lab Invest. 2005;85(3):408-15.

19. Candeliere GA, Roughley PJ, Glorieux FH. Polymerase chain reaction-based technique for the selective enrichment and analysis of mosaic arg201 mutations in G alpha s from patients with fibrous dysplasia of bone. Bone. 1997;21(2):201-6.

20. Idowu BD, Al-Adnani M, O'Donnell P, Yu L, Odell E, Diss T, et al. A sensitive mutation-specific screening technique for GNAS1 mutations in cases of fibrous dysplasia: the first report of a codon 227 mutation in bone. Histopathology. 2007;50(6):691-704.

21. Willems SM, Mohseny AB, Balog C, Sewrajsing R, Briaire-de Bruijn IH, Knijnenburg J, et al. Cellular/intramuscular myxoma and grade I myxofibrosarcoma are characterized by distinct genetic alterations and specific composition of their extracellular matrix. J Cell Mol Med. 2009;13(7):1291-301.

22. Eijkelenboom A, Kamping EJ, Kastner-van Raaij AW, Hendriks-Cornelissen SJ, Neveling K, Kuiper RP, et al. Reliable Next-Generation Sequencing of Formalin-Fixed, Paraffin-Embedded Tissue Using Single Molecule Tags. J Mol Diagn. 2016;18(6):851-63.

23. Hiatt JB, Pritchard CC, Salipante SJ, O'Roak BJ, Shendure J. Single molecule molecular inversion probes for targeted, high-accuracy detection of low-frequency variation. Genome Res. 2013;23(5):843-54.

24. Enzinger FM. Intramuscular Myxoma; a Review and Follow-up Study of 34 Cases. Am J Clin Pathol. 1965;43:104-13.

25. Gorelov VN, Dumon K, Barteneva NS, Palm D, Roher HD, Goretzki PE. Overexpression of Gs alpha subunit in thyroid tumors bearing a mutated Gs alpha gene. J Cancer Res Clin Oncol. 1995;121(4):219-24.

26. Panagopoulos I, Gorunova L, Lobmaier I, Bjerkehagen B, Heim S. Karyotyping and analysis of GNAS locus in intramuscular myxomas. Oncotarget. 2017;8(13):22086-94.

Chapter 3

Detection of PRKAR1A gene mutations in sporadic cardiac myxomas. A study of 24 cases

Elise Bekers, Diede A.G. van Bladel, Madeleine R. Berendsen, Astrid Eijkelenboom, J. Han J.M. van Krieken, Marc Ooft, Emiel Ruijter, Ad Verhagen, Uta E. Flucke, Blanca Scheijen

Virchows Archive, 2025, accepted for publication

Abstract

The benign neoplasm cardiac myxoma represents one of the hallmarks of Carney complex (CNC), a familial multiple neoplasia syndrome. About 80% of the index cases have germline mutations in *PRKAR1A* encoding the RIα regulatory subunit of cAMP-dependent protein kinase A (PKA). However, the role of *PRKAR1A* gene mutations in the pathogenesis of non-CNC-associated sporadic cardiac myxoma is less well established. Here, we investigated the presence of *PRKAR1A* gene variants in a cohort of 24 sporadic cardiac myxomas using targeted next-generation sequencing. Our study shows that 14 out of 24 cases (58%) harbor *PRKAR1A* gene mutations, represented mostly by frameshift, nonsense and splice site mutations (together 84%), leading to a premature stop codon predicted to be degraded via non-sense mediated mRNA decay. The other 16% of *PRKAR1A* genetic alterations involved missense mutations, often located in important functional domains of the regulatory subunit RIα. Notably, 64% (n=9/14) of the cases harbored more than one *PRKAR1A* gene variant, suggesting compound heterozygous mutations either in *cis* or *trans*. In conclusion, *PRKAR1A* gene mutations associated with loss of RIα function leading to increased PKA activity were observed in ~60% of sporadic cardiac myxomas, strongly supporting an essential role for PKA in mediating formation of cardiac myxoma.

Introduction

Cardiac myxoma is the most common primary tumor of the heart, manifesting itself mainly in middle-aged patients between the third and sixth decades of life, and affects woman on average twice more than men [1]. It is a benign mesenchymal neoplasm composed of stellate, ovoid or plump spindle cells in a myxoid stroma with prominent vascularization [2, 3]. Most tumors occur sporadic, but up to 10% arise as a component of the Carney Complex (CNC), a multiple neoplasia syndrome characterized by cardiac and extracardiac myxomas, mucocutaneous pigmentation, endocrine hyperactivity due to tumors in the corresponding organs, and malignant melanotic nerve sheath tumor [4, 5]. Cardiac myxomas represent the most common non-cutaneous lesions in CNC (in 20-40% of the patients), which can arise anywhere in the heart, and are often multiple and recurrent. In contrast, sporadic cardiac myxomas develop almost exclusively in the left atrium and are generally solitary without recurrence after standard surgical treatment [6]. Approximately 70% of the CNC patients show a familial history, while the remaining patients develop tumors as a result of a *de novo* germline defect. Up to 80% of CNC lesions are caused by genetic alterations affecting the *PRKAR1A* gene, located on chromosome 17q22-24 [7-10]. These contain mostly exonic and splice site mutations, while larger deletions, including those affecting promoter/enhancer regions, have been reported in only a few cases [11-14].

PRKAR1A is a tumor suppressor gene encoding for the regulatory subunit type 1 alpha (RIα) of the 3',5'-cyclic adenosine monophosphate (cAMP)-dependent protein kinase A (PKA) enzyme, which is constitutively expressed in all cell types [15]. In its inactive state, PKA is an hetero-tetramer comprised of a regulatory subunit dimer (type I subunits: RIα, RIβ; type II subunits: RIIα, RIIβ) and two catalytic subunits (three different forms: Cα, Cβ, PRKX) [16, 17]. RIα sequesters the PKA catalytic subunits and inhibits PKA kinase activation in the absence of second messenger cAMP. Mutations within the *PRKAR1A* gene result in a mutant protein or lead to non-sense mRNA lacking translation into RIα protein, also called non-sense mediated mRNA decay [10, 18]. This loss of Riα function eventually results in unrestrained activity of the PKA catalytic subunits leading to increased cell proliferation and tumor formation.

Initial reports failed to identify *PRKAR1A* mutations, loss of heterozygosity or microsatellite instability in sporadic non-syndromic cardiac myxomas [19-21]. However, in three other studies employing predominantly Sanger sequencing *PRKAR1A* variants were detected in 13 out of 19 (68%) [22], 9 of 29 (31%) [23], and

39 of 61 (64%) of such lesions [24], and in an individual case [25]. A complicating factor for mutation detection in cardiac myxomas is the relative hypocellularity, where low concentrations of genomic DNA are isolated. Therefore, genetic analysis of this tumor type will benefit from robust and sensitive techniques for mutation detection using deep targeted next-generation sequencing (tNGS). In this study, we applied two different complementary tNGS-based approaches for reliable *PRKAR1A* mutation detection in a cohort of 24 sporadic cardiac myxomas.

Materials and Methods

Patient cohort and tissue specimens

A total of 24 cases of sporadic cardiac myxoma were retrieved from the archives of the Pathology Departments of the Radboud University Medical Center (Nijmegen, The Netherlands) and Rijnstate Hospital (Arnhem, The Netherlands). Patients were diagnosed between 2000 to 2016, and showed no signs of CNC (multiple myxomas, spotty skin pigmentation, endocrine overactivity with corresponding lesions). Histopathological review of the H&E-stained slides (4µm formalin-fixed and paraffin-embedded (FFPE) tissue) was performed according to the 2021 World Health Organization criteria [26]. All samples and clinical information were collected in accordance with the Declaration of Helsinki and of Taipei.

Genomic DNA isolation

Three 20µm sections were cut from each specimen of FFPE tissue and digested at 56°C for at least 1 hour in the presence of TET-lysis buffer (10 mmol/L Tris/HCl pH8.5, 1 mmol/L EDTA pH8.0, 0.01% Tween-20) with 5% Chelex-100 (Bio-Rad, Hercules, CA, USA), 15 µg/mL GlycoBlue (Thermo Fisher Scientific, Waltham, MA, USA), and 400 µg proteinase K (Qiagen, Hilden, Germany), followed by inactivation at 95°C for 10 minutes, and centrifugation for 10 minutes at 20,000 x g. Supernatant containing genomic DNA was purified with QIAamp DNA Micro Kit (Qiagen). Alternatively, QIAamp DNA FFPE Tissue Kit (Qiagen) was used directly for genomic DNA isolation according to manufacturer's protocol. DNA concentration was measured with Qubit Broad Range Kit (Thermo Fisher Scientific).

PRKAR1A mutation analysis by next-generation sequencing

For the detection of *PRKAR1A* gene mutations two different targeted next-generation sequencing (tNGS) approaches were employed: i) Ion Torrent amplicon-NGS (Ion AmpliSeq) and ii) single molecule molecular inversion probe (smMIP) technique followed by paired-end sequencing on Illumina NovaSeq platform

(Illumina, San Diego, CA, USA). For the Ion AmpliSeq method, multiplex PCR was performed with 20 ng input DNA to amplify the intron-exon boundaries and protein-coding genomic regions of exons 2-11 of the *PRKAR1A* gene (Supplementary Table 1). After beads purification of the amplicons (Agencourt AMPure XP Beads, Beckman Coulter, Brea, CA, USA), library preparation and amplification (Ion Plus Fragment Library kit and Ion Xpress Barcode Adapters kit, Thermo Fisher Scientific) as described previously [27], the samples were pooled with equal DNA concentrations for sequencing on Ion Torrent PGM using Ion 318™ Chip Kit v2 BC (Ion Torrent™, Thermo Fisher Scientific). An automated workflow for smMIP pool and library preparation was performed on 100 ng input DNA for each sample as described previously [28], and custom molecular inversion probes (MIPs) targeting the intron-exon boundaries and protein-coding genomic regions of exons 2-11 of *PRKAR1A* (Supplementary Table 2) were included in a larger smMIP panel as reported elsewhere [29]. NGS data output was analyzed with SeqNext software (JSI Medical Systems, Ettenheim, Germany) with a minimum coverage set at n=5 total variant reads for each single nucleotide variant identified by Ion AmpliSeq (without the ability to distinguish PCR duplicates) or MIP (eliminating PCR duplicates after consensus clustering through identification of the unique molecular identifier), and a minimum variant allele frequency (VAF) of 5% for both Ion AmpliSeq and smMIP NGS datasets (minimum read depth: 100x). For mutational calling, synonymous variants, intronic variants (with exception of splice sites), and single nucleotide polymorphisms (SNPs) related to known germline variants were excluded.

Results

Clinical characteristics

The 24 cardiac myxomas analyzed were from 14 females (58%) and 10 males (42%) with a median age of 63 years (range 35-86 years), who presented without any other clinical manifestations of CNC (CM01-CM24; Table 1). All tumors but one were located in the left atrium. In one case (CM16) the tumor was spanning both, left and right cardiac chambers. All samples were tumor resection specimens. Besides surgery, no additional treatment was given. During follow-up (range 7- 23 years), there were no further events.

Table 1. Clinical characteristics patient cohort sporadic cardiac myxoma

Case number	Gender	Age at diagnosis	Location cardiac myxoma
CM01	F	54	Left atrium
CM02	F	77	Left atrium
CM03	F	72	Left atrium
CM04	F	74	Left atrium
CM05	M	66	Left atrium
CM06	F	64	Left atrium
CM07	F	38	Left atrium
CM08	M	71	Left atrium
CM09	M	62	Left atrium
CM10	M	69	Left atrium
CM11	M	63	Left atrium
CM12	F	36	Left atrium
CM13	M	39	Left atrium
CM14	F	42	Left atrium
CM15	M	55	Left atrium
CM16	M	68	Left and right atrium
CM17	F	57	Left atrium
CM18	F	73	Left atrium
CM19	M	53	Left atrium
CM20	F	57	Left atrium
CM21	F	43	Left atrium
CM22	F	86	Left atrium
CM23	M	75	Left atrium
CM24	F	35	Left atrium

Histopathology

All cases showed the characteristic features of a cardiac myxoma, represented by sparsely distributed cytological bland-looking spindle and stellate-shaped or plump cells with indistinct cell borders embedded in a myxoid matrix with prominent vascularity and signs of hemorrhage (Figure 1).

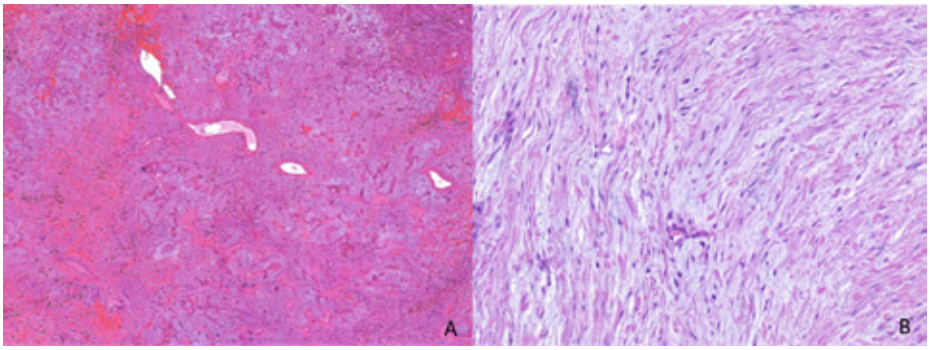

Figure 1. A. Hematoxylin and eosin (H&E) staining shows the characteristic morphology of cardiac myxoma (Case 13) with a prominent vasculature in a myxoid matrix combined with inflammatory cells and hemorrhage with hemosiderin deposits. **B.** High power view of case 18 demonstrating polygonal/stellatelesional cells with an oval nucleus with open chromatin and indistinct nucleoli and aneosinophilic cytoplasm, set in an abundant myxoid background.

PRKAR1A gene mutation analysis by two different next-generation sequencing approaches

In all cases, sufficient FFPE tissue was available for genomic DNA isolation and molecular analysis, focusing on *PRKAR1A* mutation analysis without additional copy number variation analysis. Two different complementary tNGS approaches were used (Figure 2). First, a custom Ion AmpliSeq method was designed, were the protein coding sequence and intron-exon junctions of exons 2-11 of *PRKAR1A* were amplified with oligonucleotide primers generating amplicons ranging in size from 140 to 217 nucleotides, which were prepared for sequencing on Ion Torrent platform. Secondly, the smMIP technology was used that targets genomic regions of 113 nucleotides in size, which we previously employed as a successful approach to identify novel *GNAS* mutations in intramuscular myxoma [31]. Important advantages of smMIP compared to Ion AmpliSeq relates to ability to identify PCR artefacts by the inclusion of a unique molecular identifier (UMI) sequence of (in our case) 8 random bases in the ligation probe representing $4^8 = 65,536$ single molecule possibilities. Since every smMIP molecule with an individual UMI-tag can only hybridize to one genomic DNA fragment, the UMI sequence is able to correct for PCR duplicates in the bioinformatic analysis pipeline. Furthermore, the smMIPs are

designed to capture overlapping regions on both sense and antisense DNA strands, thereby distinguishing FFPE artefacts related to single strand cytosine deamination variants from actual gene mutations detected on both DNA strands.

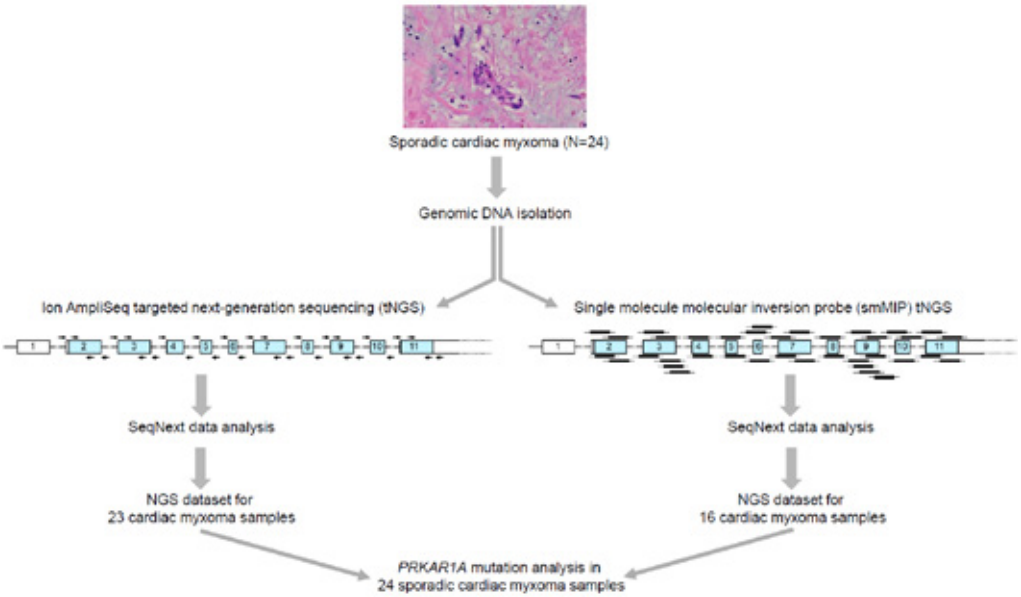

Figure 2. Schematic overview of the targeted next-generation sequencing approaches to detect *PRKAR1A* gene mutations in sporadic cardiac myxoma. On the left side the workflow of the Ion AmpliSeq method, and on the right side the single molecule molecular inversion probe (smMIP) approach is shown. The relative positions of the sense primers and smMIPs have been mapped above the *PRKAR1A* exons, while antisense primers and smMIPs are indicated below the *PRKAR1A* exons.

Identification of *PRKAR1A* gene mutations in sporadic cardiac myxoma

Each case was subjected to both tNGS approaches involving Ion AmpliSeq and smMIP-based mutation analysis of the *PRKAR1A* gene. Based on the threshold settings employed for mutation detection (see Materials and Methods) one sample (CM05) was excluded from the data analysis after Ion AmpliSeq tNGS, while eight samples (CM04, CM06, CM09, CM10, CM12, CM13, CM14, CM22) did not fulfill the criteria for *PRKAR1A* mutation detection using the smMIP approach ("No data" in Supplementary Table 3). However, for all 24 cases at least one tNGS approach provided reliable NGS datasets to investigate the presence of *PRKAR1A* gene mutations (Supplementary Table 3). Samples analyzed by both tNGS approaches showed identical results, except for one sample (CM16), where only Ion AmpliSeq detected a *PRKAR1A* variant (c.955G>A; p.Gly319Arg), but not the smMIP method.

Combining the results from both tNGS approaches, *PRKAR1A* variants were identified in 14 of 24 (58%) sporadic cardiac myxomas (Table 2). These involved a total of 25 distinct variants within the *PRKAR1A* gene, including 56% (n=14/25) frameshift mutations, 24% (n=6/25) missense mutations yielding amino acid substitutions, 16% (n=4/25) nonsense mutations resulting in a premature stop codon, and 4% (n=1/25) splice site mutation (Figure 3).

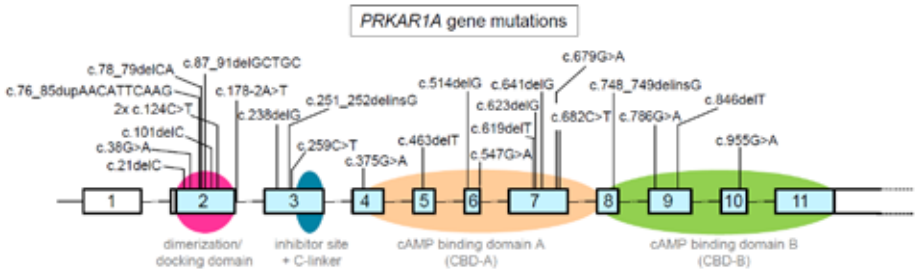

Figure 3. Summary of the identified *PRKAR1A* gene mutations (n=25) in sporadic cardiac myxoma. The different exonic regions (exon 1- exon 11) of the human *PRKAR1A* gene are shown, and coding regions are indicated in blue. The functional protein domains of the regulatory subunit RI alpha that are encoded by the different *PRKAR1A* exons are represented by the colored circles.

The frameshift mutations resulted from indels with the deletion and/or insertion of single nucleotides (n=11/14; 79%) or multiple nucleotides (n=3/14; 21%). The *PRKAR1A* mutations were distributed over all coding exons, except exon 11. The majority of variants were located in exon 2 (c.1-c.177) and exon 7 (c.550-c.708). Loss-of-function mutations resulting from frameshift and nonsense mutations together with the splice site mutation were classified as pathogenic (n=11/25; 44%) or likely pathogenic (n=8/25; 32%), while the six missense mutations were categorized as variant of uncertain significance (n=6/25; 24%) (p.Arg13His located in the dimerization/docking domain; p.Met125Ile, p.Asp183Asn, p.Asp227Asn located in c-AMP binding domain A; p.Gly319Arg located in c-AMP binding domain B; p.Pro87Ser in the C-linker region). In total, 11 out of 25 variants (44%) were previously identified in CNC patients, two additional variants detected in unrelated sporadic cardiac myxoma cases, while 12 variants represented novel genetic alterations in *PRKAR1A* (Supplementary Table 3). The median VAF of all identified variants was 17% (range 6%-38%) for Ion AmpliSeq and 24% (range 14%-44%) for smMIP, indicating that these single nucleotide variants reflected somatic mutations. Notably, 9 out of 14 (64%) cases showed more than one *PRKAR1A* variant, suggestive for the presence of compound heterozygous *PRKAR1A* mutations in sporadic cardiac myxoma. In one case (CM09) this involved two missense mutations (c.259C>T, c.679G>A), while in the other eight cases these represented a combination of either a frameshift and/or nonsense mutations.

Table 2. *PRKAR1A* gene mutation analysis in sporadic cardiac myxoma

Case number	DNA variant *PRKAR1A*	Protein alteration *PRKAR1A*	VAF Ion AmpliSeq	VAF smMIP	Effect
CM01	c.238delG	p.Asp80Metfs*49	31%	24%	Frameshift
	c.682C>T	p.Arg228Ter	25%	25%	Nonsense
CM02	c.124C>T	p.Arg42Ter	20%	20%	Nonsense
	c.178-2A>T	p.?	17%	19%	Altered splicing
CM03	c.623delG	p.Gly208Glufs*14	26%	29%	Frameshift
	c.641delC	p.Thr214Metfs*8	21%	28%	Frameshift
CM04	c.87_91delGCTGC	p.Leu30Glnfs*13	12%	No data	Frameshift
	c.251_252delinsG	p.Pro84Argfs*45	12%	No data	Frameshift
CM05	No variant detected	-	No data	NVD†	-
CM06	No variant detected	-	NVD	No data	-
CM07	No variant detected	-	NVD	NVD	-
CM08	c.748_749delinsG	p.Leu250Valfs*7	6%	No data	Frameshift
CM09	c.259C>T	p.Pro87Ser	8%	No data	Missense
	c.679G>A	p.Asp227Asn	6%	No data	Missense
CM10	No variant detected	-	-	No data	-
CM11	c.101delC	p.Ser34Leufs*95	17%	73%[#]	Frameshift
CM12	c.786G>A	p.Trp262Ter	18%	No data	Nonsense
CM13	c.21delC	p.Ala8Profs*121	9%	No data	Frameshift
	c.78_79delCA	p.Ile27Serfs*17	11%	No data	Frameshift
CM14	No variant detected	-	NVD	No data	-
CM15	c.463delT	p.Ser155Argfs*10	16%	16%	Frameshift
CM16	c.955G>A	p.Gly319Arg	10%	NVD	Missense
CM17	No variant detected	-	NVD	NVD	-
CM18	c.514delG	p.Asp172Ilefs*5	20%	14%	Frameshift
	c.846delT	p.Ile282Metfs*15	17%	23%	Frameshift
CM19	No variant detected	-	NVD	NVD	-
CM20	No variant detected	-	NVD	NVD	-
CM21	No variant detected	-	NVD	NVD	-
CM22	c.124C>T	p.Arg42Ter	7%	No data	Nonsense
	c.375G>A	p.Met125Ile	7%	No data	Missense
	c.38G>A	p.Arg13His	15%	No data	Missense
	c.547G>A	p. Asp183Asn	26%	No data	Missense
CM23	No variant detected	-	NVD	NVD	-
CM24	c.76_85dupAACATTCAAG	p.Ala29Glufs*19	33%	44%	Frameshift
	c.619delT	p.Tyr207Metfs*15	38%	36%	Frameshift

VAF, variant allele frequency; No data: too few reads; †NVD: no variant detected; [#] Relative low sequencing depth at that position with smMIP may have resulted in a skewed VAF; this value was not included in the calculation of the median VAF.

Discussion

Cardiac myxomas are the most common primary tumors of the heart with an estimated prevalence of 0.03% in the general population [32]. The pathobiology of cardiac myxomas has still remained unclear so far, but there is evidence of an obvious role for *PRKAR1A* mutations in CNC-associated cardiac myxomas [5]. However, in sporadic lesions, in the beginning it appeared more challenging to assess the role of *PRKAR1A* gene mutations. Sensitive methods involving tNGS are required to detect gene variants in hypocellular tissues at lower abundancy. Here, we presented two different tNGS methods for *PRKAR1A* gene mutation detection in 24 sporadic cardiac myxomas. One method involved Ion AmpliSeq where amplicons generated by multiplex PCR of *PRKAR1A* exonic regions were sequenced on Ion Torrent platform, while the second method used UMI-tagged MIPs to capture genomic fragments from both DNA strands of the *PRKAR1A* gene that were sequenced on an Illumina platform. Integration of both NGS datasets showed that 14 of 24 cases (58%) displayed *PRKAR1A* gene variants with an average median VAF of 21%, due to the relative low tumor percentage. This frequency is similar to the findings of two previous studies where *PRKAR1A* gene mutations were detected in 68% and 64% of sporadic cardiac myxomas, respectively [22, 24]. In the study of Maleszewski et al. they only found *PRKAR1A* gene mutations in 31% of cases. This could possibly be explained by their reported low quantity and quality of the DNA (only 26% was adequate) and the Sanger sequencing technique, which has lower sensitivity and limitations in detecting larger deletions or duplications [23].

The majority of variants that were identified by tNGS in our cases represented genetic alterations that are predicted to result in RIα loss-of-function, including fourteen frameshift and four nonsense mutations, which as a single mutation most likely result in haploinsufficiency due to non-sense mediated mRNA decay (NMD) or truncated protein resulting from a premature stop codon. These types of genetic alterations also predominate in CNC-associated *PRKAR1A* germline variants [10, 18, 20]. However, some *PRKAR1A* variants may escape NMD, especially those that cluster in cAMP binding domain A (CBD-A) [33], thereby giving rise to the expression of an altered and dysfunctional Riα protein. In addition, *PRKAR1A* mutations can also promote accelerated RIα protein degradation [34]. Similar to findings in other reported sporadic as well as CNC-associated cardiac myxomas [23, 25, 35], we furthermore identified missense mutations that mapped in the dimerization/docking domain or cAMP binding domains of RIα. Notably, mutation p.Met125Ile was located in the isoform-specific N3A motif representing the RIα homodimer interface [36], and mutation p.Asp227Asn in the hinge domain

of CBD-A, both representing allosteric hotspots [37]. However, it still remains to be established whether each of the identified missense mutations will affect the RIα function. In addition, we identified one mutation outside the *PRKAR1A* coding sequencing, representing a splice site mutation affecting RIα function, also occurring frequently in CNC associated lesions [7, 10, 18].

Another important observation from our study is that almost two-thirds of the sporadic cardiac myxomas displayed multiple *PRKAR1A* variants, in line with previous findings [24, 25]. Although, mosaicism could formerly not be excluded [38], it is very likely that the majority of these cases show *PRKAR1A* inactivation either in *cis* or *trans* by compound heterozygous mutations. Thus, the occurrence of cardiac myxoma is strongly associated with uncontrolled PKA activation, either through germline CNC-associated *PRKAR1A* mutation combined with loss-of-heterozygosity as seen in the other CNC associated lesions [8], or somatic loss-of-function mutations. Heterozygous knock-out of the *PRKAR1A* gene in mice leads to extracardiac myxomatous soft tissue tumors[22], in line with some of the CNC-associated tumors including cardiac myxomas. However, mice displaying cardiac-specific heterozygous ablation of *PRKAR1A* show no signs of cardiac tumor formation, but instead diminished cardiomyocyte hypertrophy and augmented cardiomyocyte necrosis [39, 40].

Cardiac myxomas negative for *PRKAR1A* mutation(s) may activate PKA through other molecular pathways. These include activating micro-insertions in *PRKACA* encoding the catalytic subunit Cα of PKA [41], and loss-of-function mutations in *KIF1C*, a member of the kinesin superfamily of molecular motor proteins, resulting in decreased *PRKAR1A* expression [42]. Other candidates that could affect PKA activity are regulators of RI, RII and C subunits [17, 43], but specific mutations in their genes have not yet been linked to cardiac myxoma.

In conclusion, our findings indicate that about 60% of sporadic cardiac myxoma harbor *PRKAR1A* mutations leading most often to loss of the regulatory subunit RIα, and unscheduled activation of the PKA enzyme. Notably 64% of the affected tumors show multiple *PRKAR1A* variants suggesting *PRKAR1A* inactivation by compound heterozygous mutations. This is in concert with previously published results. Further investigation using genome-wide next generation sequencing is required to investigate and identify other potential driver mutations involved in the pathogenesis of sporadic cardiac myxomas.

References

1. Velez Torres JM, Martinez Duarte E, Diaz-Perez JA, Rosenberg AE (2020) Cardiac Myxoma: Review and Update of Contemporary Immunohistochemical Markers and Molecular Pathology Adv Anat Pathol 27:380-384. doi: 10.1097/PAP.0000000000000275
2. Singhal P, Luk A, Rao V, Butany J (2014) Molecular basis of cardiac myxomas Int J Mol Sci 15:1315-1337. doi: 10.3390/ijms15011315
3. Di Vito A, Mignogna C, Donato G (2015) The mysterious pathways of cardiac myxomas: a review of histogenesis, pathogenesis and pathology Histopathology 66:321-332. doi: 10.1111/his.12531
4. Correa R, Salpea P, Stratakis CA (2015) Carney complex: an update Eur J Endocrinol 173:M85-97. doi: 10.1530/EJE-15-0209
5. Bouys L, Bertherat J (2021) MANAGEMENT OF ENDOCRINE DISEASE: Carney complex: clinical and genetic update 20 years after the identification of the CNC1 (PRKAR1A) gene Eur J Endocrinol 184:R99-R109. doi: 10.1530/EJE-20-1120
6. Griborio-Guzman AG, Aseyev OI, Shah H, Sadreddini M (2022) Cardiac myxomas: clinical presentation, diagnosis and management Heart 108:827-833. doi: 10.1136/heartjnl-2021-319479
7. Kirschner LS, Sandrini F, Monbo J, Lin JP, Carney JA, Stratakis CA (2000) Genetic heterogeneity and spectrum of mutations of the PRKAR1A gene in patients with the carney complex Hum Mol Genet 9:3037-3046. doi: 10.1093/hmg/9.20.3037
8. Kirschner LS, Carney JA, Pack SD, Taymans SE, Giatzakis C, Cho YS, Cho-Chung YS, Stratakis CA (2000) Mutations of the gene encoding the protein kinase A type I-alpha regulatory subunit in patients with the Carney complex Nat Genet 26:89-92. doi: 10.1038/79238
9. Casey M, Vaughan CJ, He J, Hatcher CJ, Winter JM, Weremowicz S, Montgomery K, Kucherlapati R, Morton CC, Basson CT (2000) Mutations in the protein kinase A R1alpha regulatory subunit cause familial cardiac myxomas and Carney complex J Clin Invest 106:R31-38. doi: 10.1172/JCI10841
10. Bertherat J, Horvath A, Groussin L, Grabar S, Boikos S, Cazabat L, Libe R, Rene-Corail F, Stergiopoulos S, Bourdeau I, Bei T, Clauser E, Calender A, Kirschner LS, Bertagna X, Carney JA, Stratakis CA (2009) Mutations in regulatory subunit type 1A of cyclic adenosine 5'-monophosphate-dependent protein kinase (PRKAR1A): phenotype analysis in 353 patients and 80 different genotypes J Clin Endocrinol Metab 94:2085-2091. doi: 10.1210/jc.2008-2333
11. Blyth M, Huang S, Maloney V, Crolla JA, Karen Temple I (2008) A 2.3Mb deletion of 17q24.2-q24.3 associated with 'Carney Complex plus' Eur J Med Genet 51:672-678. doi: 10.1016/j.ejmg.2008.09.002
12. Horvath A, Bossis I, Giatzakis C, Levine E, Weinberg F, Meoli E, Robinson-White A, Siegel J, Soni P, Groussin L, Matyakhina L, Verma S, Remmers E, Nesterova M, Carney JA, Bertherat J, Stratakis CA (2008) Large deletions of the PRKAR1A gene in Carney complex Clin Cancer Res 14:388-395. doi: 10.1158/1078-0432.CCR-07-1155
13. Ito S, Hashimoto A, Yamaguchi K, Kawamura S, Myoen S, Ogawa M, Sato I, Minato T, Miyabe S, Nakazato A, Fujii K, Mochizuki M, Fujimori H, Tamai K, Niihori T, Aoki Y, Sugawara A, Sasano H, Shima H, Yasuda J (2022) A novel 8.57-kb deletion of the upstream region of PRKAR1A in a family with Carney complex Mol Genet Genomic Med 10:e1884. doi: 10.1002/mgg3.1884
14. Palla S, Toke J, Bozsik A, Butz H, Papp J, Liko I, Kuroli E, Banvolgyi A, Hamar M, Bertherat J, Medvecz M, Patocs A (2023) Whole genome sequencing resolves 10 years diagnostic odyssey in familiar myxoma Sci Rep 13:14658. doi: 10.1038/s41598-023-41878-9
15. Bossis I, Stratakis CA (2004) Minireview: PRKAR1A: normal and abnormal functions Endocrinology 145:5452-5458. doi: 10.1210/en.2004-0900

16. Torres-Quesada O, Mayrhofer JE, Stefan E (2017) The many faces of compartmentalized PKA signalosomes Cell Signal 37:1-11. doi: 10.1016/j.cellsig.2017.05.012

17. Soberg K, Skalhegg BS (2018) The Molecular Basis for Specificity at the Level of the Protein Kinase a Catalytic Subunit Front Endocrinol (Lausanne) 9:538. doi: 10.3389/fendo.2018.00538

18. Horvath A, Bertherat J, Groussin L, Guillaud-Bataille M, Tsang K, Cazabat L, Libe R, Remmers E, Rene-Corail F, Faucz FR, Clauser E, Calender A, Bertagna X, Carney JA, Stratakis CA (2010) Mutations and polymorphisms in the gene encoding regulatory subunit type 1-alpha of protein kinase A (PRKAR1A): an update Hum Mutat 31:369-379. doi: 10.1002/humu.21178

19. Fogt F, Zimmerman RL, Hartmann CJ, Brown CA, Narula N (2002) Genetic alterations of Carney complex are not present in sporadic cardiac myxomas Int J Mol Med 9:59-60

20. Mabuchi T, Shimizu M, Ino H, Yamguchi M, Terai H, Fujino N, Nagata M, Sakata K, Inoue M, Yoneda T, Mabuchi H (2005) PRKAR1A gene mutation in patients with cardiac myxoma Int J Cardiol 102:273-277. doi: 10.1016/j.ijcard.2004.05.053

21. Mantovani G, Bondioni S, Corbetta S, Menicanti L, Rubino B, Peverelli E, Labarile P, Dall'Asta C, Ambrosi B, Beck-Peccoz P, Lania AG, Spada A (2009) Analysis of GNAS1 and PRKAR1A gene mutations in human cardiac myxomas not associated with multiple endocrine disorders J Endocrinol Invest 32:501-504. doi: 10.1007/BF03346496

22. Veugelers M, Wilkes D, Burton K, McDermott DA, Song Y, Goldstein MM, La Perle K, Vaughan CJ, O'Hagan A, Bennett KR, Meyer BJ, Legius E, Karttunen M, Norio R, Kaariainen H, Lavyne M, Neau JP, Richter G, Kirali K, Farnsworth A, Stapleton K, Morelli P, Takanashi Y, Bamforth JS, Eitelberger F, Noszian I, Manfroi W, Powers J, Mochizuki Y, Imai T, Ko GT, Driscoll DA, Goldmuntz E, Edelberg JM, Collins A, Eccles D, Irvine AD, McKnight GS, Basson CT (2004) Comparative PRKAR1A genotype-phenotype analyses in humans with Carney complex and prkar1a haploinsufficient mice Proc Natl Acad Sci U S A 101:14222-14227. doi: 10.1073/pnas.0405535101

23. Maleszewski JJ, Larsen BT, Kip NS, Castonguay MC, Edwards WD, Carney JA, Kipp BR (2014) PRKAR1A in the development of cardiac myxoma: a study of 110 cases including isolated and syndromic tumors Am J Surg Pathol 38:1079-1087. doi: 10.1097/PAS.0000000000000202

24. He J, Sun M, Li E, Hou Y, Shepard MJ, Chen D, Pacak K, Wang C, Guo L, Zhuang Z, Liu Y (2017) Recurrent somatic mutations of PRKAR1A in isolated cardiac myxoma Oncotarget 8:103968-103974. doi: 10.18632/oncotarget.21916

25. Roque A, Kimbrough T, Traner C, Baehring JM, Huttner A, Adams J, Canosa S, Sklar J, Madri JA (2019) Somatic PRKAR1A mutation in sporadic atrial myxoma with cerebral parenchymal metastases: a case report J Med Case Rep 13:389. doi: 10.1186/s13256-019-2317-z

26. Maleszewski JJ, Basso C, Bois MC, Glass C, Klarich KW, Leduc C, Padera RF, Tavora F (2022) The 2021 WHO Classification of Tumors of the Heart J Thorac Oncol 17:510-518. doi: 10.1016/j.jtho.2021.10.021

27. van Bladel DAG, van der Last-Kempkes JLM, Scheijen B, Groenen P, EuroClonality C (2022) Next-Generation Sequencing-Based Clonality Detection of Immunoglobulin Gene Rearrangements in B-Cell Lymphoma Methods Mol Biol 2453:7-42. doi: 10.1007/978-1-0716-2115-8_2

28. Eijkelenboom A, Kamping EJ, Kastner-van Raaij AW, Hendriks-Cornelissen SJ, Neveling K, Kuiper RP, Hoischen A, Nelen MR, Ligtenberg MJ, Tops BB (2016) Reliable Next-Generation Sequencing of Formalin-Fixed, Paraffin-Embedded Tissue Using Single Molecule Tags J Mol Diagn 18:851-863. doi: 10.1016/j.jmoldx.2016.06.010

29. Berendsen MR, van Bladel DAG, Hesius E, Berganza Irusquieta C, Rijntjes J, van Spriel AB, van der Spek E, Pruijt JFM, Kroeze LI, Hebeda KM, Croockewit S, Stevens WBC, van Krieken J, Groenen P, van den Brand M, Scheijen B (2023) Clonal Relationship and Mutation Analysis in Lymphoplasmacytic Lymphoma/Waldenstrom Macroglobulinemia Associated With Diffuse Large B-cell Lymphoma Hemasphere 7:e976. doi: 10.1097/HS9.0000000000000976

30. Scalise M, Torella M, Marino F, Ravo M, Giurato G, Vicinanza C, Cianflone E, Mancuso T, Aquila I, Salerno L, Nassa G, Agosti V, De Angelis A, Urbanek K, Berrino L, Veltri P, Paolino D, Mastroroberto P, De Feo M, Viglietto G, Weisz A, Nadal-Ginard B, Ellison-Hughes GM, Torella D (2020) Atrial myxomas arise from multipotent cardiac stem cells Eur Heart J 41:4332-4345. doi: 10.1093/eurheartj/ehaa156

31. Bekers EM, Eijkelenboom A, Rombout P, van Zwam P, Mol S, Ruijter E, Scheijen B, Flucke U (2019) Identification of novel GNAS mutations in intramuscular myxoma using next-generation sequencing with single-molecule tagged molecular inversion probes Diagn Pathol 14:15. doi: 10.1186/s13000-019-0787-3

32. Grebenc ML, Rosado de Christenson ML, Burke AP, Green CE, Galvin JR (2000) Primary cardiac and pericardial neoplasms: radiologic-pathologic correlation Radiographics 20:1073-1103; quiz 1110-1071, 1112. doi: 10.1148/radiographics.20.4.g00jl081073

33. Greene EL, Horvath AD, Nesterova M, Giatzakis C, Bossis I, Stratakis CA (2008) In vitro functional studies of naturally occurring pathogenic PRKAR1A mutations that are not subject to nonsense mRNA decay Hum Mutat 29:633-639. doi: 10.1002/humu.20688

34. Rhayem Y, Le Stunff C, Abdel Khalek W, Auzan C, Bertherat J, Linglart A, Couvineau A, Silve C, Clauser E (2015) Functional Characterization of PRKAR1A Mutations Reveals a Unique Molecular Mechanism Causing Acrodysostosis but Multiple Mechanisms Causing Carney Complex J Biol Chem 290:27816-27828. doi: 10.1074/jbc.M115.656553

35. Kubo H, Tsurutani Y, Sugisawa C, Sunouchi T, Hirose R, Saito J (2022) Phenotypic Variability in a Family with Carney Complex Accompanied by a Novel Mutation Involving PRKAR1A Tohoku J Exp Med 257:337-345. doi: 10.1620/tjem.2022.J051

36. Bruystens JG, Wu J, Fortezzo A, Kornev AP, Blumenthal DK, Taylor SS (2014) PKA RIalpha homodimer structure reveals an intermolecular interface with implications for cooperative cAMP binding and Carney complex disease Structure 22:59-69. doi: 10.1016/j.str.2013.10.012

37. Jafari N, Del Rio J, Akimoto M, Byun JA, Boulton S, Moleschi K, Alsayyed Y, Swanson P, Huang J, Martinez Pomier K, Lee C, Wu J, Taylor SS, Melacini G (2021) Noncanonical protein kinase A activation by oligomerization of regulatory subunits as revealed by inherited Carney complex mutations Proc Natl Acad Sci U S A 118. doi: 10.1073/pnas.2024716118

38. Kamilaris CDC, Faucz FR, Andriessen VC, Nilubol N, Lee CR, Ahlman MA, Hannah-Shmouni F, Stratakis CA (2021) First Somatic PRKAR1A Defect Associated With Mosaicism for Another PRKAR1A Mutation in a Patient With Cushing Syndrome J Endocr Soc 5:bvab007. doi: 10.1210/jendso/bvab007

39. Liu Y, Xia P, Chen J, Bandettini WP, Kirschner LS, Stratakis CA, Cheng Z (2020) PRKAR1A deficiency impedes hypertrophy and reduces heart size Physiol Rep 8:e14405. doi: 10.14814/phy2.14405

40. Liu Y, Chen J, Xia P, Stratakis CA, Cheng Z (2021) Loss of PKA regulatory subunit 1alpha aggravates cardiomyocyte necrosis and myocardial ischemia/reperfusion injury J Biol Chem 297:100850. doi: 10.1016/j.jbc.2021.100850

41. Tseng IC, Huang WJ, Jhuang YL, Chang YY, Hsu HP, Jeng YM (2017) Microinsertions in PRKACA cause activation of the protein kinase A pathway in cardiac myxoma J Pathol 242:134-139. doi: 10.1002/path.4899

42. Zhou M, Yao Y, Wang X, Zha L, Chen Y, Li Y, Wang M, Yu C, Zhou Y, Li Q, Cao Z, Wu J, Shi S, Jiang D, Long D, Wang J, Wang Q, Cheng X, Liao Y, Tu X (2023) Crosstalk between KIF1C and PRKAR1A in left atrial myxoma Commun Biol 6:724. doi: 10.1038/s42003-023-05094-5

43. Zhang X, Wang BZ, Kim M, Nash TR, Liu B, Rao J, Lock R, Tamargo M, Soni RK, Belov J, Li E, Vunjak-Novakovic G, Fine B (2022) STK25 inhibits PKA signaling by phosphorylating PRKAR1A Cell Rep 40:111203. doi: 10.1016/j.celrep.2022.111203

Supplementary Tables

Supplementary Table 1

Target region *PRKAR1A*	Ion AmpliSeq Fwd primers	Ion AmpliSeq Rev primers	Amplicon length
Exon 2-1	TCCCTGTGAATCAGTTGTCT	GCACAATAGAATCTTTGAGCAG	215
Exon 2-2	GTGAGCTCTACGTCCAGAAG	CAACTGTCACAATCACCTCATC	169
Exon 3-1	GCCGAAGGATCTCATTTTGC	CTTTAACCACTGGGTTGGGTG	140
Exon 3-2	CAGACTCAAGGGAGGATGAG	AAGTGGGTCCCAAAAGCATCC	172
Exon 4	GGAATTGTCATTTGACCTTCAG	AACAATTTGGGATCACACCC	184
Exon 5	TCACCAGATGACAGTCTGGG	TATTGCATGCTCCAGAGGCC	187
Exon 6	TCACAGTACCACTGTAAAATAAG	CTTATTGCTCGGAAGCGATC	217
Exon 7-1	GATGTCACTTGCACTTTAGG	TTTGACAGTGGCTGCTCTCG	118
Exon 7-2	TGAATGGGCAACCAGTGTTG	CACACTCTCAAACACCATGG	173
Exon 8	ACACGTCTTGGGGATATCAC	AGGCTTTTCCCAAGTCCATC	180
Exon 9-1	TGGGCATGGCTATTTGGTTG	AAGAACTCATCCCCTGGTTC	207
Exon 9-2	GTCTCTGGACAAGTGGGAAC	TCCCTCTTAGAGCGTACAAC	208
Exon 10	CCTGGGTTTGAGAGTGTGTG	CTGAGAGGTGACTTAAAGAAACC	187
Exon 11-1	CAGAAGTGCACTGCTTTAAGG	GTCTGAGCATGGGCCAAGAAC	189
Exon 11-2	TGCCACAGTTGTTGCTCGTG	GTTTGCATGAGTGAAGCATGG	199

Supplementary Table 2

smMIP probes	Probe strand	MIP sequence
PRKAR1A_EX2_2_S	Sense	GCGCTGCTCAAAGATTCTATTGTGNNNNNNNNNCTTCAGCTTCCCGATATCCGACGGTAGTGTATAGTTTATACAAGCA
PRKAR1A_EX2_3_A	Antisense	GAAAAAAACACACACATGCTTGTANNNNNNNNNCTTCAGCTTCCCGATATCCGACGGTAGTGTCACAACTGCACAATAG
PRKAR1A_EX2_1_S	Sense	ATAAATGTGGGGAGATGATGAGGNNNNNNNNNCTTCAGCTTCCCGATATCCGACGGTAGTGTGAGCTCTACGTCCAGAA
PRKAR1A_EX2_4_A	Antisense	TTGAGCAGCGCTTGAATGTTATNNNNNNNNNCTTCAGCTTCCCGATATCCGACGGTAGTGTGTAACAACTGTCACAATC
PRKAR1A_EX3_3_A	Antisense	CGGCATGTAAAGCTGGCANNNNNNNNNCTTCAGCTTCCCGATATCCGACGGTAGTGTTTAACCACTGGGTTGGGTGGAG
PRKAR1A_EX3_1_S	Sense	CAGTGGTTAAAGGTAGGAGGCGNNNNNNNNNCTTCAGCTTCCCGATATCCGACGGTAGTGTATGCCGAAGGATCTCATT
PRKAR1A_EX3_2_S	Sense	GATATTTGAATATCGGGGGGNNNNNNNNNCTTCAGCTTCCCGATATCCGACGGTAGTGTAGACTCAAGGGAGGATGAGA
PRKAR1A_EX3_4_A	Antisense	GCACCTCGTCGCCTCCTACCNNNNNNNNNCTTCAGCTTCCCGATATCCGACGGTAGTGTGATTCATTCATCAAAGGAGA
PRKAR1A_EX3_5_A	Antisense	CGTGTAGACCTCAGCGCTGATANNNNNNNNNCTTCAGCTTCCCGATATCCGACGGTAGTGTCACCCTGTTTTGTATTTT
PRKAR1A_EX3_6_A	Antisense	AGGATGCCGCATCTTCCTCNNNNNNNNNCTTCAGCTTCCCGATATCCGACGGTAGTGTTTGTACAGGATGGATGAAGTT
PRKAR1A_EX4_1_S	Sense	GAACAGGCTCTTTCTTAACACTNNNNNNNNNCTTCAGCTTCCCGATATCCGACGGTAGTGTTGGAATTGTCATTTGACC
PRKAR1A_EX4_2_A	Antisense	CTAGAAAAGAACTGAAGGTCAANNNNNNNNNCTTCAGCTTCCCGATATCCGACGGTAGTGTTACTTGAAAAATAGTGTT
PRKAR1A_EX5_1_S	Sense	GTTACGGGAGAGGAGGCGAGNNNNNNNNNCTTCAGCTTCCCGATATCCGACGGTAGTGTAGAGACATGTGAAATGTAAC
PRKAR1A_EX5_2_A	Antisense	GAGAGAAGGCCTCGTGTTACATTNNNNNNNNNCTTCAGCTTCCCGATATCCGACGGTAGTGTAAATCCTCTAGTCTCGC
PRKAR1A_EX6_1_S	Sense	GTGATTGATCAAGGAGAGACGGNNNNNNNNNCTTCAGCTTCCCGATATCCGACGGTAGTGTCACACTCTCACAGTACCA
PRKAR1A_EX6_3_A	Antisense	GTTAGAAGCATATTCCAAATTAAANNNNNNNNNCTTCAGCTTCCCGATATCCGACGGTAGTGTCTCGGAAGCGATCAAT
PRKAR1A_EX6_2_S	Sense	GATTTTGAAGGGTCATTACATCCCNNNNNNNNNCTTCAGCTTCCCGATATCCGACGGTAGTGTTTTAGGTGATGAAGGG
PRKAR1A_Ex7_5_A	Antisense	ATGTTAAAAACCCTCAAACCTTTNNNNNNNNNCTTCAGCTTCCCGATATCCGACGGTAGTGTGTTCCATAAATCAAAGC
PRKAR1A_EX7_1_S	Sense	CGAGAGCAGCCACTGTCAAAGCAANNNNNNNNNCTTCAGCTTCCCGATATCCGACGGTAGTGTAGTGTTTGTATCTAGA
PRKAR1A_EX7_2_S	Sense	GTAAGAGACCATGGTGTTTNNNNNNNNNCTTCAGCTTCCCGATATCCGACGGTAGTGTCAGTGTTGGGGAAGGAGGGAG
PRKAR1A_EX7_4_A	Antisense	TTCTCCAAAGCTCCCTCCNNNNNNNNNCTTCAGCTTCCCGATATCCGACGGTAGTGTAAATCACACTCTCAAACACCAT

Supplementary Table 2 Continued

smMIP probes	Probe strand	MIP sequence
PRKAR1A_EX8_2_A	Antisense	CACCACATAATGCTATGGAATAANNNNNNNNNCTTCAGCTTCCCGATATCCGACGGTAGTGTTTAACACACTTTACAAC
PRKAR1A_EX8_1_S	Sense	GCTAGTATGTGAGATACCCCTGNNNNNNNNNCTTCAGCTTCCCGATATCCGACGGTAGTGTATTACACGTCTTGGGGAT
PRKAR1A_EX9_3_A	Antisense	GGTGCTGTTATAAAGGTAAAAAGNNNNNNNNNCTTCAGCTTCCCGATATCCGACGGTAGTGTCTCCCTGCACCACAATC
PRKAR1A_EX9_1_S	Sense	GAGAACCAGGGGATGAGTTCNNNNNNNNNCTTCAGCTTCCCGATATCCGACGGTAGTGTAGCACCAAATAATACAGAGC
PRKAR1A_Ex9_5_A	Antisense	TAACTGCTCTGTATTATTTGNNNNNNNNNCTTCAGCTTCCCGATATCCGACGGTAGTGTCTCCCTGCACCACAATCTTC
PRKAR1A_Ex9_6_A	Antisense	ACTCTGAAAGACAAGAATCAAAATNNNNNNNNNCTTCAGCTTCCCGATATCCGACGGTAGTGTAAGAACTCATCCCCTG
PRKAR1A_EX9_4_A	Antisense	AGCTACCGTAAGACGTTCCCACTTNNNNNNNNNCTTCAGCTTCCCGATATCCGACGGTAGTGTTTTACCTCTAAAATTC
PRKAR1A_EX9_2_S	Sense	AAAGTTGTACGCTCTAAGAGGNNNNNNNNNCTTCAGCTTCCCGATATCCGACGGTAGTGTGTTTGAAGATGGGCAGAAG
PRKAR1A_Ex9_7_A	Antisense	CTCCCTGCACCACAATCTTCNNNNNNNNNCTTCAGCTTCCCGATATCCGACGGTAGTGTGAGCGTACAACTTTTTAAAG
PRKAR1A_EX10_1_S	Sense	GTTGAAGTGGGAAGATTGGGNNNNNNNNNCTTCAGCTTCCCGATATCCGACGGTAGTGTGGTAGTTAAAATTGCATAGG
PRKAR1A_EX10_3_A	Antisense	CTATAATAAAATCACCAAAAAGCTNNNNNNNNNCTTCAGCTTCCCGATATCCGACGGTAGTGTTGACTTAAAGAAACCA
PRKAR1A_EX10_2_S	Sense	GTCACCTCTCAGTGAGATATTGNNNNNNNNNCTTCAGCTTCCCGATATCCGACGGTAGTGTTTATAGGGGTCAGCTGCT
PRKAR1A_EX11_3_A	Antisense	TGGGTAACAGGCTAACTTCTANNNNNNNNNCTTCAGCTTCCCGATATCCGACGGTAGTGTGAGCATGGGCCAAGAACAC
PRKAR1A_EX11_1_S	Sense	GCTCAGACATCCTCAAACGANNNNNNNNNCTTCAGCTTCCCGATATCCGACGGTAGTGTACCCATCTTTGCTTTCTCCA
PRKAR1A_EX11_4_A	Antisense	CAAGGGGCCACGAGCAACANNNNNNNNNCTTCAGCTTCCCGATATCCGACGGTAGTGTAGGGAGGCACAGGAGGCAGAT
PRKAR1A_EX11_2_S	Sense	CTCCTCTCCCCAATCCATGNNNNNNNNNCTTCAGCTTCCCGATATCCGACGGTAGTGTTGCGTTAAGCTGGACCGACCT

Supplementary Table 3

Sample	Ion AmpliSeq c.HGVS-*PRKAR1A*	Ion AmpliSeq p.HGVS-PRKAR1A	Ion AmpliSeq reads SNV	Ion AmpliSeq VAF-PRKAR1A	smMIP c.HGVS-*PRKAR1A*
CM01	c.238delG	p.Asp80Metfs*49	1877	31%	c.238delG
	c.682C>T	p.Arg228Ter	4327	25%	c.682C>T
CM02	c.124C>T	p.Arg42Ter	915	20%	c.124C>T
	c.178-2A>T	splicing	1303	17%	c.178-2A>T
CM03	c.623delG	p.Gly208Glufs*14	7000	26%	c.623delG
	c.641delC	p.Thr214Metfs*8	1526	21%	c.641delC
CM04	c.87_91delGCTGC	p.Leu30Glnfs*13	67	12%	No data
	c.251_252delinsG	p.Pro84Argfs*45	50	12%	
CM05	No data				No variant detected
CM06	No variant detected				No data
CM07	No variant detected				No variant detected
CM08	c.748_749delinsG	p.Leu250Valfs*7	330	6%	No data
CM09	c.259C>T	p.Pro87Ser	646	8%	No data
	c.679G>A	p.Asp227Asn	1511	6%	
CM10	No variant detected				No data
CM11	c.101delC	p.Ser34Leufs*95	3094	17%	c.101delC
CM12	c.786G>A	p.Trp262Ter	214	18%	No data
CM13	c.21delC	p.Ala8Profs*121	680	9%	No data
	c.78_79delCA	p.Ile27Serfs*17	1430	11%	
CM14	No variant detected				No data
CM15	c.463delT	p.Ser155Argfs*10	1730	16%	c.463delT
CM16	c.955G>A	p.Gly319Arg	35	10%	No variant detected
CM17	No variant detected				No variant detected
CM18	c.514delG	p.Asp172Ilefs*5	905	20%	c.514delG
	c.846delT	p.Ile282Metfs*15	624	17%	c.846delT
CM19	No variant detected				No variant detected
CM20	No variant detected				No variant detected
CM21	No variant detected				No variant detected
CM22	c.124C>T	p.Arg42Ter	245	7%	No data

smMIP p.HGVS-PRKAR1A	smMIP reads SNV	smMIP VAF-PRKAR1A	Pathogenicity (ACMG scoring) §	Variant in Carney complex#	Variant in sporadic myxoma#
p.Asp80Metfs*49	508	24%	Likely pathogenic (PVS1 + PM2)	No	No
p.Arg228Ter	310	25%	Pathogenic (PVS1 + PS4 + PM2)	Yes PMID: 20358582	No
p.Arg42Ter	155	20%	Pathogenic (PVS1 + PS4 + PM2)	Yes PMID: 20358582	Yes PMID: 29262613
splicing	150	19%	Pathogenic (PVS1 + PM2)	Yes PMID: 20358582	No
p.Gly208Glufs*14	64	29%	Pathogenic (PVS1 + PS4 + PM2)	Yes PMID: 20358582	No
p.Thr214Metfs*8	42	28%	Likely pathogenic (PVS1 + PM2)	No	No
			Likely pathogenic (PVS1 + PM2)	No	Yes PMID: 29262613
			Likely pathogenic (PVS1 + PM2)	No	Yes PMID: 29262613
			Likely pathogenic (PVS1 + PM2)	No	No
			Variant of uncertain significance (PP2 +PM2)	No	No
			Variant of uncertain significance (PP2 +PM2)	No	No
p.Ser34LeufsTer95	58*	73%	Pathogenic (PVS1 + PM2)	Yes PMID: 20358582	No
			Likely pathogenic (PVS1 + PM2)	No (Yes: Indel, fs Trp262)	No
			Likely pathogenic (PVS1 + PM2)	No	No
			Pathogenic (PVS1 + PM2)	Yes PMID: 31264077	No
p.Ser155ArgfsTer10	20	16%	Pathogenic (PVS1 + PM2)	Yes PMID: 20358582	No
			Variant of uncertain significance (PP2 +PM2)	No	No
p.Asp172IlefsTer5	22	14%	Pathogenic (PVS1 + PM2)	Yes PMID: 36456122	Yes PMID: 24618615
p.Ile282MetfsTer15	62	23%	Likely pathogenic (PVS1 + PM2)	No	No
			Pathogenic (PVS1 + PS4 + PM2)	Yes PMID: 20358582	Yes PMID: 29262613

Supplementary Table 3 Continued

Sample	Ion AmpliSeq c.HGVS-*PRKAR1A*	Ion AmpliSeq p.HGVS-PRKAR1A	Ion AmpliSeq reads SNV	Ion AmpliSeq VAF-PRKAR1A	smMIP c.HGVS-*PRKAR1A*
	c.375G>A	p.Met125Ile	338	7%	
	c.38G>A	p.Arg13His	314	15%	
	c.547G>A	p.Asp183Asn	166	26%	
CM23	No variant detected				No variant detected
CM24	c.76_85dupAACATTCAAG	p.Ala29Glufs*19	6197	33%	c.76_85dupAACATTCAAG
	c.619delT	p.Tyr207Metfs*15	9709	38%	c.619delT

§ " Pathogenic" with score PVS1 + PM2 (+ PS4), and variant in Carney complex; " Likely pathogenic" with score PVS1 + PM2, but unknown variant in Carney complex; " variant of uncertain significance" with score PP2 + PM2

Frameshift mutations have been compared at the affected PRKAR1A amino acid position (column 4)

* This region was covered by < 100 reads

smMIP p.HGVS-PRKAR1A	smMIP reads SNV	smMIP VAF-PRKAR1A	Pathogenicity (ACMG scoring) §	Variant in Carney complex#	Variant in sporadic myxoma#
			Variant of uncertain significance (PP2 + PM2)	No	No
			Variant of uncertain significance (PP2 + PM2)	No	No
			Variant of uncertain significance (PP2 + PM2)	No	No
p.Ala29GlufsTer19	96	44%	Pathogenic (PVS1 + PM2)	Yes PMID: 20358582	No
p.Tyr207MetfsTer15	178	36%	Pathogenic (PVS1 + PM2)	Yes PMID: 20358582	No

Chapter 4

Myositis ossificans - Another condition with *USP6* rearrangement, providing evidence of a relationship with nodular fasciitis and aneurysmal bone cyst

Elise M Bekers, Astrid Eijkelenboom, Katrien Grünberg, Rona C Roverts, Jacky WJ de Rooy, Ingrid CM van der Geest, Joost M van Gorp, David Creytens, Uta Flucke

Ann Diagn Pathol. 2018 Jun;34:56-59

Abstract

Myositis ossificans is defined as a self-limiting pseudotumor composed of reactive hypercellular fibrous tissue and bone. *USP6* rearrangements have been identified as a consistent genetic driving event in aneurysmal bone cyst and nodular fasciitis. It is therefore an integral part of the diagnostic workup when dealing with (myo) fibroblastic lesions of soft tissue and bone. Two cases of myositis ossificans with *USP6* rearrangement were published so far. We determine herein the incidence of *USP6* rearrangement in myositis ossificans using *USP6* fluorescence in situ hybridization analysis (FISH). Of the 11 cases included, seven patients were female and four were male. Age ranged from 6 to 56 years (mean 27 years). Lesions were located in the thigh (n=5), knee (n=1), lower leg (n=1), lower arm (n=1), perineum (n=1), gluteal (n=1) and thoracic wall (n=1). All assessable cases except one (8/9) showed rearrangement of *USP6* providing evidence that myositis ossificans is genetically related to nodular fasciitis and aneurysmal bone cyst.

Introduction

Myositis ossificans is defined as a self-limiting pseudotumor composed of reactive hypercellular fibrous tissue and bone. This rapid growing and involuting lesion is mostly located in the skeletal muscle of the extremities or limb girdles of young patients and is usually interpreted as a posttraumatic lesion [1,2]. However, its cause is debated since its early description in 1892 [3].

The clinical characteristics depend on the developmental stage; the early phase is characterized by a painful swelling and within 6 weeks after onset it becomes more circumscribed and firm. Eventually, it evolves into a painless, well-demarcated hard lump with a diameter of ca. 3 to 6 cm [1].

Radiographically, soft tissue fullness is observed in the early stage. Subsequently, calcification becomes apparent with patchy and irregular densities maturing after approximately 6 weeks into a bony periphery with a radiolucent center [1].

The histological findings reflect those of the clinical symptoms and radiology. The early stage is characterized by nodular fasciitis-like features and additional development of woven bone terminally showing a prominent zonation with cancellous bone at the periphery [1,2]. In addition, entrapment of muscle fibers is often observed.

Since *USP6* rearrangement was identified as a consistent genetic driving event, initially in aneurysmal bone cyst (ABC) and later in nodular fasciitis as well, it is an integral part of diagnostic workup when dealing with (myo)fibroblastic lesions of soft tissue and bone [4-9].

Interestingly, two cases of myositis ossificans containing *USP6* rearrangements were published by Sukov et al and classified as being aneurysmal bone cysts of soft tissue [10].

We therefore set out to determine the incidence of *USP6* rearrangement in myositis ossificans using *USP6* fluorescence in situ hybridization analysis (FISH).

Material and Methods

The cases were retrieved from the authors' (referral) files. Clinical details were obtained from the referring physicians. The study was conducted in accordance with the Code of Conduct of the Federation of Medical Scientific Societies.

In all cases the tissue was fixed in 4% buffered formalin, routinely processed including decalcification, if needed, and embedded in paraffin; 2-4 µm thick sections were stained with hematoxylin and eosin.

USP6 FISH detection was performed on paraffin sections of 4µm. Slides were mounted and dried for 45 minutes at 55°C. They were deparaffinized in xylene for 5 minutes, rehydrated in ethanol (99,5%) and demineralized water. Pretreatment with 10mM Sodiumcitrate (pH=6.0) at 96°C for 10 minutes followed and after cooling down, rinsing in demineralized water. Slides were rinsed with 0,01 M HCL for 5 minutes and cells were digested by 200 U/ml pepsin (0,01M HCL) for 15 minutes at 37°C. To remove pepsin, slides were rinsed 3x shortly with 0,01M HCl and rinsed with PBS. Slides were fixated in 1% formaldehyde/PBS for 5 minutes. After that, slides were rinsed shortly with PBS and demineralized water and finally dehydrated in increasing ethanol series and are dried.

For the ISH staining, 10µl *USP6* (Kreatech, KBI-00094 split probe, Leica, Rijswijk, The Netherlands) was applied per pre-treated slide. The probe incubated area were covered with a cover glass and sealed with photo glue. The slides were denaturated at 80°C for 10 minutes and hybridization overnight at 37°C. After hybridization the slides were washed in 2xSSC at 42°C for 5 minutes to remove the cover glass, washed for 1x1 minutes and 1x2 minutes in 2xSSC-NP40 3% washbuffer at 73°C and rinsed with 2xSSC for 5 minutes (covered). Slides were dehydrated again in increasing ethanol series to demineralized water and are dried. Slides were covered with Vectashield mounting medium with DAPI (Vector, Brunschwig, Amsterdam, The Netherlands) and stored at 4°C.

USP6 signals were scored by two independent experienced technicians and considered positive if at least 20% of the 50 counted cells showed split signals. Slides were scored using a Leica DM4000 (Leitz) fluorescence microscope with a Leica DFC310 FX camera and LAS AF software.

As positive control, we included 10 samples of nodular fasciitis and 10 aneurysmal bone cysts.

Results

Clinical and FISH results are summarized in Table 1. Of the 11 patients included, seven were female and four were male. The age ranged from 6 to 56 years (mean 27 years). Lesions were located in the thigh (n=5), knee (n=1), lower leg (n=1), lower arm (n=1), perineum (n=1), gluteal (n=1) and thoracic wall (n=1).

Table 1. Clinical characteristics and FISH results

Case #	Sex/age	Site	*USP6* FISH (% of nuclei)
1	f/24	Perineum	>50
2	f/19	Lower leg	34
3	m/28	Lower arm	Failed
4	m/44	Thoracic wall	20
5	m/25	Thigh	25
6	f/17	Thigh	50
7	f/38	Thigh	30
8	f/32	Thigh	50
9	f/8	Knee	25
10	m/56	Thigh	<10
11	f/6	Gluteal	Failed

f, female; m, male

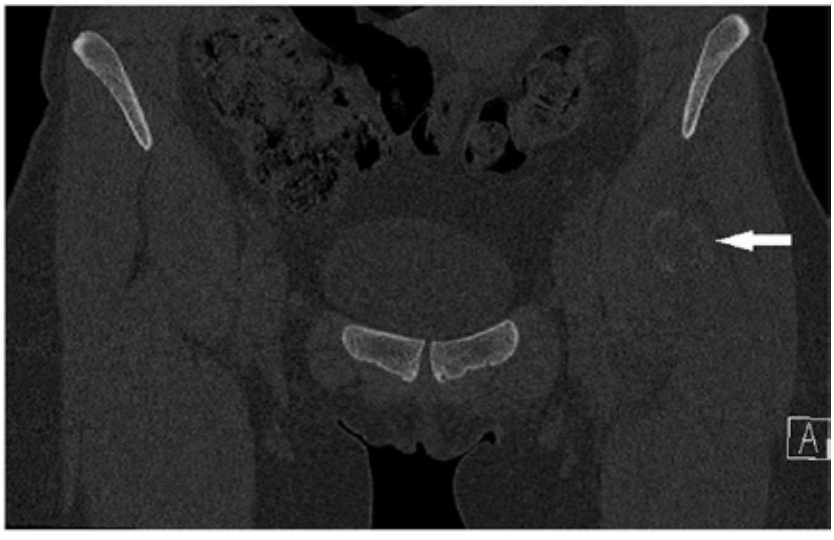

Figure 1. By CT, a diffuse swelling of the proximal rectus femoris muscle with faint peripheral calcifications was seen (Case 8).

By computed tomography, coronal reconstruction, bone window, a diffuse swelling of the proximal rectus femoris muscle with faint peripheral calcifications was seen (Case 8) (Figure 1). On MRI, TSE T2-weighted coronal image with fat saturation of the same patient showed a sharply delineated lesion with inhomogeneous high signal intensity with peripheral low signal intensity (Figure 2).

Six patients underwent resection, in the remaining patients, only a biopsy was taken until now.

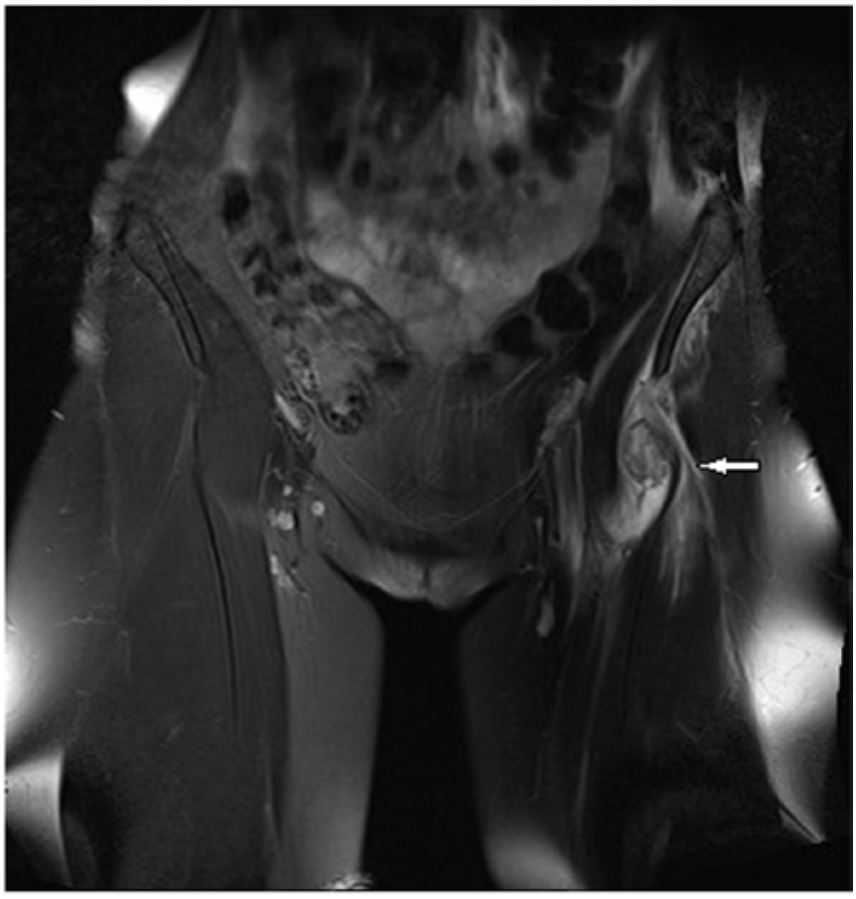

Figure 2. On MRI, a sharply delineated lesion with inhomogeneous high signal intensity with peripheral low signal intensity was observed.

Grossly, all lesions were located in the voluntary muscle. The resection specimens had an ill-defined, firm and grey-white appearance with gritty areas. Small cystic spaces were seen in one case (Case 3). Microscopically, the lesions showed an infiltrative

growth with entrapped muscle fibers. Nodular fasciitis-like areas with tissue culture-like myofibroblasts intermingled with woven bone maturating peripherally were seen in all cases. There was osteoblast rimming without atypia. Scattered around, osteoclastic giant cells in a varying number were observed (Figure 3). ABC-like pseudocystic spaces were present in only one case (Case 3, Figure 4).

Using FISH, *USP6* rearrangement were shown in eight out of 11 cases with one case being negative (<10% signals) (Figure 5). Two cases repeatedly failed for analysis, probably related to decalcified end stage areas (Table 1).

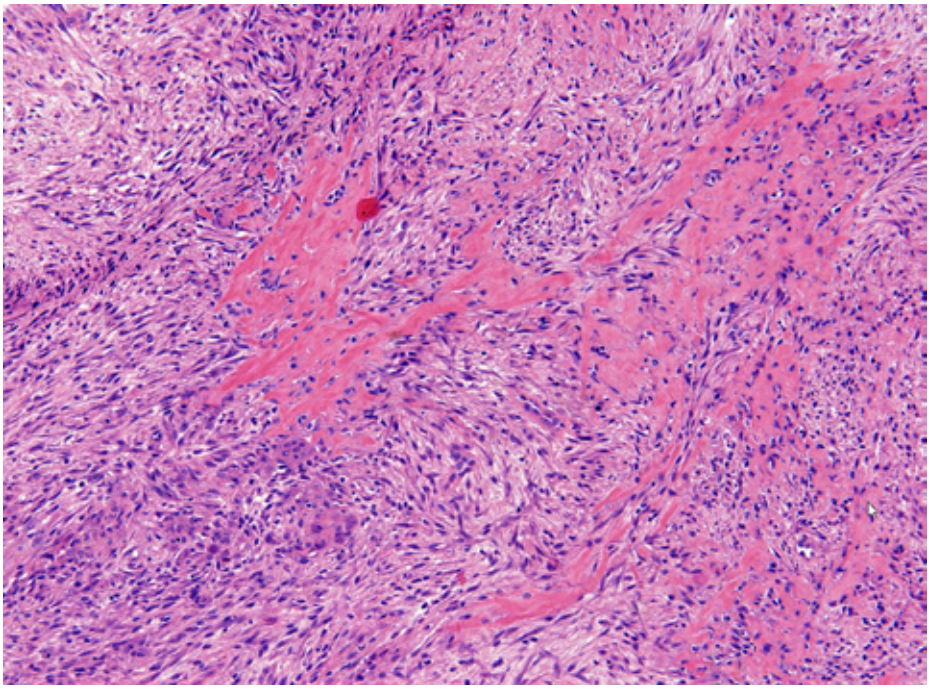

Figure 3. Classical features of myositis ossificans showing tissue culture-like myofibroblasts intermingled with woven bone were seen in all cases.

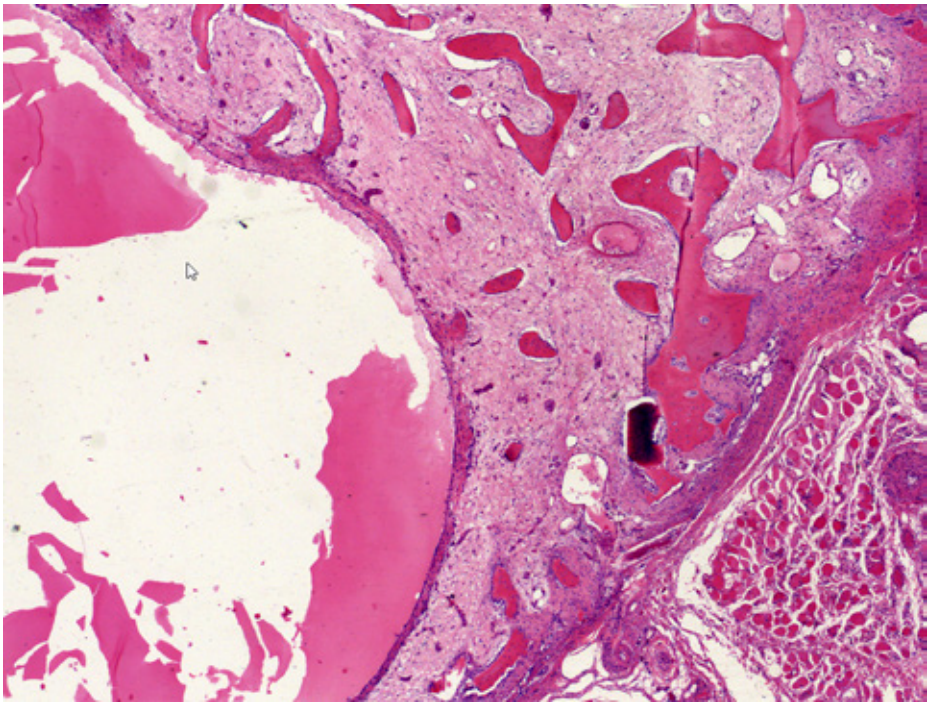

Figure 4. ABC-like pseudocystic spaces were present in case 3.

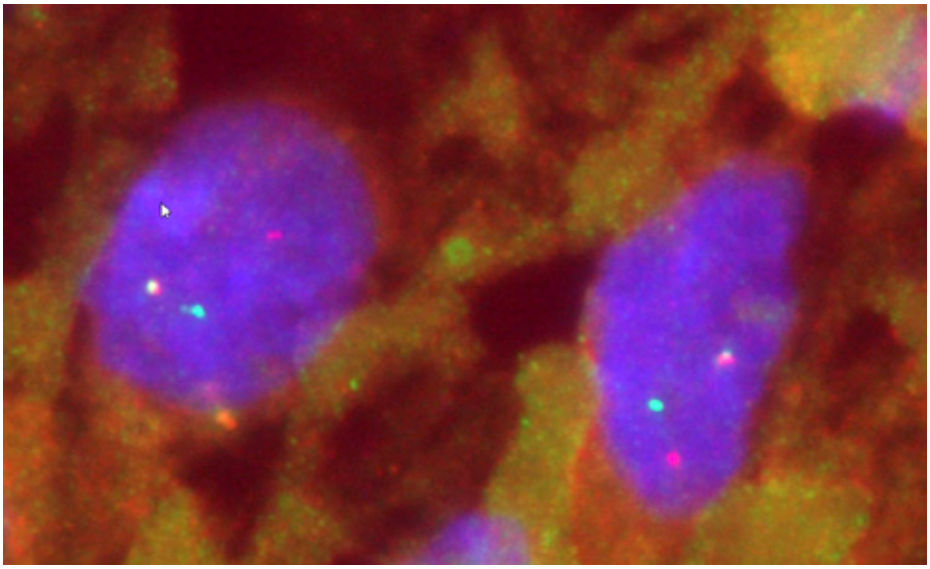

Figure 5. Using FISH, break apart signals of *USP6* were seen in 8/9 cases demonstrating rearrangement.

Discussion

Nodular fasciitis, myositis ossificans and aneurysmal bone cyst share clinicopathologic characteristics. First, they mainly occur in young patients. Second, the soft tissue lesions, nodular fasciitis and myositis ossificans, are of short duration with rapid growth and secondary involution, also called transient neoplasms [1,2,5,11,12].

All three entities are microscopically related by the presence of bland looking tissue culture like (myo)fibroblastic cells. Osteoclasts are mainly present in the two bone forming lesions and secondary pseudocystic changes are possible in all three neoplasms although they are most prominent in aneurysmal bone cyst, as expected. In exceptional cases, nodular fasciitis shows metaplastic bone formation, called fasciitis ossificans [1,2,11,12].

Another neoplasm clinicopathologically related to aneurysmal bone cyst is giant cell lesion of small bones [13].

The most convincing argument for these conditions forming a spectrum rather than distinct entities is the presence of *USP6* rearrangement (4,5,7,8,13]. This is supported by our study with rearrangement in eight out of nine cases (89%).

Interestingly, the presence of *USP6* rearrangement has also been described in a subset of cellular fibromas of the tendon sheath, retrospectively assigned to nodular fasciitis [14].

USP6 (ubiquitin specific protease) is one of deubiquinating enzymes involved in several cellular processes as intracellular trafficking, protein turnover, inflammatory signaling, and cell transformation [7,11]. It has been shown that the *USP6* fusion genes result in *USP6* overexpression due to promoter switch. This in turn leads to tumorigenesis, osteoblastic maturation, osteolysis, inflammation and neovascularisation [7]. Jak1-STAT3, c-Jun/AP-1 and Wnt signaling are the known involved pathways [15,16,18].

There is a variety of fusion partners described in ABC which are mainly functionally assigned to the fibroblastic-osteoblastic lineage (*CDH11,TRAP150, ZNF9, OMD, COL1A1, RUNX2, PAFAH1B1, CTNNB1, SEC31A, E1F1, FOSL2, STAT3*) [7,17]. The common *USP6* fusion partner of nodular fasciitis is *MYH9*, normally expressed in subcutaneous fibroblasts [7]. Recently found novel fusion genes are *RRBP1, CALU,*

MIR22HG, SPARC, THBS2, COL6A2 and *CTNNB1*. The latter in overlap with aneurysmal bone cyst [8].

What fusion genes are present in myositis ossificans remain to be elucidated as *USP6* FISH has been performed. From the literature it is known that one of the *USP6* rearranged cases of myositis ossificans showed a fusion with *COL1A1*. The other case was negative for *CDH11* [7,10].

The most important entity that myositis ossificans must be distinguished from is extraskeletal osteosarcoma. This very rare tumor shows histologically atypical neoplastic osteoblast-like cells with pleomorphic nuclei. The typical zonation of bone is absent [1].

Other benign fibro-osseous conditions which could be considered in the differential diagnosis are subungual exostosis, florid reactive periostitis, bizarre parosteal osteochondromatous proliferation, and fibro-osseous pseudotumor of digits. However, the clinicopathological features are different with occurrence usually in fingers and toes and absence of the bone zonation pattern [1].

Simple excision is the optimal treatment of myositis ossificans and recurrence is exceptional [2].

In conclusion, we have identified *USP6* rearrangements in a series of myositis ossificans cases. We therefore argue that this entity belongs to the group of clonal transient neoplasms also including nodular fasciitis and aneurysmal bone cyst.

References

1. Rosenberg AE. Pseudosarcomas of soft tissue. Arch Pathol Lab Med 2008;132:579-586.
2. Rosenberg AE, Oliveira AM. Myositis ossificans and fibro-osseous pseudotumour of digits. In Fletcher CDM, Bridge JA, Hogendoorn PCW, Mertens F (Eds.): WHO classification of tumours of soft tissue and bone. IARC:Lyon 2013; pp 50-51.
3. Taylor WJ. Myositis ossificans with a report of two cases – one traumatic, the other non-traumatic. Ann Surg 1903;37:825-833.
4. Oliveira AM, Hsi BL, Weremowicz S, Rosenberg AE, Dal Cin P, Joseph N, Bridge JA, Perez-Atayde AR, Fletcher JA. *USP6 (Tre2)* fusion oncogenes in aneurysmal bone cyst. Cancer Res 2004;64:1920-1923.
5. Erickson-Johnson MR, Chou MM, Evers BR, Roth CW, Seys AR, Jin L, Ye Y, Lau AW, Wang X, Oliveira AM. Nodular fasciitis: a novel model of transient neoplasia induced by *MYH9-USP6* gene fusion. Laboratory Investigation 2011; 91:1427-1433.
6. Amary MF, Hongtao Ye, Berisha F, Tirabosco R, Presneau N, Flanagan AM. Detection of *USP6* gene rearrangement in nodular fasciitis: an important diagnostic tool. Virchows Arch 2013;463:97-98.
7. Oliveira AM, Chou MM. USP6-induced neoplasms: the biologic spectrum of aneurysmal bone cyst and nodular fasciitis. Hum Pathol 2014;45:1-11.
8. Patel NR, Chrisinger JS, Demicco EG, Sarabia SF, Reuther J, Kumar E, Oliveira AM, Billings SD, Bovee JV, Roy A, Lazar AJ, Lopez-Terrada DH, Wang WL. *USP6* activation in nodular fasciitis by promotor-swapping gene fusions. Mod Pathol 2017; 30:1577-1588.
9. Li HR, Tai CF, Huang HY, Jin YT, Chen YT, Yang SF. *USP6* gene rearrangement differentiate primary paranasal sinus solid aneurysmal bone cyst from other giant cell-rich lesions, report of a rare case. Hum Pathol 2017.
10. Sukov WR, Franco MF, Erickson-Johnson M, Chou MM, Unni KK, Wenger DE, Wang X, Oliveira AM. Frequency of *USP6* rearrangements in myositis ossificans, brown tumor, and cherubism: molecular cytogenetic evidence that a subset of "myositis ossificans-like lesions" are the early phases in the formation of soft-tissue aneurysmal bone cyst. Skeletal Radiol 2008;37:321-327.
11. Lazar A, Evans HL, Oliveira AM. Nodular fasciitis. In Fletcher CDM, Bridge JA, Hogendoorn PCW, Mertens F (Eds.): WHO classification of tumours of soft tissue and bone. IARC:Lyon 2013; pp 46-47.
12. Nielsen GP, Fletcher JA, Oliveira AM. Aneurysmal bone cyst. In Fletcher CDM, Bridge JA, Hogendoorn PCW, Mertens F (Eds.): WHO classification of tumours of soft tissue and bone. IARC:Lyon 2013; pp348-349.
13. Agaram NP, LeLoarer FV, Zhang L, Hwang S, Athanasian EA, Hameed M, Antonescu CR. *USP6* gene rearrangements occur preferentially in giant cell reparative granulomas of the hands and feet but not in gnathic location. Hum Pathol 2014;45:1147-1152.
14. Carter JM, Wang X, Dong J, Westendorf J, Chou MM, Oliveira AM. *USP6* genetic rearrangements in cellular of fibroma of the tendon sheath. Mod Pathol 2016;29:865-869.
15. Madan B, Walker MP, Young R, Quick L, Orgel KA, Ryan M, Gupta P, Henrich IC, Ferrer M, Marine S, Roberts BS, Arthur WT, Berndt JD, Oliveira AM, Moon RT, Virshup DM, Chou MM, Major MB. *USP6* oncogene promotes Wnt signaling by deubiquitylating Frizzleds. Proc Natl Acad Sci U S A 2016;113:E2945-2954.
16. Quick L, Young R, Henrich IC, Wang X, Asmann YW, Oliveira AM, Chou MM. Jak1-STAT3 signals are essential effectors of the *USP6/TRE17* oncogene in tumorigenesis. Cancer Res 2016;76:5337-5347.

17. Guseva NV, Jaber O, Tanas MR, Stence AA, Sompallae R, Schade J, Fillman AN, Miller BJ, Bossler AD, Ma D. Anchored multiplex PCR for targeted next-generation sequencing reveals recurrent and novel *USP6* fusions and upregulation of *USP6* expression in aneurysmal bone cyst. Genes Chromosomes Cancer 2017;56:266-277.

18. Li L, Yang H, Li T, Feng J, Chen W, Ao L, Shi X, Lin Y, Liu H, Zheng E, Lin Q, Bu J, Zeng Y, Zheng, Xu Y, Liao Z, Lin J, He Y, Lin D. The ubiquitin-specific protease USP6 regulates the stability of the c-Jun protein. Mol Cell Biol 2018.

Chapter 5

Fibro-osseous pseudotumor of digits - Expanding the spectrum of clonal transient neoplasms harboring *USP6* rearrangement

Uta Flucke, Sarah J Shepard, Elise M Bekers, Roberto Tirabosco, Paul J van Diest, David Creytens, Joost M van Gorp

Ann Diagn Pathol. 2018 May 12;35:53-55.

Abstract

Fibro-osseous pseudotumors of the digits (FOPD) is a rare self-limiting lesion composed of bland looking hypercellular fibrous tissue and bone. *USP6* rearrangement is a consistent genetic finding in aneurysmal bone cyst, nodular fasciitis, myositis ossificans and giant cell lesions of small bones. We report herein the occurrence of *USP6* rearrangement in fibro-osseous pseudotumors of the digits using fluorescence in situ hybridization analysis (FISH). Of the five patients included, three were female and two were male. The age ranged from 33 to 72 years (mean 48 years). Lesions arose in the palm (n=2), thenar (n=1), middle finger (n=1) and great toe (n=1). All patients underwent resection. Four cases (80%) harbored *USP6* rearrangements showing that fibro-osseous pseudotumors of digits belongs to the spectrum of clonal transient neoplasms including aneurysmal bone cyst, nodular fasciitis, myositis ossificans and giant cell lesion of small bones.

Introduction

Fibro-osseous pseudotumor of digits (FOPD) is a very rare bone producing condition showing otherwise nodular fasciitis-like features. It originates in the soft tissue predominantly of the hands and more rarely of the wrist and feet. Fingers, especially the index finger are reported as preference sites. In comparison to other digital fibro-osseous lesions there is no primary relationship with the periosteum [1-6]. Although, the age range is broad the mean age is in the 4th decade. Precedent traumata were reported in only a subset of cases making a relationship uncertain [1-3]. Pain and swelling of short duration are the usual clinical symptoms [1-3,6]. Radiologically, a soft tissue mass with variable mineralization is seen, often with development of a peripheral bone rim depending on duration [2,3]. Attachment to the periosteum or osseous surface has been rarely observed most probably being a secondary phenomenon due to the close relationship of tissues at these sites [3].

Because of the clinicopathological features lesions were linked to myositis ossificans and interpreted as being reactive [1-5].

Recently, we identified *USP6* rearrangements in myositis ossificans [7]. This arose the question whether FOPD has corresponding genetic characteristics. We therefore analyzed FOPD cases using *USP6* fluorescence in situ hybridization analysis (FISH).

Material and Methods

The cases were retrieved from the authors' (referral) files. Clinical details were obtained from the referring physicians. The study was conducted in accordance with the Code of Conduct of the Federation of Medical Scientific Societies of the Netherlands, Great Britain and Belgium.

In all cases the tissue was fixed in 4% buffered formalin, routinely processed including decalcification, if needed, and embedded in paraffin; 2-4 µm thick sections were stained with hematoxylin and eosin.

USP6 FISH detection was performed on paraffin sections of 4µm. Slides were mounted and dried for 45 minutes at 55°C. They were deparaffinized in xylene for 5 minutes, rehydrated in ethanol (99,5%) and demineralized water. Pretreatment with 10mM Sodiumcitrate (pH=6.0) at 96°C for 10 minutes followed and after cooling down, rinsing in demineralized water. Slides were rinsed with 0,01 M HCL

for 5 minutes and cells were digested by 200 U/ml pepsin (0,01M HCL) for 15 minutes at 37°C. To remove pepsin, slides were rinsed 3x shortly with 0,01M HCl and rinsed with PBS. Slides were fixated in 1% formaldehyde/PBS for 5 minutes. After that, slides were rinsed shortly with PBS and demineralized water and finally dehydrated in increasing ethanol series and are dried.

For the ISH staining, 10µl *USP6* (Kreatech, KBI-00094 split probe, Leica, Rijswijk, The Netherlands) was applied per pre-treated slide. The probe incubated area were covered with a cover glass and sealed with photo glue. The slides were denaturated at 80°C for 10 minutes and hybridization overnight at 37°C. After hybridization the slides were washed in 2xSSC at 42°C for 5 minutes to remove the cover glass, washed for 1x1 minutes and 1x2 minutes in 2xSSC-NP40 3% washbuffer at 73°C and rinsed with 2xSSC for 5 minutes (covered). Slides were dehydrated again in increasing ethanol series to demineralized water and are dried. Slides were covered with Vectashield mounting medium with DAPI (Vector, Brunschwig, Amsterdam, The Netherlands) and stored at 4°C.

USP6 signals were scored by two independent experienced technicians and considered positive if at least 20% of the 50 counted cells showed split signals. Slides were scored using a Leica DM4000 (Leitz) fluorescence microscope with a Leica DFC310 FX camera and LAS AF software.

Positive controls were used throughout.

Results

Clinical and FISH results are summarized in Table 1. Of the five patients included, three were female and two were male. The age ranged from 33 to 72 years (mean 48 years). Lesions arose in the palm (n=2), thenar (n=1), middle finger (n=1) and great toe (n=1). All patients underwent resection.

Grossly, the resection specimens showed ill-defined (multi)nodular lesions with a firm grey-white appearance with gritty areas.

Microscopically, in all cases a (multi)nodular infiltrative proliferation of plump, tissue culture-like bland looking myofibroblasts was seen merging with osteoid and woven bone sometimes with maturating areas peripherally. There was osteoblast

rimming without atypia. Mitotic activity was readily identified. Osteoclast-like giant cells were variably present in all cases (Figure 1).

Using FISH, *USP6* rearrangements were observed in four out of the five cases (Table 1, Figure 2).

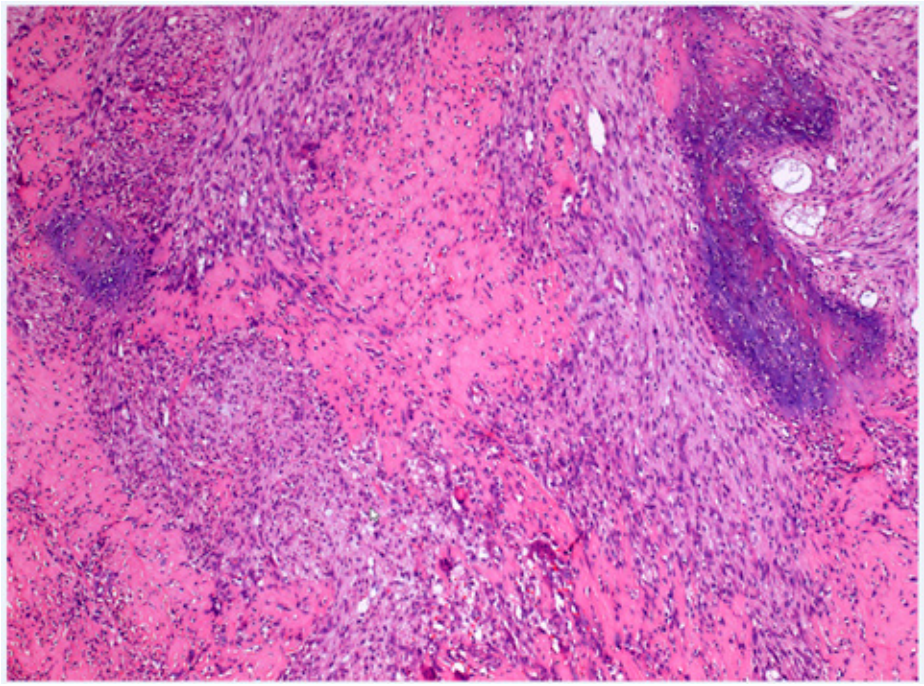

Figure 1. Classical features of FOPD showing tissue culture-like myofibroblasts merged with osteoid and woven bone were seen in all cases (Case 3).

Table 1. Clinical characteristics and FISH results

Case #	Sex/age	Site	*USP6* FISH (% of nuclei)
1	f/45	Palm	23
2	m/50	Palm	21
3	m/42	Great toe	22
4	f/33	Middle finger	30
5	f/72	Thenar	<10

f, female; m, male

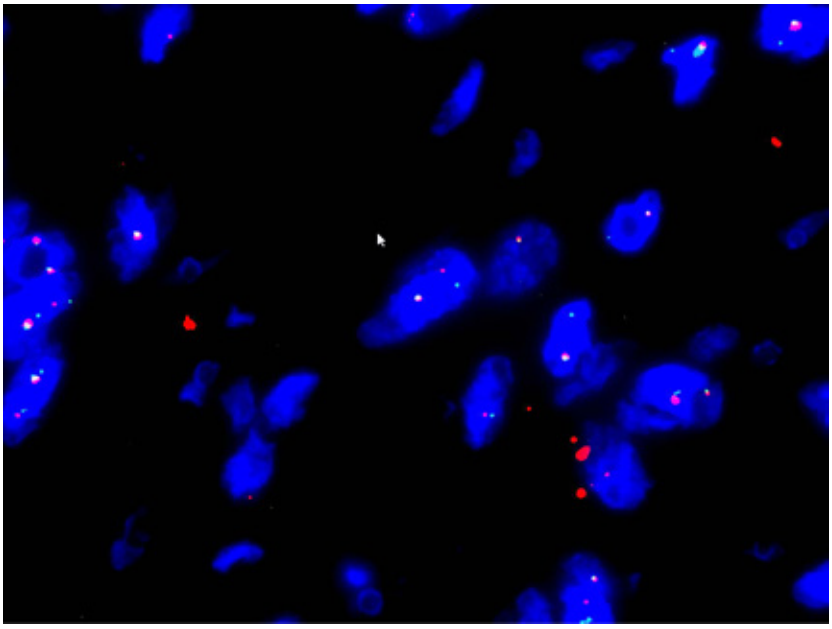

Figure 2. Using FISH break apart, signals of *USP6* were observed in 4/5 cases demonstrating rearrangement (Case 3).

Discussion

Fibro-osseous pseudotumor of digits is defined as a classic pseudosarcomatous lesion usually occurring in the superficial soft tissue of the fingers, especially on the proximal phalanx region, and less frequently on the toes [1-6]. It shares clinicopathological and especially genetic characteristics with nodular fasciitis, myositis ossificans, aneurysmal bone cyst and giant cell lesion of small bones [5,7-12]. These myofibroblastic tissue culture-like and variable bone-producing lesions are transient neoplasms with short duration, rapid growth and secondary involution [7,12]. Pseudocystic changes are most often present in aneurysmal bone cysts and more rarely in myositis ossificans, which is sometimes referred by some authors as aneurysmal bone cyst of soft tissue [7,13,14].

Osteoid and woven bone formations in FOPD are haphazardly distributed with sporadic occurrence of a zonation pattern as seen in myositis ossificans [1,2,6]

In contrast to the initial large FOPD series by Dupree and Enzinger in 1986, Chaudhry et al [6] discussed a more variable anatomic distribution emphasizing the morphological overlap within the above mentioned soft tissue lesions.

The presence of *USP6* rearrangements, the genetic hallmark of all of these neoplasms underpins that they are biologically related [7-12], although the fusion partner of *USP6* in the mentioned lesions is usually different with *CDH11* and *MYH 9* being the most common in aneurysmal bone cysts and nodular fasciitis, respectively [12]. What genetic partners are present in FOPD and whether there is overlap with the other related conditions need to be investigated.

The detection of *USP6* rearrangement can be useful for diagnostic purposes when interpretation of immature bone is challenging because of lack of the bone architecture with peripheral maturation and osteoblast rimming especially in small biopsies [4,7].

Other acral fibro-osseus soft tissue lesions as florid reactive periostitis, subungual exostosis and bizarre parosteal osteochondromatous proliferation (Nora's lesion) are differential diagnoses. These lesions in contrast develop on the surfaces of small bones and share with FODP rapid growth and the nodular fasciitis-like appearance with mineralization, haphazardly arranged woven bone. The fibrous component is usually most prominent at the periphery and overlies cellular hyaline cartilage that undergoes enchondral ossification at its base which is different from FODP [4].

The known genetic changes in Nora's lesion are a t(1;17) translocation [15] and in subungual exostosis a t(X;6) leading to rearrangements of *COL12A1* and *COL4A5* [16-18].

The diagnosis of extraosseous or surface osteosarcoma is of paramount importance because of the clinical consequences demanding neoadjuvant chemo- and/or radiotherapy and extended surgery. However, these tumortypes are extremely rare at acral sites and severe cytological atypia along with more aggressive features on imaging, would lead to the correct diagnoses in most cases [1,4,6].

Synovial sarcoma may also originate at acral sites and may produce bone, however these tumors consist of cellular fascicles of monomorphic spindle cells with elongated nuclei in its monophasic fibrous form. Furthermore, the immunoprofile with positivity for EMA and keratins and the X;18 translocation with SS18-SSX1/2 is specific for this malignant tumor [19].

Prognosis of FOPD is excellent with recurrence in exceptional cases. Complete excision is the treatment of choice [1-3].

In conclusion, we have identified *USP6* rearrangements in a series of fibro-osseous pseudotumors of the digits. We therefore argue that this entity belongs to the group of clonal transient neoplasms also including nodular fasciitis, myositis ossificans, aneurysmal bone cyst and giant cell lesion of small bones. *USP6* FISH can be helpful when considering malignancy on clinicopathological grounds.

References

1. Dupree WB, Enzinger FM. Fibro-osseous pseudotumor of the digits. Cancer 1986; 58:2103-2109.
2. De Silva MV, Reid R. Myositis ossificans and fibroosseous pseudotumor of digits: a clinicopathological review of 64 cases with emphasis on diagnostic pitfalls. Int J of Surg Pathol 2003;11:187-195.
3. Moosavi CA, Al-Nahar LA, Murphey MD, Fanburg-Smith JC. Fibroosseous pseudotumor of the digit: a clinicopathologic study of 43 new cases. Ann Diagn Pathol 2008;12:21-28.
4. Rosenberg AE. Pseudosarcomas of soft tissue. Arch Pathol Lab Med 2008;132:579-586.
5. Rosenberg AE, Oliveira AM. Myositis ossificans and fibro-osseous pseudotumour of digits. In Fletcher CDM, Bridge JA, Hogendoorn PCW, Mertens F (Eds.): WHO classification of tumours of soft tissue and bone. IARC:Lyon 2013; pp 50-51.
6. Chaudhry IH, Kazakov DV, Michal M, Mentzel T, Luzar B, Calonje E. Fibro-osseous pseudotumor of the digit: a clinicopathological study of 17 cases. J Cutan Pathol 2010;37:323-329.
7. Bekers EM, Eijkelenboom A, Grünberg K, Roverts RC, de Rooy JW, van der Geest IC, van Gorp JM, Creytens D, Flucke U. Myositis ossificans – another condition with USP6 rearrangement, providing evidence of a relationship with nodular fasciitis and aneurysmal bone cyst. Ann Diagn Pathol 2018;34:56-59.
8. Oliveira AM, Hsi BL, Weremowicz S, Rosenberg AE, Dal Cin P, Joseph N, Bridge JA, Perez-Atayde AR, Fletcher JA. *USP6 (Tre2)* fusion oncogenes in aneurysmal bone cyst. Cancer Res 2004;64:1920-1923.
9. Erickson-Johnson MR, Chou MM, Evers BR, Roth CW, Seys AR, Jin L, Ye Y, Lau AW, Wang X, Oliveira AM. Nodular fasciitis: a novel model of transient neoplasia induced by *MYH9-USP6* gene fusion. Laboratory Investigation 2011; 91:1427-1433.
10. Amary MF, Hongtao Ye, Berisha F, Tirabosco R, Presneau N, Flanagan AM. Detection of *USP6* gene rearrangement in nodular fasciitis: an important diagnostic tool. Virchows Arch 2013;463:97-98.
11. Agaram NP, LeLoarer FV, Zhang L, Hwang S, Athanasian EA, Hameed M, Antonescu CR. *USP6* gene rearrangements occur preferentially in giant cell reparative granulomas of the hands and feet but not in gnathic location. Hum Pathol 2014;45:1147-1152.
12. Oliveira AM, Chou MM. USP6-induced neoplasms: the biologic spectrum of aneurysmal bone cyst and nodular fasciitis. Hum Pathol 2014;45:1-11.
13. Nielsen GP, Fletcher CD, Smith MA, Rybak L, Rosenberg AE. Soft tissue aneurysmal bone cyst: a clinicopathological study of five cases. Am J Surg Pathol 2002;26:64-69.
14. Sukov WR, Franco MF, Erickson-Johnson M, Chou MM, Unni KK, Wenger DE, Wang X, Oliveira AM. Frequency of *USP6* rearrangements in myositis ossificans, brown tumor, and cherubism: molecular cytogenetic evidence that a subset of "myositis ossificans-like lesions" are the early phases in the formation of soft-tissue aneurysmal bone cyst. Skeletal Radiol 2008;37:321-327.
15. Endo M, Hasegawa T, Tashiro T, Yamaguchi U, Morimoto Y, Nakatani F, Shimoda T. Bizarre parosteal osteochondromatous proliferation with a t(1;17) translocation. Virchows Arch 2005;447:99-102.
16. Zambrano E, Nose V, Perez-Atayde AR, Gebhardt M, Hresko MT, Kleinman P, Richkind KE, Kozakewich HP. Distinct chromosomal rearrangement in subungual (Duuytren) exostosis and bizarre parosteal osteochondromatous proliferation (Nora lesion). Am J Surg Pathol 2004;28:1033-1039.
17. Nilsson M, Domanski HA, Mertens F, Mandahl N. Molecular cytogenetic characterization of recurrent breakpoints in bizarre parosteal osteochondromatous proliferation (Nora's lesion). Hum Pathol 2004;35:1063-1069.

18. Storlazzi CT, Wozniak A, Panagopoulos I, Sciot R, Mandahl N, Mertens F, Debiec-Rychter M. Rearrangement of the COL12A1 and COL4A5 genes in subungual exostosis: molecular cytogenetic delineation of the tumor-specific translocation t(X;6)(q13-14;q22). Int J Cancer 2006;118:1972-1976.

19. Suurmeijer AJH, de Bruijn D, Geurts van Kessel A, Miettinen MM. Synovial sarcoma. In Fletcher CDM, Bridge JA, Hogendoorn PCW, Mertens F (Eds.): WHO classification of tumours of soft tissue and bone. IARC:Lyon 2013; pp 213-215.

Chapter 6

Soft tissue angiofibroma: Clinicopathologic, immunohistochemical and molecular analysis of 14 cases

Elise M Bekers, Patricia JTA Groenen, Marian AJ Verdijk, Winny L Raaijmakers-van Geloof, Paul Roepman, Robert Vink, Natalie DB Gilhuijs, Joost M van Gorp, Judith VMG Bovée, David H Creytens, Adrienne M Flanagan, Albert JH Suurmeijer, Thomas Mentzel, Elsa Arbajian, Uta Flucke

Genes Chromosomes Cancer. 2017 Oct;56(10):750-757.

Abstract

Soft tissue angiofibroma is rare and has characteristic histomorphological and genetic features. For diagnostic purposes, there are no specific antibodies available. Fourteen lesions (6 females, 8 males; age range 7-67 years) of the lower extremities (12) and trunk (2) were investigated by immunohistochemistry, including for the first time *NCOA2*. *NCOA2* was also tested in a control group of other spindle cell lesions. The known fusion-genes (*AHRR-NCOA2* and *GTF2I-NCOA2*) were examined using RT-PCR in order to evaluate their diagnostic value. Cases in which no fusion gene was detected were additionally analysed by RNA sequencing. All cases tested showed nuclear expression of *NCOA2*. However, this was not specific since other spindle cell neoplasms also expressed this marker in a high percentage of cases. Other variably positive markers were EMA, SMA, desmin and CD34. STAT6 was negative in the cases tested. By RT-PCR for the most frequently observed fusions, an *AHRR-NCOA2* fusion transcript was found in 9/14 cases. *GFT2I-NCOA2* was not detected in the remaining cases (n53). RNA sequencing revealed three additional positive cases; two harbored a *AHRR-NCOA2* fusion and one case a novel *GAB1-ABL1* fusion. Two cases failed molecular analysis due to poor RNA quality. In conclusion, the *AHRR-NCOA2* fusion is a frequent finding in soft tissue angiofibroma, while *GTF2I-NCOA2* seems to be a rare genetic event. For the first time, we report a *GAB1-ABL1* fusion in a soft tissue angiofibroma of a child. Nuclear expression of *NCOA2* is not discriminating when compared with other spindle cell neoplasms.

Introduction

Soft tissue angiofibroma (STAF), a recently defined benign soft tissue tumor entity, is rare and has characteristic histomorphological and genetic features with a recurrent chromosomal translocation t(5;8)(p15;q13), resulting in a consistent rearrangement of *NCOA2* in a subset of cases [1,2]. The histologic diagnostic clue is a prominent vascular network consisting mainly of uniform small vessels [1]. However, this feature may not be convincing in cellular areas. Moreover, myxoid change in other soft tissue lesions, such as solitary fibrous tumor (SFT) or cellular angiofibroma, can also reveal a prominent vasculature with small branching vessels [3-5], rendering diagnosis of STAF somewhat uncertain.

Chimeric fusion proteins represent targets for potential tumor-specific diagnostic immunohistochemistry assays. Examples of a robust immunohistochemical assays include antibodies for *STAT6* in SFT showing nuclear relocation due to fusion with *NAB2* [6,7] and *CAMTA* for epithelioid hemangioendothelioma, which is upregulated due to the fusion with the promotor of the *WWTR1* gene [8,9].

Possible aberrant expression of *NCOA2* (nuclear receptor co-activator 2) as a consequence of the involvement in the STAF fusion protein could be a novel diagnostic target as there is no specific immunohistochemical marker for STAF so far [1].

Molecular analysis is an additional diagnostic adjunct, especially in biopsies of tumor types without a specific immunohistochemical profile but with tumor-related therapeutic consequences (e.g., myxoid liposarcoma, another potential mimic of STAF) [1,10-12].

The aim of our work was to examine the diagnostic value of STAFs known fusion genes (*AHRR-NCOA2* and *GTF2I-NCOA2*) by studying their occurrence in a cohort of 14 lesions using RT-PCR for the most frequent reported fusions and RNA sequencing. In addition, we examined immunohistochemically the expression of *NCOA2* in STAF and other benign and malignant spindle cell tumors to determine if it could be a potential immunohistochemical marker for STAF.

Methods

Cases were collected from the authors' files or referral files and reviewed. Clinical information, including follow-up, was obtained from the referring clinicians. The

study was conducted in accordance with the Code of Conduct of the Federation of Medical Scientific Societies. The tissues of all samples were formalin fixed and paraffin embedded; 2-4 µm thick sections were performed. Slides were hematoxylin and eosin stained. Immunohistochemistry was done by the Brightvision technique (Immunologic, The Netherlands). Antibodies are listed in Table 1. Appropriate positive and negative controls were used.

Table 1. Details of used antibodies

Antibody	Clone	Dilution	Source
NCOA2	Polyclonal	1:1600	ITK Diagnostics BV, Uithoorn, The Netherlands
STAT6	YE361	1:80	Abcam, Cambridge, UK
CD34	QBEnd/10	1:80	Immunologic, Duiven, The Netherlands
EMA	E29	1:250	DAKO, Glostrup, Denmark
SMA	1A4	1:30000	Sigma, Saint Louis, USA
S100	Polyclonal	1:10000	DAKO, Glostrup, Denmark
Desmin	Clone33	1:100	Klinipath BV, Duiven, The Netherlands
Pan-CK	MNF116	1:500	DAKO, Glostrup, Denmark
Pan-CK	AE1/3	1:50	Immunologic, Duiven, The Netherlands

Table 2. NCOA2 staining in other soft tissue tumors including mimics

Tumortype	Nuclear NCOA2 expression
Intramuscular myxoma	3/4
Juxtaarticular myxoma	1/1
Odontogenic myxoma	1/1
Myxoid liposarcoma	6/6
Myxofibrosarcoma	6/6*
Cellular angiofibroma	3/3
LGFMS	2/2
Solitary fibrous tumor	10/14
Mesenchymal chondrosarcoma	1/1
Schwannoma	5/5
MPNST	2/4
GIST	5/5
Leiomyoma	6/6 (<50%)

* one case only partly positive (< 50%)

LGFMS, low-grade fibromyxoid sarcoma; MPNST, malignant peripheral nerve sheath tumor; GIST, gastrointestinal stroma tumor

We included a group of 58 cases consisting of mimics of STAF, as listed in Table 2. Cases were scored positive when at least 50% of the tumor cell nuclei showed a strong immunoreactivity. A seminoma was used as positive control as proposed by the manufacturer.

Reverse transcriptase-Polymerase chain reaction (RT-PCR)

According to standard procedures, RNA was extracted using RNA-Bee-RNA isolation reagent (Bio-Connect BV, Huissen, the Netherlands). Quantity and quality were determined by NanoDrop measurement (Fisher Scientific, Landsmeer, the Netherlands). cDNA synthesis was conducted using Superscript II (Invitrogen Life Technologies Europe, Bleiswijk, the Netherlands) and random hexamers (Promega Nederland, Leiden, the Netherlands).

The cDNA was tested by RT-PCR for the *HMBS* (hydroxymethylbilase synthase) housekeeping gene using the following primers forw150 5′-TGCCAGAGAAGAGTGTGGTG-3′, rev150 5′-ATGATGGCACTGAACTCCTG-3′, forw250 5′- CTGGTAACGGCAATGCGGCT-3′, rev250 5′- TTCTTCTCCAGGGCATGTTC-3′.

For detection of the *AHRR-NCOA2* fusion t(5;8)(p15;q13), the following primers were used for *AHRR* (at 5p15, accession number NM 020731.1) forward primers P928 (exon 9): CCGCAGCGGAGATGAAAATG and P930 (exon 10): GTAAAAGCCACCACCAGTCTG. For *NCOA2* (at 8q13, accession number NM 006540.2) reverse primers P929 (exon 16): CAAGTCATCTGGAGAACTGC, P931 (exon 14): CCATTCTCCAGATGGCATAG were used.

For the detection of the *GTF2I-NCOA2* fusion, resulting from the t(7;8)(q11;q13), forward primers 1380 (GACCAAAGGCCAATGAGCTA, exon 13) and 1436 (AAGCGGAAAGTGAGGGAGTT, exon 13) for *GTF2I* and reverse primers 3368 (GCAGGATGTGGACATAGCAA, exon 16) and 3402 (CAGGAGAGCTCCCTCATCAC, exon 16) for *NCOA2* were used.

For the detection of the *GAB1-ABL1* fusion, forward primer 1913 (CGTGGATAGGAACCTCAAGC, exon 6) and reverse primer 689 (GGTTGGGGTCATTTTCACTG, exon 2) were used.

PCR products were evaluated by agarose gel electrophoresis. The sequence of the differently sized PCR-products was obtained using Sanger sequencing.

Negative controls for RT-PCR were 1 myxofibrosarcoma, 1 spindle cell liposarcoma, 1 solitary fibrous tumor, 1 dedifferentiated liposarcoma. For positive control of the *GTF2I-NCOA2* fusion see Arbajian et al [13].

RNA sequencing

mRNA with DV200 values >40 could be extracted from 5 FFPE blocks using Qiagen's RNeasy FFPE Kit (Qiagen, Valencia, CA, USA), as described [14]. mRNA libraries were prepared from 20-50 ng of RNA, depending on the DV200 value, using the capturing chemistry of the TruSeq RNA Access Library Prep Kit (Illumina). Paired-end 85 nt reads were generated from the mRNA libraries on a NextSeq 500 (Illumina). Sectioning, RNA extraction, library preparation, sequencing and bioinformatic analysis were performed as described [14].

ChimeraScan and FusionCatcher, using default settings, were used to identify candidate fusion transcripts from the sequence data [15, 16]. The GRCh37/hg19 build was used as the human reference genome.

Results

Clinical data

Clinical data are presented in Table 3. Of the fourteen patients, six were female and eight were male. The age ranged from 7 to 67 years (median 50 years; mean 49 years). Anatomical sites were upper leg (five), knee (four), lower leg (one), foot (two), upper back (one) and flank (one). Seven neoplasms were located subcutaneously, three in muscle and two deep to the fascia. In the two lesions of the foot, the anatomic plane was difficult to asses. Magnetic resonance imaging (MRI) of case 6 showed a juxta-articular, sharply demarcated lesion of the knee that had a diffuse iso-intense signal in T1 and a hyperintense pattern in T2 (Figure 1). All lesions were completely excised. Follow-up information, available for 10 patients, ranged from 3 months to 4 years (median interval 2 years and 3 months). There was no evidence of disease in any of the cases.

Table 3. Clinical data

Case	sex/age	localization	size (cm)	Resection status	Follow up
1	m/46 y	knee, sc	1.6	R0	NED, 2 years
2	m/45 y	upper leg, im	4.0	R0	NED, 2.5 years
3	f/52 y	upper leg, im	3.0	R0	NED, 1 year
4	f/42 y	upper leg, sc	3.5	R0	NED, 3.5 years
5	m/62 y	upper back, sc	3.5	R0	NED, 3.5 years
6	f/56 y	knee, sf	5.0	R0	NED, 3.5 years
7	f/63 y	knee, sc	4.0	R0	NED, 4 years

Table 3. Continued

Case	sex/age	localization	size (cm)	Resection status	Follow up
8	m/67 y	upper leg, sc	4.3	R0	NED, 3 months
9	m/49y	dorsal foot	1.4	R0	NA
10	m/56y	lower leg, sc	2.2	R0	NA
11	f/48y	flank, sc	3.7	R0	NED, 10 months
12	m/61y	knee, sf	8.7	R0	NA
13	f/36y	upper leg, im	7.0	R0	NA
14	m/7y	foot	2.0	2.0	NED, 4 months

M, male; f, female; y, year; sc, subcutaneous; im, intramuscular; sf, subfascial, NED, no evidence of disease; NA, not available

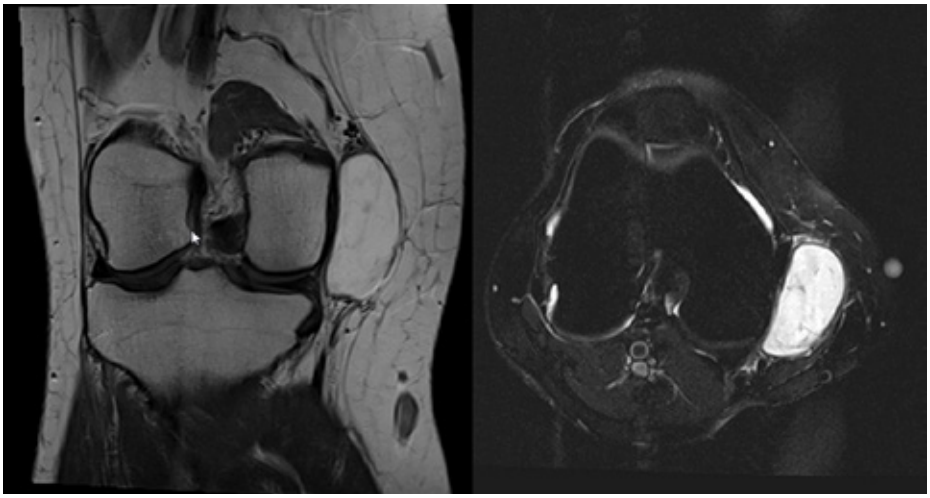

Figure 1. MRI of case 6 showed a juxta-articular, sharply demarcated lesion that had a diffuse isointense signal in T1 and a hyperintense pattern in T2.

Gross findings

Most of the tumors were well-circumscribed and (multi)nodular; the size ranged from 1.6 – 8.7 cm (mean 3.9 cm). The cut surface appeared solid, white to yellow-tan and glistening.

Histological findings

Ten neoplasms were sharply demarcated and surrounded by a pseudocapsule (Figure 2). Infiltration into fat, striated muscle and connective tissue were seen in the remaining four cases.

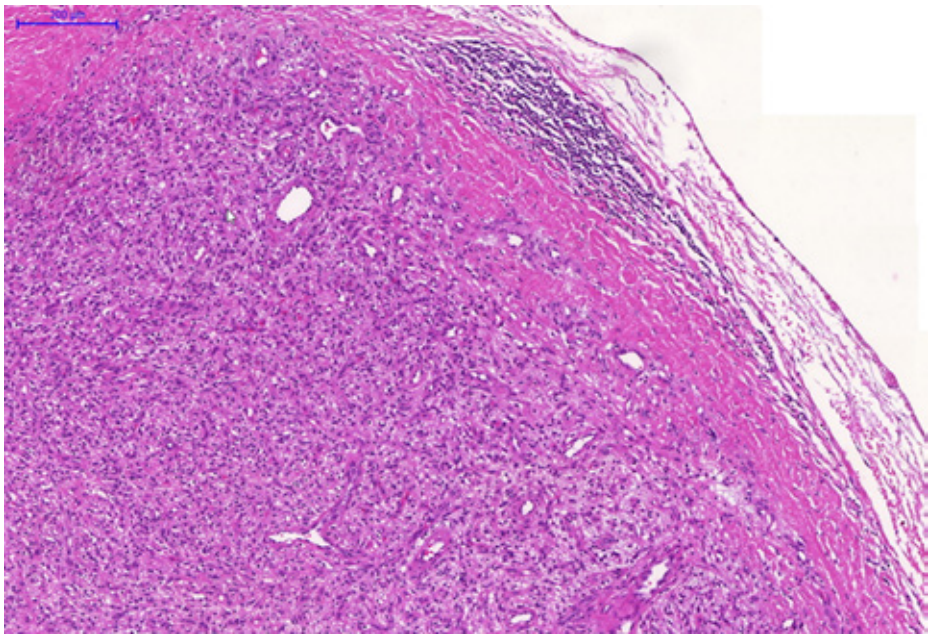

Figure 2. Most tumors were well-circumscribed and surrounded by a pseudocapsule.

Most lesions showed variable cellularity (Figures 3-5) with predominantly low cellularity in three tumors. Neoplasms were composed of haphazardly arranged, bland-looking spindle cells. Nuclei were round to oval or tapering with somewhat histiocytoid appearance (Figures 4 and 5). In some cases, prominent nucleoli were seen. Binucleated cells were obvious in four cases (cases 1, 3, 4 and 5). Mitoses did not exceed 1 per 10 high power fields. The cytoplasm was inconspicuous. There was no atypia. All cases possessed a prominent, evenly distributed network of small blood vessels (Figures 2- 5). In addition, larger hemangiopericytoma-like vessels were seen in eight cases (Figure 3). The background consisted of fine collagen bundles and was myxoid in the poor cellular areas. In few cases

hyalinization was focally observed. Thick collagen bundles were present in cases 2, 10 and 11 (Figure 6) and inclusion of mature adipocytes was a feature of four cases (5, 7, 10, 11) (Figure 7). Case 14, remarkable because of a novel fusion gene (see below), showed a similar morphology with variable cellularity, bland-looking fibroblasts and a prominent network of capillaries and in some areas larger hemangiopericytoma-like vessels (Figure 8).

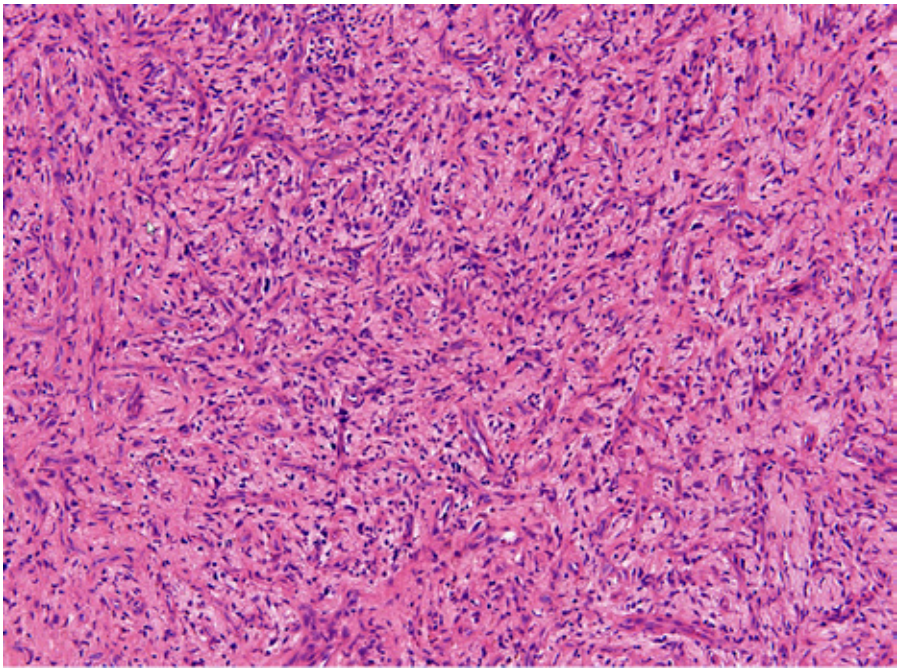

Figure 3. A prominent complex vascular network with medium-sized and small thin-walled vessels were characteristic.

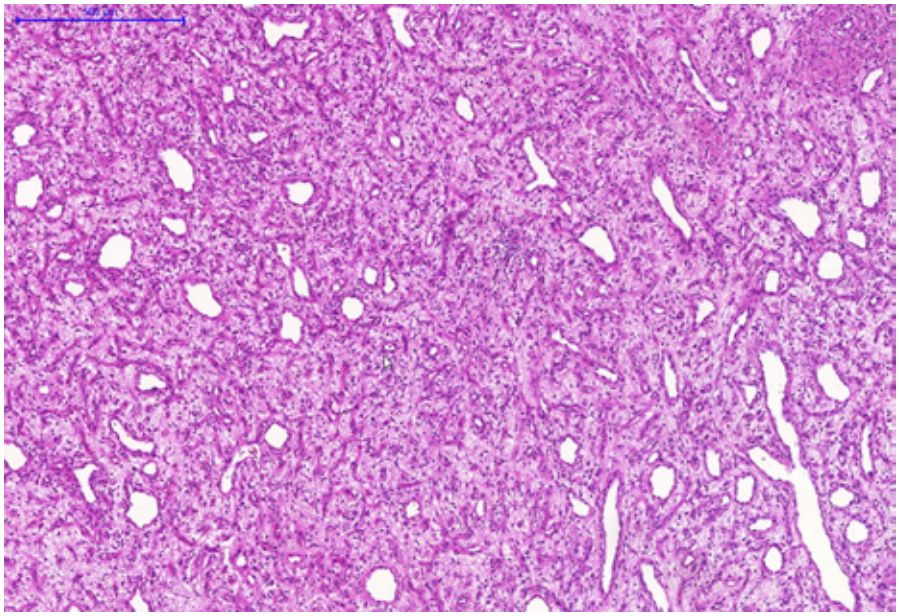

Figure 4. Innumerable uniform branching vessels were seen in all lesions.

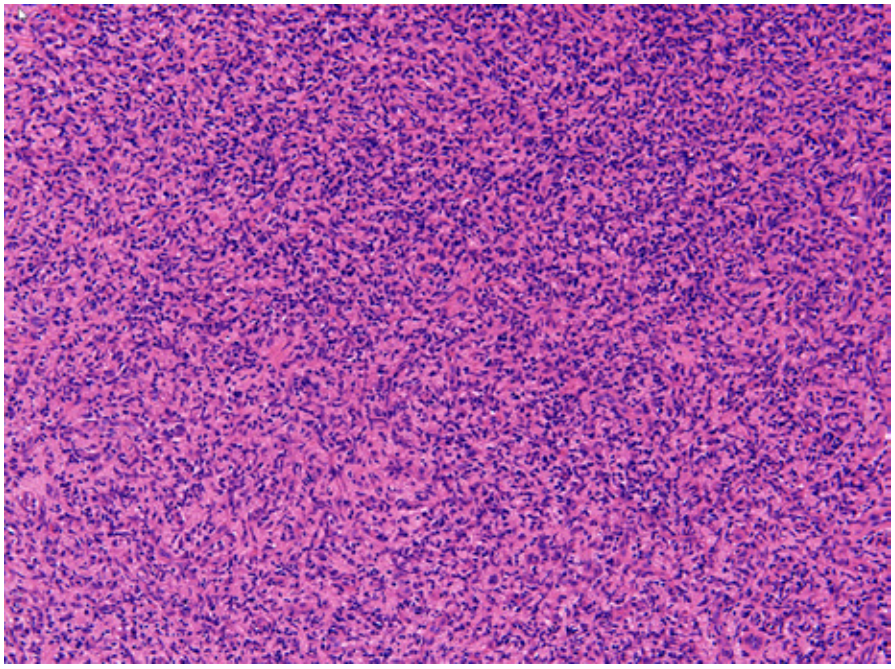

Figure 5. In cellular aras, the vessels were more inconspicuous.

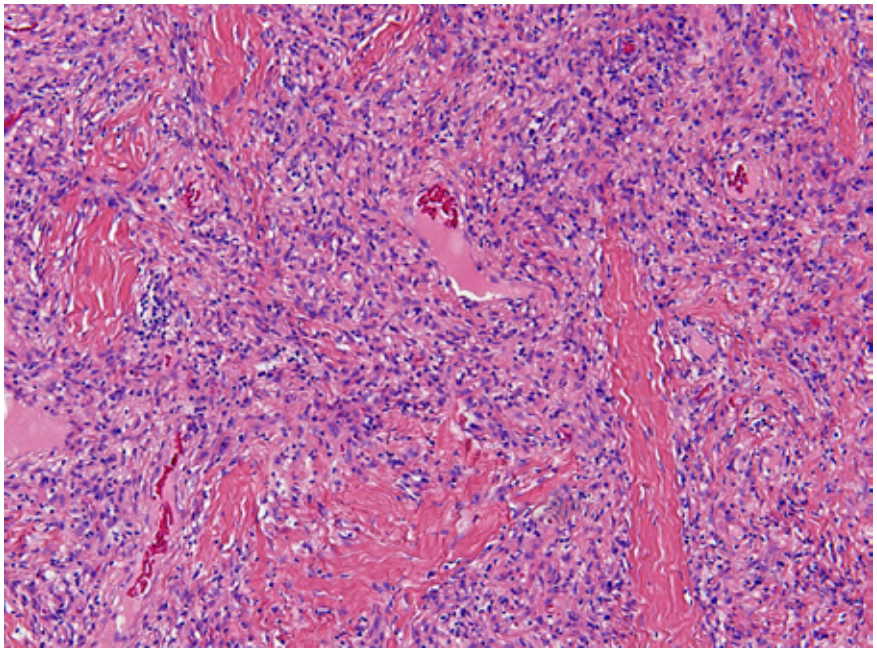

Figure 6. Thick collagen bundles were seen in Case 2.

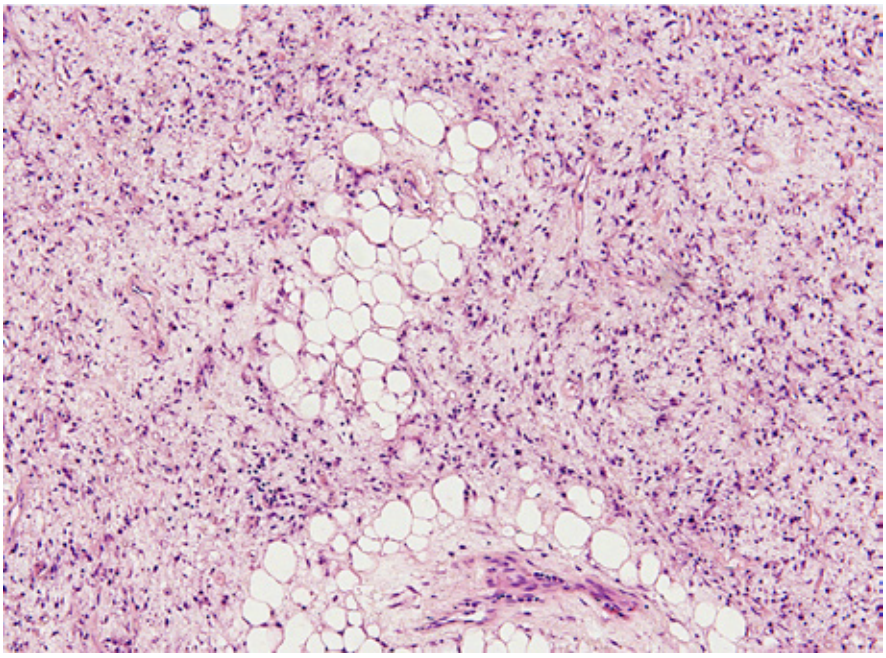

Figure 7. Inclusion of mature adipocytes can be present (Case 5).

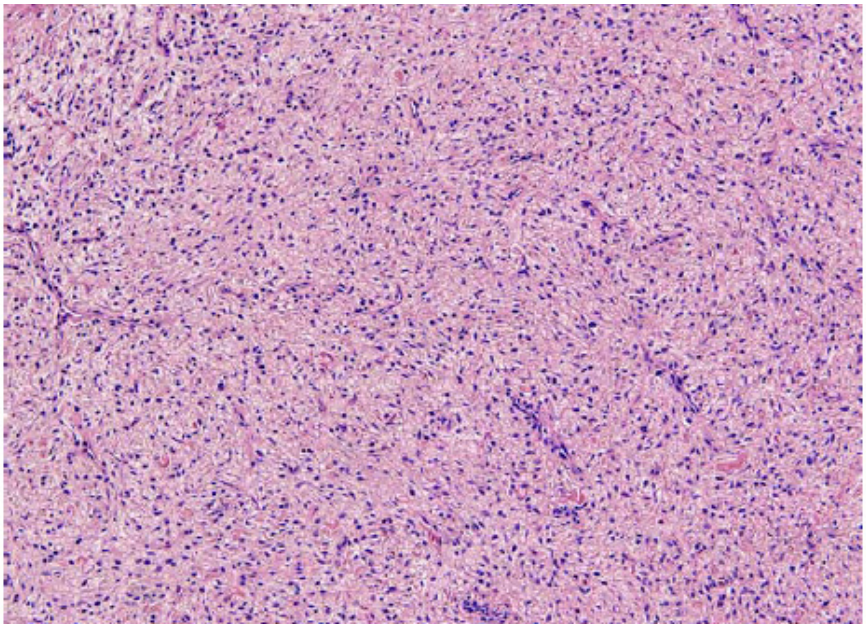

Figure 8. Case 14 was remarkable for its novel *GAB1-ABL1* fusion showed a typical morphology.

Immunohistochemical findings

The results are shown in Table 4. Nine cases tested showed nuclear staining for *NCOA2* (Figure 9). However, differential diagnoses of STAF and other spindle cell lesions were also positive (Table 2). Nuclear expression was also seen in normal tissue including connective tissue, endothelial cells and smooth muscle. Adipocytes showed variable positivity and epithelial cells of the rete testis and seminiferous tubules showed a cytoplasmic reactivity.

CD34 staining was seen in one of thirteen cases (Figure 10). EMA positivity was demonstrated in seven out of nine cases with a focal expression in five cases. Desmin was focally positive in two of six examined cases. Alpha smooth muscle actin was focally detected in two of eleven cases. S100, Pan-CK (AE or MNF116) and STAT6 were negative in all cases tested (n=11, n=4, n=5, respectively).

Table 4. Immunohistochemical results

Case	CD34	EMA	Desmin	ASMA	S100	CK	STAT6	NCOA2
1	-	f+	f+	-	nd	nd	nd	+
2	-	+	nd	-	-	- (MNF116)	nd	+
3	-	+	nd	-	nd	nd	nd	+
4	-	-	-	-	-	nd	nd	+
5	+	nd	f+	-	-	nd	nd	+
6	-	nd	-	nd	-	- (AE)	-	+
7	nd	nd	nd	-	-	nd	-	+
8	-	-	nd	-	-	nd	nd	+
9	-	f+	nd	f+	-	nd	nd	+
10	-	nd	nd	nd	-	nd	nd	nd
11	-	f+	-	f+	-	- (AE)	-	nd
12	-	nd	nd	-	nd	nd	-	nd
13	-	f+	nd	-	-	nd	-	nd
14	-	f+	-	nd	-	- (MNF116)	nd	nd
n	1/13	7/9	2/6	2/11	0/11	0/4	0/5	9/9

f, focal expression; nd, not done

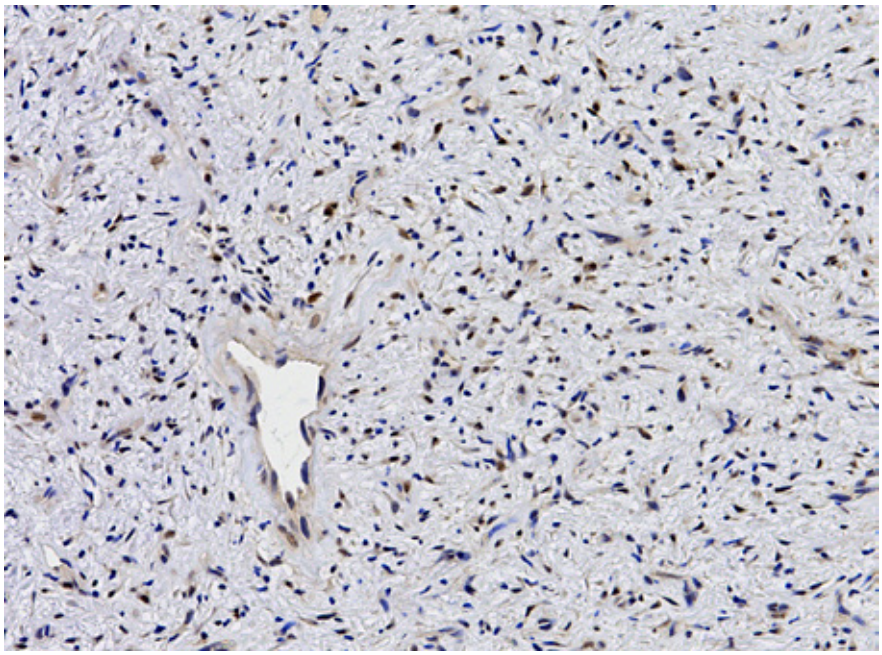

Figure 9. All cases of STAF but also other spindle cell lesion showed nuclear expression of NCOA2 (Case 2).

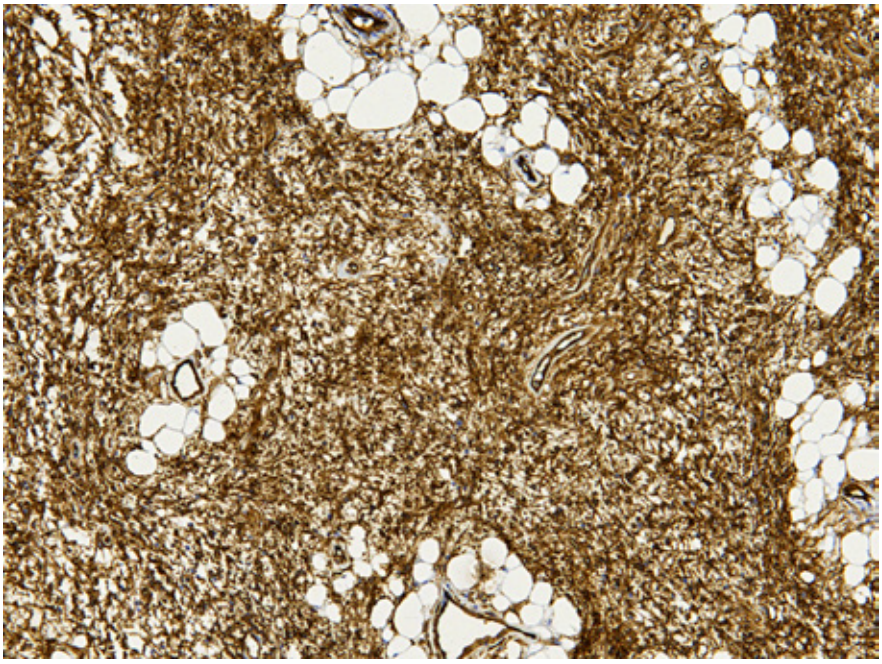

Figure 10. Case 5 was positive for CD34.

Molecular genetic findings

Molecular genetic results are presented in Table 5. Using RT-PCR, nine out of fourteen cases were shown to harbor a *AHRR-NCOA2* fusion gene, with exon combinations were exon 10-14 (four cases) (Figure 11), exon 10-16 (two cases), exon 9-16 (two cases) and exon 9-14 (+insertion) (one case); also one case was shown to harbor a *GAB1-ABL1* fusion of exons 6 and 2, respectively. *GTF2I-NCOA2* was not detected in the remaining cases (n=3). None of the cases of the control group harbored a transcript of these fusion genes.

RNA seq and subsequent bioinformatics analyses revealed the presence of *AHRR-NCOA2* fusion transcripts in cases 6 and 12. The exon combinations were ex 8-11 in both. Case 14 displayed a *GAB1-ABL1* fusion transcript of exons 6 and 2, according to both ChimeraScan and FusionCatcher algorithms.

Two cases failed for analysis due to poor RNA quality.

Table 5. Molecular data (RT-PCR and NGS results)

Case	*AHRR-NCOA2*	*GTF2I-NCOA2*	*GAB1-ABL1*
1	ex 10-14	na	
2	ex 9-14*	na	
3	ex 10-14	na	
4	ex 10-14	na	
5	ex 10-16	na	
6	ex 8-11**	neg	
7	x	x	
8	ex 9-16	na	
9	x	x	
10	ex 10-14	na	
11	ex 9-1	na	
12	ex 8-11**		
13	ex 10-16		
14			ex6-ex2**

Ex, exon; nd, not detected; na, not analyzed; neg, negative, x, failed for analysis (poor RNA quality);* plus an insertion, ** NGS

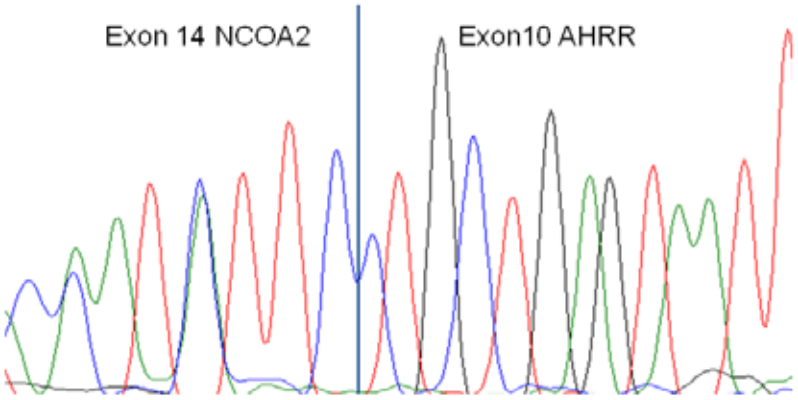

Figure 11. Sequence of the RT-PCR product showed a fusion between exon 10 of *AHRR* and exon 14 of *NCOA2* in four cases.

Discussion

Recurrent fusion genes, recognized as driver mutations, are being discovered in a growing number of tumor types, resulting in a specific transcription program of different target genes, which in turn has clinicopathological implications [17-19]. One example of such a tumor type is the recently delineated benign mesenchymal lesion STAF, which has, in addition to a distinct fibrovascular histological appearance, a *AHRR- NCOA2* fusion transcript in a large subset of cases [2, 20].

AHRR (aryl hydrocarbon receptor repressor) regulates the activity of the corresponding receptor (AHR) and is as a putative tumor suppressor. The coding gene is located on 5p15 [2,21]. *NCOA2* (nuclear receptor coactivator 2), located on 8q13.3, normally enhances chromatin remodeling and facilitates transcription of nuclear hormone receptor target genes with influence on cell growth, development and homeostasis [2,22-24]. It has been shown that the *AHRR-NCOA2* chimeric protein is able to activate the *AHR* signaling due to the retained transcriptional activation domain of *NCOA2*, resulting in neoplastic transformation [2].

In accordance to the series investigated by Jin et al [2] and Yamada et al [20], our data suggest that *AHRR-NCOA2* is the most common fusion gene in STAF with in-frame fusion transcripts of exon 10-14 (n = 4), exon 10-16 (n = 2), exon 9-16 (n = 2), exon 9-14 (n = 1) and exon 8-11 (n = 2). The exon combination 8-11 was found by RNA sequencing and has not been reported previously. Additional reciprocal

NCOA2-AHRR and in one case further fusion genes, *NCOA2-ETV4*, *ETV4-AHRR*, *P4HA2-TBCK* and *TBCK-P4HA2*, have been reported [2, 20, 25]. *GTF2I-NCOA2*, the result of a t(7;8;14)(q11;q13;q31), has been described as an alternative fusion gene in a single case [13]. However, neither we nor others have detected it, suggesting that may be a less common genetic event [13,20].

The *NCOA2* gene is a partner in fusions involved in other soft tissue tumors, such as mesenchymal chondrosarcoma, and infantile spindle cell and alveolar rhabdomyosarcoma demonstrating a role in both benign and malignant soft tissue tumorigenesis [23, 24, 26]. *NCOA2* FISH can be a diagnostic aid in these different tumor types, especially in FFPE samples with poor RNA quality, as shown in several studies [20, 23, 24, 26-28].

To find an immunohistochemical surrogate marker for tumor types harboring *NCOA2* fusion proteins, we investigated for the first time a *NCOA2* antibody (with epitope of the carboxyterminal region because of the preserved C-terminal domains in the fusion protein). In particular, soft tissue angiofibroma and mesenchymal chondrosarcoma are good candidates because of the absence of specific immunohistochemical profile [1,10]. However, we found nuclear immunoreactivity in most of the control cases, demonstrating that this antibody is not suitable for diagnostic purposes.

For the first time, we report *GAB1-ABL1* being another alternative fusion gene in STAF. The fusion was first detected by RNA-seq and subsequently confirmed by RT-PCR. *GAB1* (Grb2-associated binding protein 1), located on 4q31, belongs to a family of scaffolding proteins closely related to the insulin receptor substrates interacting with several growth factors and interleukin receptors. It is involved in the integration of different signal transductions including the MAPK and PI3K cascades [29]. *ABL1* (Abelson tyrosin protein kinase 1), located on 9q34, is a proto-oncogene with cell cycle function involved in a variety of cellular processes, including cell division, adhesion and differentiation. It is known to be involved in myeloid and lymphoblastic leukemias as part of the Philadelphia chromosome [30].

In conclusion, the *AHRR-NCOA2* fusion is a frequent finding in STAF, while the *GTF2I-NCOA2* fusion seems to be a rare genetic event. For the first time, we report a *GAB1-ABL1* fusion transcript in a soft tissue angiofibroma of a child. In this study, immunohistochemical nuclear expression of *NCOA2* was not helpful in discriminating soft tissue angiofibroma from other spindle cell neoplasms.

References

1. Mariño-Enríquez A, Fletcher CD: Angiofibroma of soft tissue: clinicopathologic characterization of a distinctive benign fibrovascular neoplasm in a series of 37 cases. Am J Surg Pathol 2012, 36:500-508.
2. Jin Y, Möller E, Nord KH, Mandahl N, Von Steyern FV, Domanski HA, Mariño-Enríquez A, Magnusson L, Nilsson J, Sciot R, Fletcher CD, Debiec-Rychter M, Mertens F: Fusion of the AHRR and NCOA2 Genes through a recurrent translocation t(5;8)(p15;q13) in soft tissue angiofibroma results in upregulation of aryl hydrocarbon receptor target genes. Genes Chromosomes Cancer 2012, 51:510-520.
3. Nucci MR, Granter SR, Fletcher CD: Cellular angiofibroma: a benign neoplasm distinct from angiomyofibroblastoma and spindle cell lipoma. Am J Surg Pathol 1997, 21:636-644.
4. De Saint Aubain Somerhausen N, Rubin BP, Fletcher CD: Myxoid solitary fibrous tumor: a study of seven cases with emphasis on differential diagnosis. Mod Pathol 1999, 12:463-471.
5. Flucke U, van Krieken JH, Mentzel T: Cellular angiofibroma: analysis of 25 cases emphasizing its relationship to spindle cell lipoma and mammary-type myofibroblastoma. Mod Pathol 2011, 24:82-89.
6. Schweizer L, Koelsche C, Sahm F, Piro RM, Capper D, Reuss DE, Pusch S, Habel A, Meyer J, Gock T, Jones DT, Mawrin C, Schiitenhelm J, Becker A, Heim S, Simon M, Herold-Mende C, Mechtersheimer G, Paulus W, Konig R, Wiestler OD, Pfister SM, von Deimling A: Meningeal hemangiopericytoma and solitary fibrous tumors carry the NAB2-STAT6 fusion and can be diagnosed by nuclear expression of STAT6 protein. Acta Neuropathol 2013, 125:651-658.
7. Doyle LA, Vivero M, Fletcher CD, Mertens F, Hornick JL: Nuclear expression of STAT6 distinguishes solitary fibrous tumor from histologic mimics. Mod Pathol 2013, 27:390-395.
8. Doyle LA, Fletcher CD, Hornick JL: Nuclear expression of CAMTA1 distinguishes epithelioid hemangioendothelioma from histologic mimics. Am J Surg Pathol 2016, 40: 94-102.
9. Shibuya R, Matsuyama A, Shiba E, Harada H, Yabuki K, Hisaoka M: CAMTA is a useful immunohistochemical marker for diagnosing epithelioid haemangioendothelioma. Histopathology 2015, 67: 827-835.
10. Fletcher CD, Bridge JA, Hogendoorn, PC, Mertens F (Eds.): WHO classification of tumours of soft and bone. IARC:Lyon 2013
11. Wortman JR, Tirumani SH, Tirumani H, Shinagare AB, Jagannathan JP, Hornick JL, Ramaiya NH: Neoadjuvant radiation in primary extremity liposarcoma: correlation of MRI features with histopathology. Eur Radiol 2015.
12. Wang WL, Katz D, Araujo DM, Ravi V, Ludwig JA, Trent JC, Patel SR, Lin PP, Guadagnolo A, Lòpez-Terrada D, Dei Tos AP, Lewis VO, Lev D, Pollock RE, Zagars GK, Benjamin RS, Madewell JE, Lazar AJ: Extensive adipocytic maturation can be seen in myxoid liposarcomas treated with neoadjuvant doxorubicin and ifosfamide and pre-operative radiation therapy. Clin Sarcoma Res 2012;2:25.
13. Arbajian E, Magnusson L, Mertens F, Domanski HA, Vult von Steyern F, Nord KH: A novel GTF2I/NCOA2 fusion gene emphasizes the role of NCOA2 in soft tissue angiofibroma. Genes Chromosomes Cancer 2012, 52:330-331.
14. Walther C, Hofvander J, Nilsson J, Magnusson L, Domanski HA, Gisselsson D, Tayebwa J, Doyle LA, Fletcher CDM, Mertens F (2015) Gene fusion detection in formalin-fixed paraffin-embedded benign fibrous histiocytomas using fluorescence in situ hybridization and RNA sequencing. Lab Invest 95:1071-1076

15. Iyer MK, Chinnaiyan AM, Maher CA. ChimeraScan: a tool for identifying chimeric transcription in sequencing data. Bioinformatics 2011; 27: 2903-2904.

16. Nicorici D, Satalan M, Edgren H, Kangaspeska S, Murumägi A, Kallioniemi O, Virtanen S, Kilkku O (2014) FusionCatcher – a tool for finding somatic fusion genes in paired-end RNA sequencing data. bioRxiv doi https://doi.org/10.1101/011650

17. Antonescu CR, Dal Cin P: Promiscuous genes involved in recurrent chromosomal translocations in soft tissue tumours. Pathology 2014, 46:105-112.

18. Mertens F, Antonescu CR, Hohenberger P, Ladanyi M, Modena P, D'Incalci M, Casali PG, Aglietta M, Alvegard T: Translocation-related sarcomas. Semin Oncol 2009, 36:312-323.

19. Rabbitts TH: Commonality but diversity in cancer gene fusions. Cell 2009, 137:391-395.

20. Yamada Y, Yamamoto H, Kohashi K, Ishii T, Iura K, Maekawa A, Bekki H, Otsuka H, Yamashita K, Tanaka H, Hiraki T, Mukai M, Shirakawa A, Shinnou Y, Jinno M, Yanai H, Taguchi K, Maehara Y, Iwamoto Y, Oda Y. Histological spectrum of angiofibroma of soft tissue: histological and genetic analysis of 13 cases. Histopathology 2016;69:459-469

21. Hahn ME, Allan LA, Sherr DH: Regulation of constitutive and inducible AHR signaling: complex interactions involving the AHR repressor. Biochem Pharmaco 2009, 77:485-497.

22. Hong H, Kohli K, Garabedian MJ, Stallcup MR: GRIP1, a transcriptional coactivator for the AF-2 transactivation domain of steroid, thyroid, retinoid, and vitamin D receptors. Mol Cell Biol 1997, 17:2735-2744.

23. Sumegi J, Streblow R, Frayer RW, Dal Cin P, Rosenberg A, Meloni-Ehrig A, Bridge JA: Recurrent t(2;2) and t(2;8) translocations in rhabdomyosarcoma without the canonical PAX-FOXO1 fuse PAX3 to members of the nuclear receptor transcriptional coactivator family. Genes Chromosomes Cancer 2010, 49:224-236.

24. Wang L, Motoi T, Khanin R, Olshen A, Mertens F, Bridge J, Dal Cin P, Antonescu CR, Singer S, Hammed M, Bovee JV, Hogendoorn PC, Socci N, Ladanyi M: Identification of a novel, recurrent HEY1-NCOA2 fusion in mesenchymal chondrosarcoma based on a genome-wide screen of exon-level expression data. Genes Chromosomes Cancer 2012, 51:127-139.

25. Panagopoulos I, Gorunowa L, Viset T, Heim S. Gene fusions AHRR-NCOA2, NCOA2-ETV4, ETV4-AHRR, P4HA2-TBCK, TBCK-P4HA2 resulting from the translocations t(5;8;17)(p15;q13;q21) and t(4;5)(q24;q31) in a soft tissue angiofibroma. Oncol Rep 2016;36:2455-2462

26. Mosquera JM, Sboner A, Zhang L, Kitabayashi N, Chen CL, Sung YS, Wexler LH, LaQualia MP, Edelmann M, Sreekantaiah C, Rubin MA, Antonescu CR: Recurrent NCOA2 gene rearrangement in congenital/infantile spindle cell rhabdomyosarcoma. Genes Chromosomes Cancer 2013, 53:779-787.

27. Edgar MA, Lauer SR, Bridge JA, Rizzo M: Soft tissue angiofibroma: report of 2 cases of a recently described tumor. Hum Pathol 2013, 44:438-441.

28. Sugita S, Aoyama T, Kondo K, Keira Y, Ogino J, Nakanishi K, Kaya M, Emori M, Tsukahara T, Nakajima H, Takagi M, Hasegawa T: Diagnostic utility of NCOA2 fluorescence in situ hybridization and Stat6 immunohistochemistry staining for soft tissue angiofibroma and morphologically similar fibrovascular tumors. Hum Pathol 2014, 45:1588-1596.

29. Chen L, Du-Cuny L, Moses S, Dumass S, Song Z, Rezaeian AH, Lin HK, Meuillet EJ, Zhang S. Novel inhibitors induce large conformational changes of GAB1 pleckstrin homology domain and kill breast cancer cells. PLoS Comput Biol 2015;11:e1004021

30. Desogus A, Schenone S, Brullo C, Tintori C, Musumeci F. Bcr-ABL tyrosine kinase inhibitors: a patent review. Expert opin Ther pat 2015;25:397-412

Chapter 7

Myxoid liposarcoma of the foot: a study of 8 cases

Elise M Bekers, Wangzhao Song, Albert JH Suurmeijer, Johannes J Bonenkamp, Ingrid C van der Geest, Petra M Braam, Marieke JM Ploegmakers, Ingrid ME Desar, Bastiaan BJ Tops, Joost M van Gorp, David H Creytens, Thomas Mentzel, Uta Flucke

Ann Diagn Pathol. 2016 Dec;25:37-41.

Abstract

Introduction: Myxoid liposarcoma (MLS) is the only translocation-associated liposarcoma-subtype. It classically originates in the deep soft tissues of the thigh. At distal sites of the extremities, this tumor is exceedingly rare. We present a series of eight cases occurring in the foot/ankle.

Results: Two female and six male patients, aged between 32 to 77 years (mean 54.3 years) were identified. Tumor size ranged from 1. to 10 cm (mean 6.8 cm). Two lesions eroded bone. All tumors were treated by excision and seven by (neo) adjuvant radiotherapy. R0 status was reached in two cases with one case followed by metastasis in the groin. All other cases were documented with R1 (n=2) or R2 (n=4) resection status. In one patient, the follow-up status was unknown. All other patients were alive 15-135 (mean 55.8) months after initial diagnosis.

We conclude that myxoid liposarcoma at acral sites are exceedingly rare, and in this series, prognosis was good irrespective of resection status. Clinicians and pathologists have to be aware because this sarcoma type shows a peculiar clinical behavior with high radio- and chemosensitivity and metastatic spread to extra-pulmonary sites.

Introduction

Myxoid liposarcoma (MLS) is the only translocation-associated liposarcoma-subtype recapitulating more or less normal lipogenesis [1-3]. The specific fusion genes *FUS-DDIT3* and, more rarely, *EWSR1-DDTI3* are the result of the t(12;16)(q13;p11) and t(12;22)(q13;q12), respectively [3-5].

MLS is the most common liposarcoma arising in children, adolescents and young adults [6-9]. It comprises up to 35% of all liposarcomas and has, in one-third of cases, the tendency to metastasize to other soft tissue sites including mediastinum and retroperitoneum, and also to bone, lung and liver with a consecutive fatal outcome. The classical localization (two-thirds of the cases) is the deep soft tissues of the thigh [3, 6, 10]. Cases of the retroperitoneum are almost exclusively metastases with some exceptions [11-13]. At distal sites of the extremities, this tumor is exceedingly rare [6, 14-18], and the first case was documented by Booker in 1965 [15]. We here present a series of eight cases occurring in the foot/ankle.

Material and Methods

Patient data

The cases were collected retrospectively from the authors (referral) files. The study was performed in accordance with the Code of Conduct of the Federation of Medical Scientific Societies in the Netherlands and Germany.

In each case, 4-mm-thick sections of formalin-fixed, paraffin-embedded (FFPE) material were stained with haematotoxylin and eosin. The histological diagnoses were revised (UF, EB) and classified according to the 2013 WHO criteria. From each case, 1 representative paraffin tissue block (four biopsies and four resection specimens) containing the largest area and highest tumor percentage of viable tumor was selected for fluorescence in situ hybridization (FISH) and reverse transcriptase polymerase chain reaction (RT-PCR) analysis.

Fluorescence in situ hybridization (FISH)

Four-micrometer paraffin sections of selected tissue blocks were treated and made accessible to the DNA probes as described earlier in ten Heuvel et al [19]. The used probes were as follows: a telomeric 120-kilobase (kb) probe labeled with Spectrum Orange and a centromeric 334-kb probe labeled with Spectrum Green for *EWSR1*

and a telomeric 500-kb probe labeled with Spectrum Orange and a centromeric 270-kb probe labeled with Spectrum Green for *FUS*.

Slides were visually evaluated using a Leica DMR fluorescence microscope equipped with appropriate filters for 4,6-diamidino-2-phenylindole, Spectrum Orange, and Spectrum Green. Tumors (MLS) scored positive for *FUS* and *EWSR1* translocations when several areas contained at least 31% of tumor cell nuclei for *EWSR1* and 13% for *FUS*, and had clearly split orange and green signals (separated by at least 3 signal diameters from an oppositely colored signal).

Reverse transcriptase-Polymerase chain reaction (RT-PCR)

RNA was extracted from FFPE tissues using RNA-Bee-RNA isolation reagent (Bio-Connect BV, Huissen, the Netherlands) according to standard procedures. RNA quantity and quality were determined by NanoDrop measurement (Fisher Scientific, Landsmeer, the Netherlands) and, subsequently, cDNA synthesis was performed using Superscript II (Invitrogen Life Technologies Europe, Bleiswijk, the Netherlands) and random hexamers (Promega Nederland, Leiden, the Netherlands).

The cDNA was tested by the RT-PCR for the *HMBS* (hydroxymethylbilase synthase) housekeeping gene using the primers forw150 5'-TGCCAGAGAAGAGTGTGGTG-3', rev150 5'-ATGATGGCACTGAACTCCTG-3', forw250 5'- CTGGTAACGGCAATGCGGCT-3', rev250 5'- TTCTTCTCCAGGGCATGTTC-3'.

For detection of the *EWSR1-DDIT3* fusion, 5'-TCCTACAGCCAAGCTCCAAGTC-3' forward primer and 5'-GACTCAGCTGCCATCTCTGC-3' reverse primer were used. For the *FUS-DDIT3* fusion, 5'- GACAGCAGAACCAGTACAACAGCAG-3' and '5-CCGTGGTGGCTTCAATAAATTTG-3' forward primers and 5'-GCTTTCAGGTGTGGTGATGTATGAAG-3' and 5'-GACTCAGCTGCCATCTCTGC-3' reverse primers were used. The PCR-products were analyzed by agarose gel electrophoresis and Sanger-sequencing.

Results

Patient characteristics

Patient characteristics are presented in Table 1. In brief, eight patients were included of which two females and six males with an age range of 32 to 77 years (mean 54.3 years; median 57.5 years). Tumor size ranged from 1.1 to 10 cm (mean 6.8 cm; median 6.5 cm). In four patients, the tumor was localized between

metatarsal 1 and 2, one (case 2) between metatarsal 2 and 5 and in two patients (case 6 and 8), it was distal in the ankle with extension on the dorsum of the foot. In patient one, the specific location, apart from being located in the foot, was unknown. Two lesions (case 3 and 5) eroded bone with a pathological fracture as clinical presentation in case 3. All lesions were treated by excision/resection and seven patients received (neo)adjuvant radiotherapy. R0 status was reached in two cases, followed by a metastasis in the groin 7 months later in case 5. All other cases were documented with R1 (n=2) or R2 (n=4) resections without recurrences or metastases. Seven patients were alive after initial diagnosis with follow-up range from 15 to 135 months (mean 55.8; median 41.5 months). For patient eight no follow-up information was available.

Table 1. Clinical data

Case	Age(y)/Sex	Tumorsize (cm)	Site	Treatment	Rec/met (months)	Follow-up (months)
1	65/m	**10**	Foot	TNF, perfusion, R2	No	NED (135)
2	77/m	**7**	Foot	R1, adjuv RT	No	NED (94)
3	60/m	**3.5**	Foot	R1, adjuv RT	No	NED (15)
4	39/m	**1.1**	Foot	Neoadjuv RT, R1	No	NED (85)
5	55/m	**4.5**	Foot	Neoadjuv RT, R0	Groin (7)	NED (15)
6	32/m	**6**	Foot/ankle	Neoadjuv RT, R2	No	NED (58)
7	34/f	**4**	Foot	Neoadjuv RT, R0	No	NED (19)
8	72/f	**6.5**	Foot/ankle	R0	NA	NA

Y, years; f, female; m, male; rec/met, recurrence/metastases; TNF, tumor necrosis factor; R, resection status; adjuv, adjuvant; neo-adjuv, neo-adjuvant; RT, radiotherapy; NED no evidence of disease, NA not available

Radiology

Magnetic resonance imaging (MRI), exemplarily described in case 5, showed an well-defined intermetatarsal soft tissue mass with cortical destruction of the adjoining metatarsal bone and involvement of one of the neurovascular bundles (Fig. 1). This heterogeneous mass contained myxoid areas, fatty tissue (less than 25%) and necrotic components. Imaging after contrast agent showed a peripheral nodular enhancement. Six months after radiotherapy there was an increase in size, bone involvement and heterogeneous enhancement on MRI with central necrosis. Nine months after radiotherapy and total resection, a lesion in the right groin was found with ultrasonography. This lesion showed a lipomatous aspect, suspicious for metastatic disease.

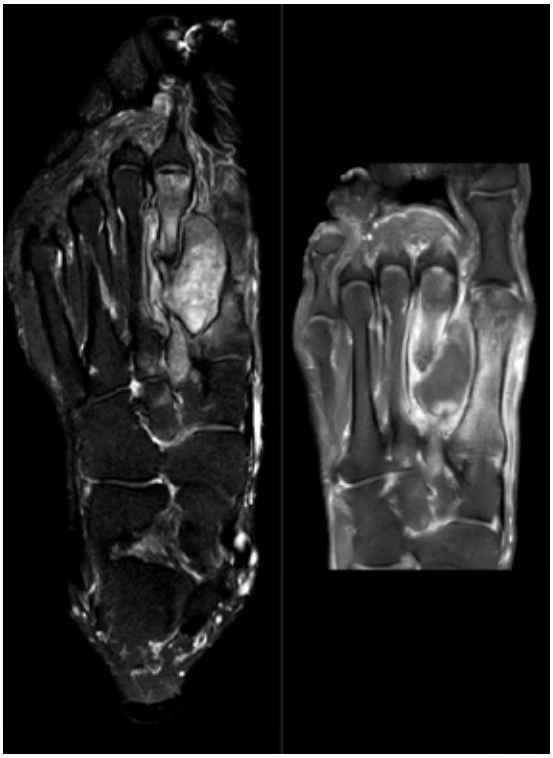

Figure 1. MRI shows a well-defined intermetatarsal soft tissue mass with cortical destruction of the adjoining metatarsal bone and involvement of one of the neurosvascular bundels.

Histology

Most cases showed a typical histology of myxoid liposarcoma with a nodular growth pattern of relatively low cellularity with enhancement of cells at the periphery of the nodules. There was a proliferation of uniform bland, round to oval-shaped primitive cells intermingled with a variable amount of lipoblasts of different stages in an abundant myxoid stroma (Figure 2). In case 1 an additional nested pattern of primitive cells was seen and Case 4 showed areas of extensive maturation and slightly pleomorphic nuclei (Figure 3). A delicate plexiform ('chicken-wire') capillary vasculature was present throughout the tumors. Two cases had mainly a hypercellular morphology with more large round cells with increased nuclear/cytoplasmic ratio, distinct nucleoli and a little amount of intervening myxoid stroma (Figure 4). In two of the five neo-adjuvant treated cases prominent necrosis and/or hyalinization were found with only minimal viable tumor as a result of radiotherapy. The remaining three tumors were mainly vital. The groin metastasis of case 5 presented with a prominent round cell pattern. Percentages of the round cell component are shown in Table 2.

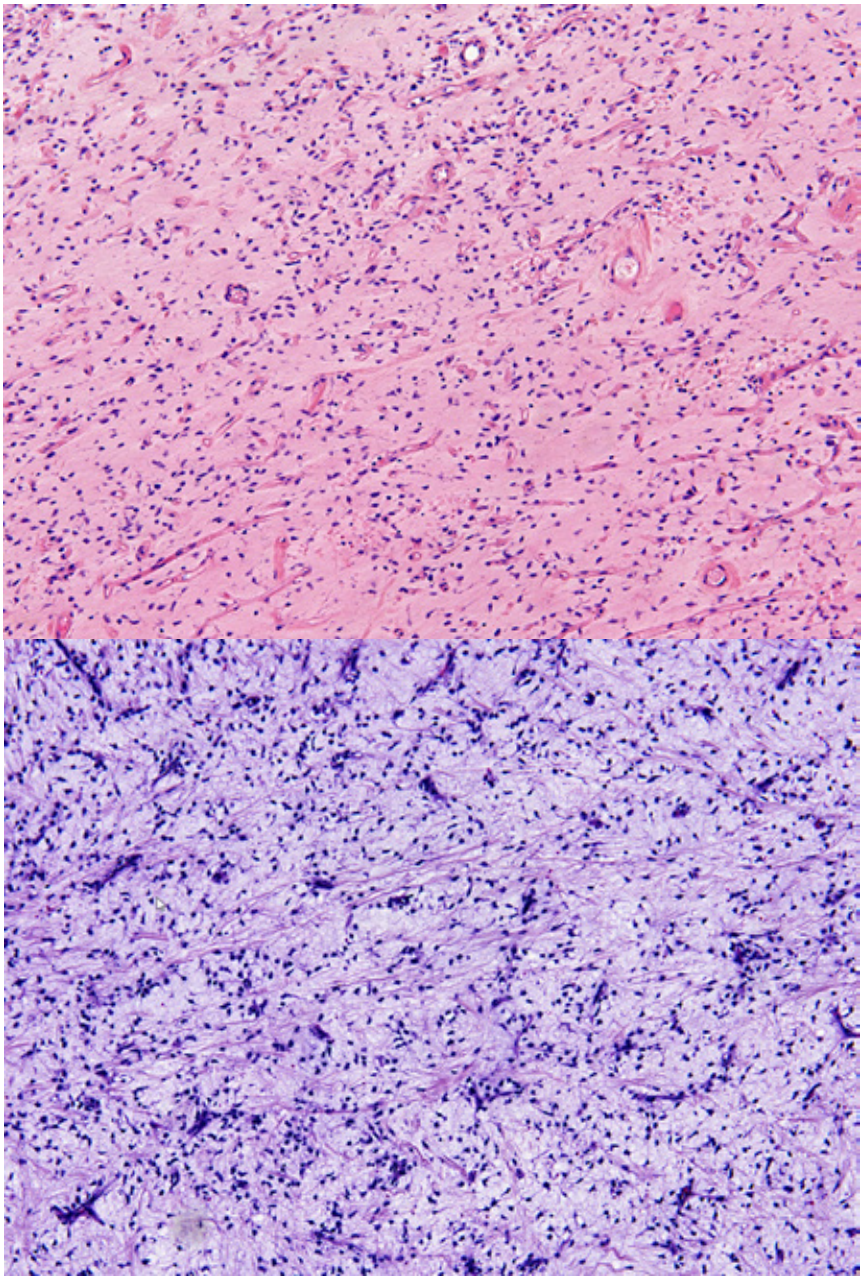

Figure 2. Typical histology of MLS with uniform cells intermingled with a variable amount of lipoblasts in an abundant myxoid stroma and delicate plexiform capillary vasculature (hematotoxylin and eosin stain, 100x)

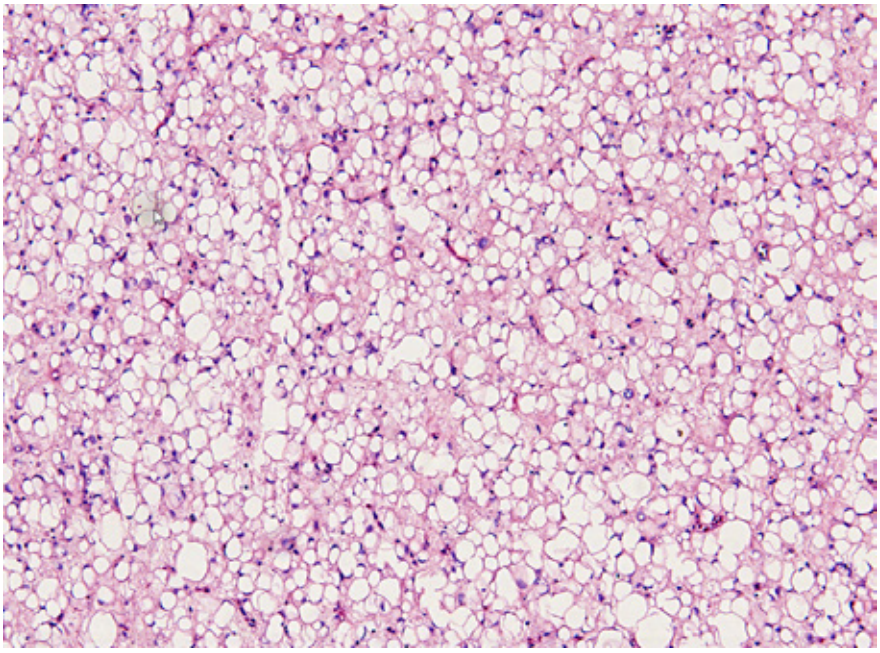

Figure 3. Areas of extensive lipomatous differentiation after radiotherapy (hematotoxylin and eosin stain, 100x)

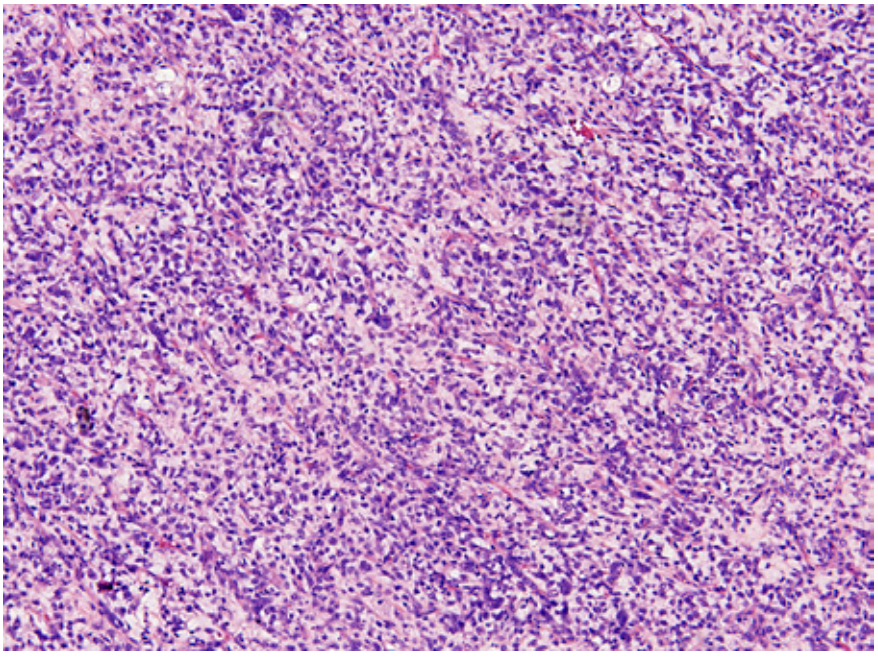

Figure 4. Hypercellular areas with round cell morphology was seen in cases 1 and 2 (hematotoxylin and eosin stain, 100x)

Molecular genetics

Genetic results are listed in Table 2. All cases were investigated using RT-PCR and/or FISH.

Five cases tested by FISH showed a *FUS* rearrangement in three cases and an *EWSR1* rearrangement in two cases. Of the seven cases analyzed using RT-PCR, three harbored a *FUS-DDIT3* fusion and one case an *EWSR1-DDIT3* fusion. One case positive for FISH (*FUS* rearrangement) was negative by RT-PCR (Fig. 5). The other three cases tested using FISH had insufficient RNA quality for RT-PCR.

Table 2. Histological and molecular data

Case	RC component	FISH rearrangement/RT-PCR (fusion gene)
1	>5% (R)	FUS/neg
2	>5% (R)	EWSR1/NI
3	0% (R)	EWSR1/NI
4	<5% (R)	FUS/NI
5	0% (R), >5% (M)	ND/FUS-DDIT3
6	<5% (R)	ND/FUS-DDIT3
7	<5% (R)	ND/EWSR1-DDIT3
8	0% (R)	FUS/NI

RC, round cell; R, resection specimen; B, biopsy; M, metastasis; neg, negative; NI not interpretable due to poor RNA quality; ND, not done

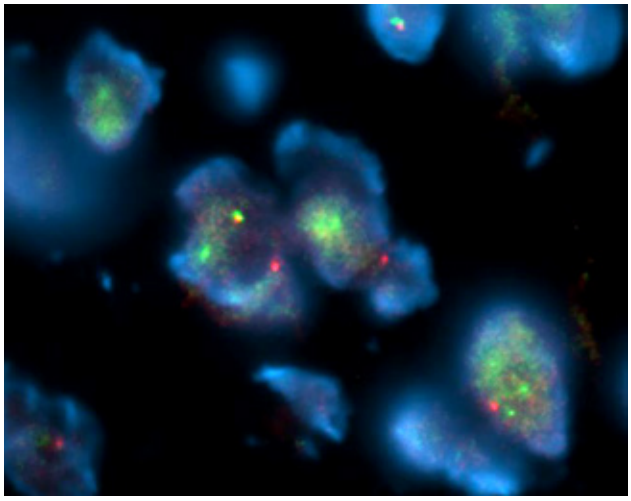

Figure 5. *FUS* FISH with breakapart signal indicating a *FUS* rearrangement

Discussion

Soft tissue sarcomas are a heterogeneous group of tumors with a large spread in biological behavior, prognosis and requested treatment modalities. The right diagnosis, strongly dependent of clinical pattern, radiological evaluation and in particular adequate pathology, is critical in order to propose the best treatment. Atypical presentation of MLS is important to recognize, due to its ability to widespread metastasize while normally being known as a radiotherapy and chemotherapy sensitive tumor [2, 12, 20-22]. This is even more important when adequate surgical margins are difficult to reach, such as in the foot and ankle.

Usually MLS are located in the deep soft tissues of the thigh. However, rarely, they can occur in atypical localization such as head and neck, skin/subcutis, mediastinum, retroperitoneum as well as acral sites [6, 10, 13-19, 22-28]. In these cases, an adapted treatment approach will possibly be administered.

We discuss herein eight cases of MLSs arising in the foot/ankle, which is very unusual for liposarcomas in general and for MLSs in particular, with MLSs ranging from low-grade tumors with a low metastatic potential to high-grade neoplasms (including "round cell" liposarcoma) with a poor prognosis [10, 29, 30].

Anatomic site often has prognostic impact as for example shown for (lipo)sarcoma localized in the retroperitoneum/peritoneum where tumor free margins can often not be obtained in comparison to surgically amenable sites as extremities [3, 6].

Whether localization of MLSs in the distal extremities is linked to better outcome is not clearly understood and in our cohort, only one of our patients showed metastatic spread soon after primary treatment. All other patients had no evidence of disease even after incomplete resection and the presence of a round cell component above 5%. Nevertheless, late metastases in MLS are reported [2, 13, 19].

Usually, on MRI, MLSs are well-delineated lobulated masses with homogenous signal intensity. A more variable/inhomogeneous appearance as shown in one of our cases might suggest a round cell component [29, 31].

The classical histology of MLSs consisting of small uniform primitive cells and lipoblasts in different stages of maturation set in a prominent myxoid matrix with pools of mucine and the typical chickenwire-like capillary network leads to a straightforward diagnosis even in needle biopsies [8]. High-grade tumors can

be more challenging as they are characterized by sheets of primitive round cells without intervening myxoid stroma and a less obvious vasculature. Rarely, one can encounter a peculiar nested pattern, stromal hyalinization, an obviously adipocytic component and hemangiopericytoma vasculature, which can hamper the diagnosis [6, 8, 18]. Fusion gene detection (*FUS/EWSR1-DDIT3*) is then a useful ancillary test, as specific immunohistochemistry is lacking [3, 7, 10, 13, 18].

Differential diagnoses of MLS in the foot could be benign fatty lesions with secondary myxoid changes such as lipoma or syndromal overgrowth tissue, as they are more common at acral sites in comparison to MLS [32-34]. Chondroid lipoma may also arise at acral sites but the constituent cells are commonly hibernoma-like and chondroblast-like with eosinophilic cytoplasm set in a chondroid matrix. There is no plexiform capillary vasculature [35, 36]. The recently described benign entity angiofibroma of soft tissue, also known for its resemblance to MLS because of branching thin walled blood vessels, a possible myxoid stroma, and a facultative lipomatous component, could be another alternative diagnosis. Although lipoblasts are not described [37]. Well differentiated liposarcoma with myxoid changes may imitate a chicken-wire vasculature but shows nuclear atypia in stromal and fat cells which is morphologically most discriminating [34]. Myxofibrosarcomas and myxoinflammatory fibroblastic sarcomas are characterized by obvious atypical cells not seen in MLS [3]. Myxoid areas of lipoblastoma can be histomorphologically indistinguishable from MLS; however, most affected patients are younger than 10 years [38].

In high-grade lesions other small round cell tumors as Ewing sarcoma, synovial sarcoma, alveolar rhabdomyosarcoma, angiomatoid fibrous histiocytoma and solitary fibrous tumor should be ruled out [34]. Of note, none of these tumors show lipoblasts or a chickenwire vasculature. In addition, all of the mentioned differential diagnoses harbor a different genetic profile and most of the lesions have a distinct immunophenotype. However, a possible overlapping *EWSR1* rearrangement in a subset of MLSs, Ewing sarcomas and angiomatoid histiocytomas should be kept in mind [3].

In conclusion MLSs rarely originate in the distal extremities and show a good prognosis in most cases, at least in our limited series. Clinicians and pathologists should be aware because MLS are biologically different from other (lipo) sarcomas with high radio- and chemosensitivity and a high prevalence of extra-pulmonary metastases.

References

1. Bolen JW, Thorning D. Benign lipoblastoma and myxoid liposarcoma: a comparative light- and electron-microscopic study. Am J Surg Pathol 1980;4:163-174
2. Haniball J, Sumathi VP, Kindblom LG, Abdu A, Carter SR, Tillman RM, Jeys L, Spooner D, Peake D, Grimer RJ. Prognostic factors and metastatic patterns in primary myxoid/round-cell liposarcoma. Sarcoma 2011; article ID 538085, 10 pages
3. Fletcher CD, Bridge JA, Hogendoorn PC, Mertens F (Eds). WHO classification of tumours of soft tissue and bone. IARC, Lyon, France 2013
4. Panagopoulos I, Hoglund M, Mertens F, Mandahl N, Mitelman F, Aman P. Fusion of the EWS and CHOP genes in myxoid liposarcoma. Oncogene 1996;12:489-494
5. Panagopoulos I, Mertens F, Isaksson M, Mandahl N. A novel FUS/CHOP chimera in myxoid liposarcoma. Biochem Biophys Res Commun 2000;279:838-845
6. Evans HL, Soule EH, Winkelmann RK. Atypical lipoma, atypical intramuscular lipoma, and well differentiated retroperitoneal liposarcoma: a reappraisal of 30 cases formerly classified as well differentiated liposarcoma. Cancer 1979; 43:574-584
7. Allagio R, Coffin C.M., Weiss S.W. et al. Liposarcomas in young patients: a study of 82 cases occuring in patients younger than 22 years of age. Am J Surg Pathol 2009; 33:645-58
8. Fritchie K, Goldblum JR, Tubbs RR, Sun Y, Carver P, Billings SD, Rubin BP. The expanded histological spectrum of myxoid liposarcoma with an emphasis on newly described patterns: implications for diagnosis on small needle biopsies. Am J Clin Pathol 2012;137:229-239
9. Dadone B, Refae S, Lemarié-Delaunay C, Bianchini L, Pedeutour F. Molecular cytogenetics of pediatric adipocytic tumors. Cancer Genet 2015;208:469-481
10. Dei Tos AP. Liposarcomas: diagnostic pitfalls and new insights. Histopathology 2014;64:38-52.
11. Estourgie SH, Nielsen GP, Ott MJ. Metastatic patterns of extremity myxoid liposarcoma and their outcome. J Surg Oncol 2002; 80:89-93
12. de Vreeze RS, de Jong D, Tielen IH, Ruijter HJ, Nederlof PM, Haas RL, van Coevorden F. Primary retroperitoneal myxoid/round cell liposarcoma is a nonexisting disease: immunohistochemical and molecular analysis. Mod Pathol 2009;22:223-231
13. Setsu N, Mototaka M, Wakai S, Nakatani F, Kobayashi E, Chuman H, Hiraoka N, Kawai A, Yoshida A. Primary retroperitoneal myxoid liposarcoma. Am J Surg Pathol 2016;40:1286-1290
14. Chang H, Hajdu SI, Collin C, Brennan MF. The prognostic value of histologic subtypes in primary extremity liposarcoma. Cancer 1989;64:1514-1520
15. Werd MB, DeFronzo DJ, Landsman AS, Surprenant M, Sakoff M. Myxoid liposarcoma of the ankle. J Foot Ankle Surg 1995;35:465-474
16. Nishio J, Isayama T, Yoshimura I, Ohjimi H, Iwasaki H, Naito M. Myxoid liposarcoma of the ankle: a case report. J Foot Ankle Surg 2012;51:76-79
17. Buehler D, Marburger TB, Billings SD. Primary subcutaneous myxoid liposarcoma: a clinicopathologic review of three cases with molecular confirmation and discussion of the differential diagnosis. J Cutan Pathol 2014;41:907-915
18. Iwasaki H, Ishiguro M, Nishio J, Aoki M, Yokoyama R, Yokoyama K, Taguchi K, Nabeshima K. Extensive lipoma-like changes of myxoid liposarcoma: morphologic, immunohistochemical, and molecular cytogenetic analyses. Virch Arch 2015;466:453-464

19. Ten Heuvel SE, Hoekstra HJ, van Ginkel RJ, Bastiaannet E, Suurmeijer AJ. Clinicopathologic prognostic factors in myxoid liposarcoma: a retrospective study of 49 patients with long term follow-up. Ann Surg Oncol 2007;14:222-229
20. Fiore M, Grosso F, Lo Vullo S, Pennacchioli E, Stacchiotti S, Ferrari A, Collini P, Lozza L, Mariani L, Casali PG, Grochi A. Myxoid/round cell and pleomorphic liposarcomas: prognostic factors and survival in a series of patients treated at a single institution. Cancer 2007;109:2522-2531
21. Sheah K, Ouelette HA, Torriani M, Nielsen GP, Kattapuram S, Bredella MA. Metastatic myxoid liposarcomas: imaging and histologic findings. Skeletal Radiol 2008;37:251-258
22. Wang WL, Katz D, Araujo DM, Ravi V, Ludwig JA, Trent JC, Patel SR, Lin PP< Guadagnolo A, Lopez-Terrada D, Dei Tos AP, Lewis VO, Lev D, Pollock RE, Zagars GK, Benjamin RS, Madewell JE, Lazar AJ. Extensive adipocytic maturation can be seen in myxoid liposarcomas treated with neoadjuvant doxorubicin and ifosfamide and pre-operative radiation therapy. Clin Sarcoma Res 2012;2:25
23. Dei Tos AP, Mentzel T, Fletcher CD. Primary liposarcoma of the skin: a rare neoplasm with unusual high grade features. Am J Dermatopathol 1998;20:332-338
24. Golledge J, Fisher C, Rhys-Evans PH. Head and neck liposarcoma. Cancer 1995;15:76:1051-1058
25. Hahn HP, Fletcher CD. Primary mediastinal liposarcoma: clinicopathologic analysis of 24 cases. Am J Surg Pathol 2007;31:1868-1874
26. Davis EC, Ballo MT, Luna MA, Patel SR, Roberts DB, Nong X, Sturgis EM. Liposarcoma of the head and neck: the University of Texas M.D. Anderson Cancer Center Experience. Head Neck 2009;31:28-36
27. Kudo H, Inaoka T, Tokuyama W, Hiruta N, Nakagawa K, Hayashi A, Terada H. Round cell liposarcoma arising in the left foot: MRI and PET findings. Jpn J Radiol 2012;30:852-857
28. Ortega P, Suster D, Falconieri G, Zambrano E, Moran CA, Morrison C, Suster S. Liposarcoma of the posterior mediastinum: clinicopathologic study of 18 cases. Mod Pathol 2015;28:721-731
29. Wortman JR, Tirumani SH, Jagannathan JP, Tirumani H, Shinagare AB, Hornick JL, Ramaiya NH. Primary extremity liposarcoma: MRI features, histopathology, and clinical outcome. J Comput Assist Tomogr 2016;00:00-00
30. Smith TA, Easley KA, Goldblum JR. Myxoid/round cell liposarcoma of the extremities. A clinicopathologic study of 29 cases with particular attention to extent of round cell liposarcoma. Am J Surg Pathol 1996;20:171-180
31. Tateishi U, Hasegawa T, Beppu Y, Kawai A, Satake M, Moriyama N. Prognostic significance of MRI findings in patients with myxoid-round cell liposarcoma. Am J Roentgenol. 2004;182:725-31
32. Laskin WB, Fetsch JF, Michal M, Miettinen M. Sclerotic (fibroma-like) lipoma: a distinctive lipoma variant with a predilection for the distal extremities. Am J Dermatopathol 2006;28:308-316
33. Martinez-Lopez A, Blasco-Morente G, Perez-Lopez I, Herrera-Garcia JD, Lugue-Valenzuela M, Sanchez-Cano D, Lopez-Gutierrez JC, Ruiz-Villaverde R, Tercedor-Sanchez J. CLOVES syndrome: review of a PIK3CA-related overgrowth spectrum (PROS). Clin Genet. 2016
34. Miettinen M (Ed). Modern soft tissue pathology. Tumors and non-neoplastic conditions. Cambridge University Press, NY, USA 2010
35. Meis JM, Enzinger FM. Chondroid lipoma. A unique tumor simulating liposarcoma and myxoid chondrosarcoma. Am J Surg Pathol 1993;17:1103-1112

36. Flucke U, Tops BB, de Saint Aubain Somerhausen N, Bras J, Creytens DH, Kusters B, Groenen PJ, Verdijk MA, Suurmeijer AJ, Mentzel T. Presence of C11orf95-MKL2 is a consistent finding in chondroid lipomas: a study of eight cases. Histopathology 2013;62:925-930

37. Mariño-Enrìquez A, Fletcher CD. Angiofibroma of soft tissue: clinicopathologic characterization of a distinctive benign fibrovascular neoplasm in a series of 37 cases. Am J Surg Pathol 2012;36:500-508

38. Coffin CM, Lowichik A, Putnam A. Lipoblastoma (LPB): a clinicopathologic and immunohistochemical analysis of 59 cases. Am J Surg Pathol 2009;33:1705-1712

Chapter 8

Multifocal occurrence of extra -abdominal desmoid type fibromatosis - A rare manifestation. A clinicopathological study of 6 sporadic cases and 1 hereditary case

Elise M Bekers, Danique LM van Broekhoven, Thijs van Dalen, Johan J Bonenkamp, Ingrid CM van der Geest, Jacky WJ de Rooy, Joost M van Gorp, David H Creytens, Wendy WJ de Leng, Blanca Scheijen, Astrid Eijkelenboom, Uta Flucke

Ann Diagn Pathol. 2018 Apr 21;35:38-41.

Abstract

Desmoid-type fibromatosis, also called desmoid tumor, is a locally aggressive myofibroblastic neoplasm that usually arises in deep soft tissue with significant potential for local recurrence and displays an unpredictable clinical course.

β-catenin, the genetic key player of desmoid tumors shows nuclear accumulation due to mutationas that prevent its degradation leading to activation of Wnt signaling and myofibroblastic cell proliferation. The corresponding hot spot mutations are located in exon 3 of the *CTNNB1* gene or alternatively, in the *APC* tumor suppressor gene, most often as a germline mutation.

Multifocal desmoid tumors are very rare and clinical characteristics are poorly understood. Here we present seven cases of multifocal desmoid in six sporadic and one familial case.

Four female and three male patients, aged between 7 and 30 years (mean 18.4 years) were identified in a cohort of 1392 cases. Tumors were located in (distal) extremities, thorax, breast, abdominal wall, shoulder, and neck. Four patients showed a *CTNNB1* mutation and one an *APC* germline mutation. In two sporadic cases no *CTNNB1* mutation was identified. Four patients showed (multiple) recurrences and one patient was lost to follow-up.

In conclusion, multifocal desmoid tumors is a very rare disease and may occur in sporadic cases that are characterized by recurrent *CTNNB1* mutations. However, the underlying pathogenesis of multifocal desmoid tumors remains poorly understood with often aggressive clinical behavior and challenging therapeutical management.

Introduction

Desmoid-type fibromatosis, or desmoid tumor, is a locally aggressive, infiltrative growing myofibroblastic lesion with unpredictable clinical behavior. It may originate at any part of the body with extremities, abdominal wall and mesentery being the most common sites [1]. The peak incidence is in the third decade [1].

Desmoid tumors arise sporadically in approximately 90% of the cases with the remaining 10% being familial [1]. Dysregulation of the Wnt signaling pathway is characteristic in both settings with β-catenin being the key player. In sporadic cases, the most common activating mutations are located in exon 3 of the *CTNNB1* gene (chr 3p22.1) coding for β-catenin. Alternatively, in the remaining sporadic cases and the familial cases that occur in the context of Gardner syndrome (a form of familial adenomatous polyposis), there is a somatic or germline inactivating mutation or allelic deletion in the *APC* tumor suppressor gene (5q22.2) [1-4]. Both mechanisms lead to stabilization of β-catenin with cytoplasmatic and subsequently nuclear accumulation. Withhin the nucleus, β-catenin acts as a transcription factor regulating cell proliferation of myofibroblastic cells [1,5,6].

In the recent years, a paradigm shift in terms of treatment modalities has taken place for desmoids tumors and the overall management is increasingly complex. It has been shown that invasive treatment should be used with caution because of the potential of recurrence, irrespective of the margin status [5, 7-9]. In this context, mutational analysis of *CTNNB1* can give prognostic information, where the hot spot mutation p.Ser45Phe (p.S45F), has been proposed as a possible marker for recurrence [10-12].

Single cases of multifocal desmoid tumors have been described [13-15], but their genetic and clinical characteristics are not well understood. We describe herein a series of multifocal desmoid tumors and their mutational status to pay attention on these rare cases.

Material and Methods

The cases were collected from the authors' files and the nationwide network and registry of histopathology and cytopathology in the Netherlands. Clinical data and follow-up were obtained from the patient records. The study was performed in accordance with the Code of Conduct of the Federation of Medical Scientific Societies in the Netherlands.

In all cases the tissue was fixed in 4% buffered formalin and embedded in paraffin; 2-4 µm thick sections were stained with hematoxylin and eosin and immunohistochemically by the labelled Streptavidin Biotin technique using a commercially available antibody against β-catenin (BD Biosciences, clone 14, dilution 1:100). Appropriate positive and negative controls were used throughout.

DNA was isolated from formalin-fixed, paraffin-embedded material (without decalcification) by proteinase K digestion and the crude DNA extract was used in a standard PCR. The hot spot region for *CTNNB1* was amplified using primers: 5'-ATGGCCATGGAACCAGACAGA-3' and 5'-GCTACTTGTTCTTGAGTGAAGGACTG-3'. The region most frequently mutated in *APC* (NM_000038.5: amino acids 1200-1580) was amplified using the following primer pairs: 1) 5'-CAGATATTCCTTCATCACAGAAAC-3' and 5'-GGAGTATCTTCTACACAATAAGTCTG-3', 2) 5'-GCCACTTGCAAAGTTTCTTC-3' and 5'-TCACAGGATCTTCAGCTGACCT-3', 3) 5'-TCAGACGACACAGGAAGCAGAT-3' and 5'-TTTTGGGTGTCTGAGCACCACT-3', 4) 5'-AGCCAGGCACAAAGCTGTTGAA-3' and 5'-TGTCCAGGGCTATCTGGAAGATCA-3', 5) 5'-ACCATGCAGTGGAATGGTAAGTGG-3' and 5'-TGGAAGAACCTGGACCCTCTGAA-3', 6) 5'-TGGACCTAAGCAAGCTGCAGTA-3' and 5'-CTGCTCTGATTCTGTTTCATTCCCATTGT-3', 7) 5'-TCTGAGCCTCGATGAGCCATTT-3' and 5'-ACGTGATGACTTTGTTGGCATGG-3'. All PCR products were analyzed by fluorescent di-deoxysequencing.

Results

Out of 1392 cases, seven cases with multifocal desmoid tumors were selected; clinicopathological and genetic results are summarized in Table 1. Of the seven patients four were female and three were male. Age ranged from 7-30 years (mean 18.4 years). Lesions were located in knee and gluteus (1), thigh and lower leg (1), thigh and foot (2), trunk, shoulder and neck (1), lower leg and back (1) and both mammae (1). In all cases neoplasms were resected. (Multiple) local recurrences were reported in 4 patients. Two patients experienced no recurrences so far and one patient was lost to follow-up. One patient was additionally treated with systemic (Lucrin, LHRH antagonist, Tamoxifen) and radiation therapy and one patient with radiotherapy only.

Coronal contrast-enhanced spinecho T1-weighted MR-images with fat saturation of the buttock and proximal (Figure 1) and distal (Figure 2) posterior side of the right lower leg in Case 1 showed an irregular lesion compatible with desmoid tumor. The extension of the lesion is displayed between the white arrows.

Histologically, all cases showed classical features of desmoid tumor according to the current WHO classification of tumors of soft tissue and bone [16]: lesions consisted of long fascicles myofibroblastic cells with monomorphous elongated nuclei. There was a variable collagenous background with sometimes coarse collagen bundles. Myxoid features were sometimes focally present. Small vessels were found parallel to the fascicles of tumor cells. A perivascular edema was often seen (Figure 3).

Immunohistochemically, nuclear expression of beta catenin was detected in all cases (Figure 4).

By Sanger sequencing, mutations in *CTNNB1* were found in four cases with p.(Thr41Ala) being the most frequent (n=3) (Figure 5). One case harbored a p.(Ser45Phe) mutation. Two sporadic cases showed no *CTNNB1* mutation and one case was known with a germline *APC* mutation.

In case 1, 5 and 7 two lesions each were tested and yielded the same mutation.

Table 1. Clinicopathological and genetic results

Case nr.	Sex (m/f)	Age of first presentation (y)	Tumor localisations	Therapy	*CTNNB1* Mutation status	Recurrence (after n months)
1	m	13	Knee and gluteus	Resection	c.121A>G* p.Thr41Ala	No
2	f	24	Breasts (left + right)	Resection	no mutation found	No
3	m	17	Upper leg and hallux	Resection	c.134C>T; p.Ser45Phe	Upper leg (10) and hallux (63)
4	f	27	Upper leg and lower leg	Resection	c.121A>G p.Thr41Ala	Lost to follow-up
5	m	11	Upper leg and hallux	Resection	c.121A>G* p.Thr41Ala	Hallux (36)
6	f	30	Abdominal wall, thorax, back, shoulder, neck	Resection, Lucrin, LHRH antagonist, Tamoxifen, RT	no mutation found	Multiple in all locations (6)
7	f	7	Ankle, back and lower leg	Resection	*APC* mutation* (Gardner)	Ankle (7, 18 and 28), back (10)

M, male; f, female; * mutation in two lesions tested

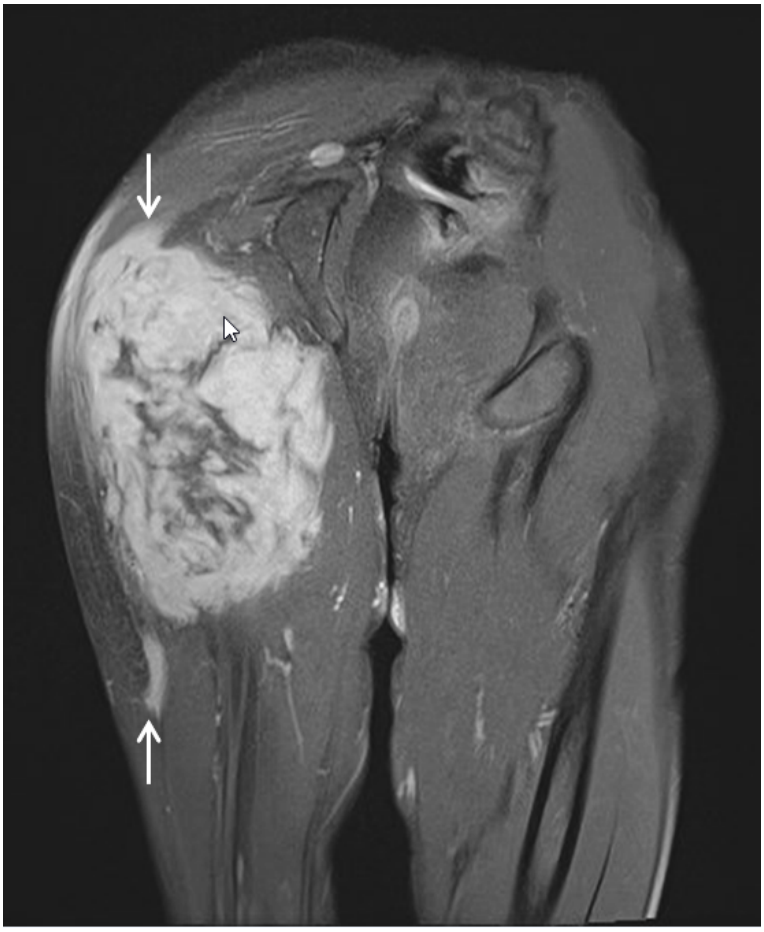

Figure 1. Coronal contrast-enhanced spinecho T1-weighted MR-images with fat saturation of the buttock and proximal posterior side of the right lower leg showed an irregular lesion compatible with desmoid tumor. The extension of the lesion is displayed between the white arrows (Case 1).

Figure 2. Coronal contrast-enhanced spinecho T1-weighted MR-images with fat saturation of the knee/distal posterior side of the right lower leg showed the second desmoid tumor. The extension of the neoplasm is displayed by the white arrows (Case 1).

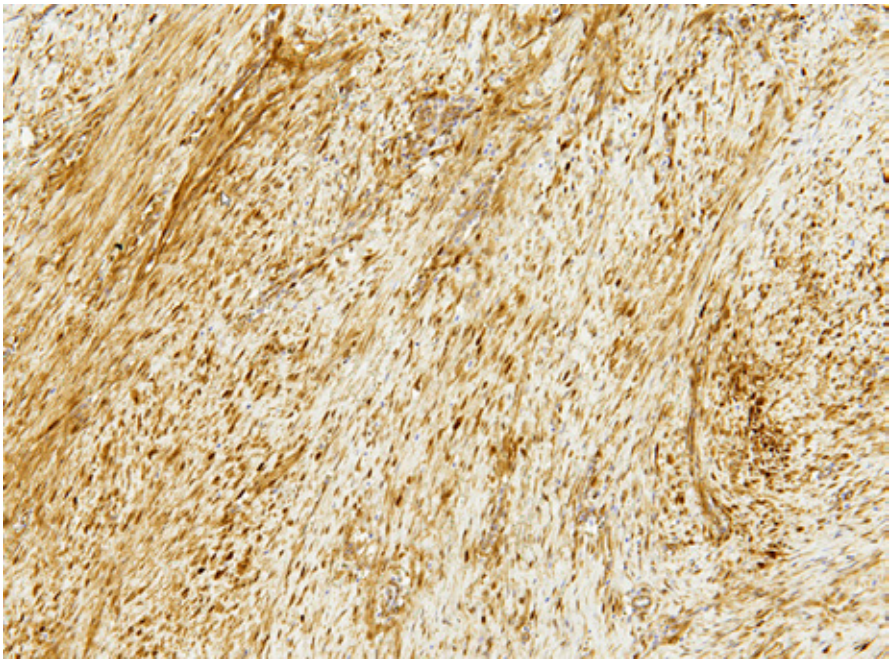

Figure 3. Classical features of desmoid tumor showing long fascicles of monomorphic elongated myofibroblasts were seen in all cases.

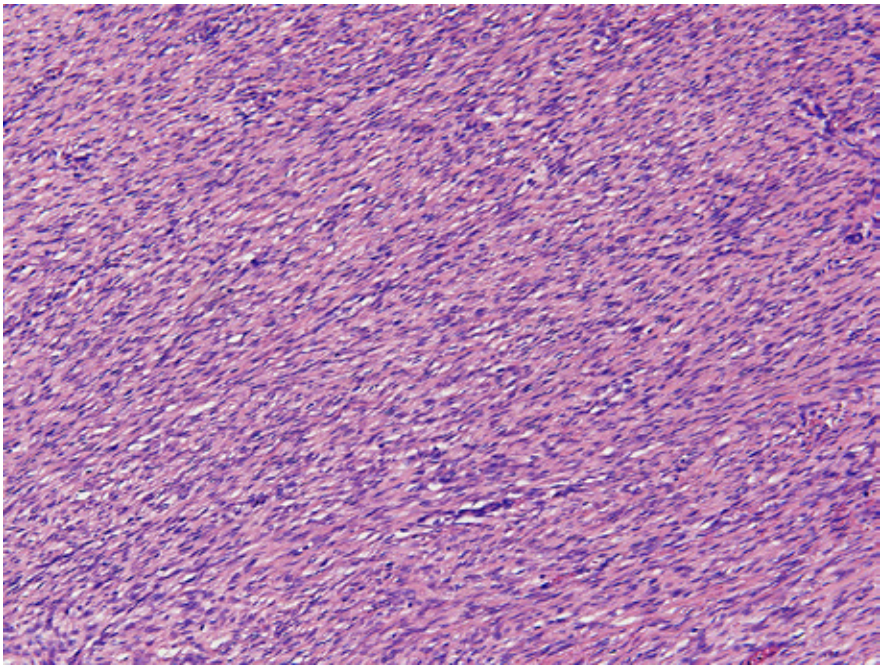

Figure 4. Immunohistochemistry showed nuclear accumulation of β-catenin in all cases.

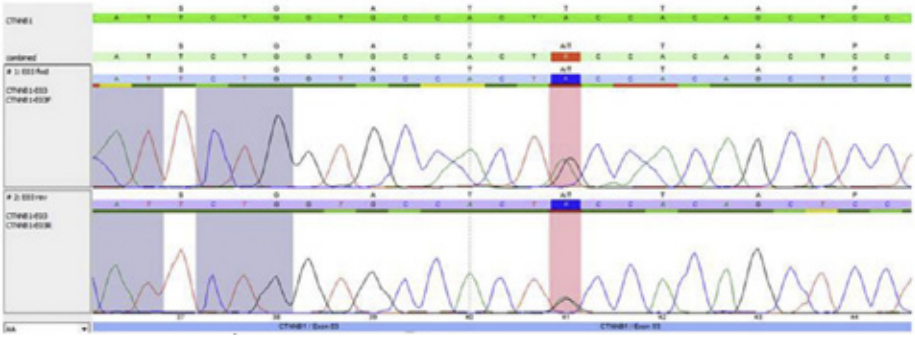

Figure 5. By Sanger sequencing, a c.121A > G (p.Thr41Ala) were detected in three cases.

Discussion

It has been shown that desmoid-type fibromatosis derives from mesenchymal progenitor cells (MPC) harboring a mutation in the *CTNNB1* gene with consecutive β-catenin stabilization [6]. The nuclear accumulated protein binds to transducing beta-like protein leading to expression of several Wnt/APC/β-catenin pathway target genes including proliferation-stimulating factors such as S100A4 resulting in growth of myofibroblastic cells [1].

The capacity of circulation of mesenchymal progenitor cells including *CTNNB1* mutated MPCs could explain multifocal development of this tumor type [6]. This is reflected by the occurrence of the same mutation in the different lesions tested per patient in our series (n=3). However, cases of multifocal desmoid tumors are exceedingly rare and mostly known in patients with germline *APC* mutations and a subsequent second somatic hit [4]. Different *CTNNB1* mutations in multifocal diseases are also reported hypothesizing that genetic alterations can take place in different stages of myofibroblastic progenitor cells [15].

Our small series consist of mainly sporadic multifocal cases and shows that clinical management is naturally more difficult than in the common unilocular cases. In terms of age, localization and mutational status the herein described cases are similar to solitary cases representing young aged patients with lesions mainly in the lower extremities [1].

The course of desmoid tumors is unpredictable, as spontaneous regression, long-lasting stable disease and disease progression can occur. Reliable and validated predictive factors are lacking [1]. In several studies it has been shown that mutational status of the hot spots influences prognosis with p.Ser45Phe (p.S45F)

CTNNB1 mutation being a risk factor for local recurrence after curative intended surgery [10-12]. Nevertheless this is not confirmed by others [17,18].

In terms of mutational status and associated prognosis of multifocal lesions, we cannot draw any conclusion since our series is very small and one case is known with an *APC* germline mutation. However, p.Thr41Ala (p.T41A) is the most common genetic event in our series.

In our cases, recurrences were common (4/7 cases) and surgical intervention limited in some cases due to additional mutilation.

Multimodality treatment including systemic (targeted) therapy could be of special interest [9,19] and identification of reliable clinical or genomic biomarkers predicting behavior of (multifocal) desmoid tumors is needed to facilitate a more patient tailored approach for successful management.

References

1. Penel N, Chibon F, Salas S. Adult desmoid tumors: biology, management and ongoing trials. Curr Opin Oncol 2017;29:268-274.
2. Tejpar S, Nollet F, Li C, Wunder JS, Michils G, Dal Cin P, Van Cutsem E, Bapat B, van Roy F, Cassiman JJ, Alman BA. Predominance of beta-catenin mutations and beta-catenin dysregulation in sporadic aggressive fibromatosis (desmoid tumor). Oncogene 1999;18:6615-6620.
3. Salas S, Chibon F, Noguchi T, Terrier P, Ranchere-Vince D, Lagarde P, Benard J, Forget S, Blanchard C, Dômont J, Bonvalot S, Guillou L, Leroux A, Mechine-Neuville A, Schöffski P, Laë M, Collin F, Verola O, Carbonelle A, Vescovo L, Bui B, Brouste V, Sobol H, Aurias A, Coindre JM. Molecular characterization by array comparative genomic hybridization and DNA sequencing of 194 desmoid tumors. Genes Chromosomes Cancer 2010;49:560-568.
4. Lips DJ, Barker N, Clevers H, et al. The role of APC and β-catenin in the aetiology of aggressive fibromatosis (desmoid tumors). Eur J Surg Oncol 2009,35:3-10.
5. Kattentidt Mouravieva AA, Geurts-Giele IR, de Krijger RR, van Noesel MM, van de Ven CP, van den Ouweland AM, Kromosoeto JN, Dinjens WN, Dubbink HJ, Smits R, Wagner A. Identification of familial adenomatosis carriers among children with desmoid tumours. Eur J Cancer 2012;48:1867-1874.
6. Wu C, Nik-Amini S, Nadesan P, Stanford WL, Alman BA. Aggressive fibromatosis (desmoid tumor) is derived from mesenchymal progenitor cells. Cancer Res 2010;70:7690-7698.
7. Janssen ML, van Broekhoven DL, Cates JM, et al. Meta-analysis of the influence of surgical margin and adjuvant radiotherapy on local recurrence after resection of sporadic desmoid-type fibromatosis. Br J Surg 2017;104:347-357.
8. Broekhoven DL, Grünhagen DJ, van Dalen T, van Coevorden F, Bonenkamp HJ, Been LB, Bemelmans MH, Dijkstra SD, Colombo C, Gronchi A, Verhoef C. Tailored beta-catenin mutational approach in extra-abdominal sporadic desmoid tumor patients without therapeutic intervention. BMC Cancer 2016;16:686
9. Eastley N, McCulloch T, Esler C, Hennig I, Fairbairn J, Gronchi A, Ashford R. Extra-abdominal desmoid fibromatosis: A review of management, current guidance and unanswered questions. Eur J Surg Oncol 2016;42:1071-108.
10. Lazar AJ, Tuvin D, Hajibashi S, Habeeb S, Bolshakov S, Mayordomo-Aranda E, Warneke CL, Lopez-Terrada D, Pollock RE, Lev D. Specific mutations in the β-catenin gene (CTNNB1) correlate with local recurrence in sporadic desmoid tumors. Am J Pathol 2008;173:1518-1527.
11. Colombo C, Miceli R, Lazar AJ, Perrone F, Pollock RE, Le Cesne A, Hartgrink HH, CleatoWn-Jansen AM, Domont J, Bovée JV, Bonvalot S, Lev D, Gronchi A. CTNNB1 45F mutation is a molecular prognosticator of increased postoperative primary desmoid tumor recurrence: an independent, multicenter validation study. Cancer 2013;119:3696-3702.
12. Van Broekhoven DL, Verhoef C, Grünhagen DJ, van Gorp JM, den Bakker MA, Hinrichs JW, de Voijs CM, van Dalen T. Prognostic value of CTNNB1 gene mutation in primary sporadic aggressive fibromatosis. Ann Surg Oncol 2015;22:1464-1470
13. Shimoyama T, Hiraoka K, Shoda T, Hamada T, Fukushima N, Nagata K. Multicentric extraabdominal desmoid tumors arising in bilateral lower limbs. Rare Tumors 2010;2:e12.
14. Garg P, Chufal SS, Gupta N, Pant P, Thapliyal NC. Multicentric aggressive mammary fibromatosis with cytological features and review of literature. J Clin Diagn Res 2014;8:FD01-FD03

15. Doyen J, Duranton-Tanneur V, Hostein I, Karanian-Philippe M, Chevreau C, Breibach F, Coutts M, Dadone B, Saint-Paul MC, Gugenheim J, Duffaud F, Pedouteur F. Spatio-temporal genetic heterogeneity of CTNNB1 mutations in sporadic desmoid type fibromatosis lesions. Virchows Arch 2016;468:369-374.

16. Goldblum JR, Fletcher JA. Desmoid-type fibromatosis. In Fletcher CDM, Bridge JA, Hogendoorn PCW, Mertens F (Eds.): WHO classification of tumours of soft tissue and bone. IARC: Lyon 2013; Wpp 72-73.

17. Dômont J, Salas S, Lacroix L, Brouste V, Saulnier P, Terrier P, Ranchère D, Neuville A, Leroux A, Guillou L, Sciot R, Collin F, Dufresne A, Blay JY, Le Cesne A, Coindre JM, Bonvalot S, Bénard J. High frequency of β-catenin heterozygous mutations in extra-abdominal fibromatosis: a potential molecular tool for disease management. Br J Cancer 2010:102:1032-1036.

18. Mullen JT, DeLaney TF, Rosenberg AE, Le L, Iafrate AJ, Kobayashi W et al. B-catenin mutation status and outcomes in sporadic desmoid tumors. Oncologist 2013;18:1043-1049.

19. Heinrich MC, McArthur GA, Demetri GD, Joensuu H, Bono P, Herrmann R, Hirte H, Cresta S, Koslin DB, Corless CL, Dirnhofer S, van Oosterom AT, Niklova Z, Dimitrijevic S, Fletcher JA. Clinical and molecular studies of the effect of imatinib on advanced aggressive fibromatosis (desmoid tumor). J Clin Oncol 2006;24:1195-1203.

Chapter 9

Summary

Soft tissue tumors are relatively rare, comprising a large and broad spectrum of diagnostic entities. Due to overlapping features, they are often diagnostically challenging. In recent years, substantial advances have been made in identifying recurrent genomic alterations for each of the different entities, which has led to a great progress in our understanding of biological mechanisms underlying soft tissue tumor pathogenesis and created new valuable diagnostic tools. These new pathogenetic insights have led and will continuously lead to reclassification and subclassification of diagnostic entities, and will shape a more nuanced and clinically relevant classification of soft tissue tumors (**chapter 1**).

In this respect, we have studied recurrent genetic changes in multiple tumor types using different molecular techniques with the main topic focused on myxoid tumors, including intramuscular myxomas and cardiac myxomas. Additionally, the expanding spectrum of tumors with *USP6* gene rearrangements were described. Finally, gene fusions in soft tissue angiofibroma and myxoid liposarcoma, and mutations of the *CTNNB1* oncogene in the rare multifocal occurrence of desmoid fibromatosis were included.

Myxoid soft tissue tumors are characterized by their abundant extracellular matrix material. They represent a heterogeneous group of tumors ranging from localized benign lesions without invading growth properties to high-grade sarcomas. There is considerable clinical and morphological overlap between the different entities, creating problems in differential diagnosis. Immunohistochemistry is usually of little help since the different tumor types display no specific immunoprofile. Complementary approaches, such as molecular diagnostics, can corroborate the diagnosis in several lesions within the group of myxoid tumors [1].

Intramuscular myxoma (IM), as discussed in **chapter 2**, is usually a hypocellular tumor, often with hypercellular areas [2, 3]. Especially on small biopsies these tumors can easily be confused with low-grade fibromyxoid sarcoma or low-grade myxofibrosarcoma [4, 5]. The prevailing view is that driver mutations of this neoplasm are exclusively located in codon 201 within exon 8 of the *GNAS* gene (hotspot mutations c.601C>T and c602G>A), encoding the stimulatory G-protein alpha subunit that activates the enzyme adenylate cyclase. Due to the low cellularity and somatic mosaicism in most of these lesions, mutation detection can be quite challenging and the presence of a mutation can be easily missed [6-8]. In our study, we used the sensitive next-generation sequencing (NGS)-based approach employing single-molecule tagged molecular inversion probes (smMIP) to investigate the prevalence of *GNAS* mutations in IM [9, 10]. The smMIP technique combines multiplex analysis with

single-molecule tagging, also named unique molecular identifiers (UMIs). Since our approach involved *GNAS* whole exon 8 and 9 sequencing, this allowed detection of four additional mutations that previously were not described in IM. We identified one c.680A>G mutation in exon 9, and three novel mutations in exon 8. One mutation at position c.601, namely c.601C>A, has previously been reported in fibrous dysplasia, while two mutations at position c.602, which included c.602G>C and c.602G>T, were only reported in sporadic endocrine tumors so far [11-14].

The cAMP-dependent protein kinase, or protein kinase A (PKA) is part of a signal transduction cascade. PKA regulates complex protein phosphorylation networks that eventually lead to a wide spectrum of physiological functions, ranging from stereoidogenesis in the adrenal cortex to stem cell maintenance in the hair follicle (Figure 1) [15]. There are multiple pathways involving PKA that are well known, for example the Ras pathway and the transforming growth factor-β pahway (TGF-β). The most recent studied pathway is the Gαs-PKA pathway with mutations seen in *GNAS*, *PRKACA* and *PRKAR1A.*

The mechanism of tumorigenesis in IM is not fully understood, but the prevailing view is that *GNAS* mutations in skeletal muscle mesenchymal stem cells (MSCs) lead to a myxoid phenotype [16]. A remarkable similarity is present in the case of cardiac myxomas, where inactivating mutations in *PRKAR1A,* also involved in the Gαs-PKA pathway as mentioned earlier, thought to arise in the endocardial MSCs also lead to a myxoid phenotype suggesting that mutations in the PKA pathway could be responsible for the myxoid nature of these tumors [17].

In **chapter 3** we discuss the topic of cardiac myxomas, a benign myxoid neoplasm which is one of the hallmarks of Carney Complex (CNC), a familial multiple neoplasia syndrome, which displays in about 80% of the index cases germline mutations in *PRKAR1A* encoding the RIα regulatory subunit of cAMP-dependent protein kinase A (PKA). Mutations within the *PRKAR1A* gene result in a mutant protein or lead to non-sense mRNA lacking translation into RIα protein, also called non-sense mediated mRNA decay [18, 19]. This loss of RIα function eventually results in unrestrained activity of the PKA catalytic subunits leading to increased cell proliferation and tumor formation. However, the role of *PRKAR1A* gene mutations in the pathogenesis of non-CNC-associated sporadic cardiac myxoma is less well established.

Like IM the relative hypocellularity of this tumor and the following low concentration of isolated DNA will benefit from sensitive techniques for mutation detection. We investigated the presence of *PRKAR1A* gene mutations using two complementary

targeted next-generation sequencing techniques (Ion Torrent amplicon-NGS (Ion AmpliSeq) and single molecule molecular inversion probe (smMIP) technique) in a cohort of 24 sporadic cardiac myxoma. Our studies showed that 14 out of 24 (58%) sporadic cardiac myxoma harbor *PRKAR1A* gene mutations, represented mostly by frameshift, nonsense and splice site mutations (together 84%), leading to a premature stop codon and predicted to be degraded via non-sense mediated mRNA decay. The other 16% of *PRKAR1A* genetic alterations involved missense mutations, often located in important functional domains of the regulatory subunit RIα. Notably, 64% (n=9/14) of the sporadic cardiac myxoma cases harbored more than one *PRKAR1A* gene variant, suggesting compound heterogenous either in *cis* or *trans*. In conclusion, *PRKAR1A* gene mutations associated with loss of RIα function leading to increased PKA activity were observed in ~60% of sporadic cardiac myxoma cases, strongly supporting an essential role for PKA in mediating cardiac myocyte cell proliferation and myxoma tumorigenesis as observed by Di Vito et al. [17].

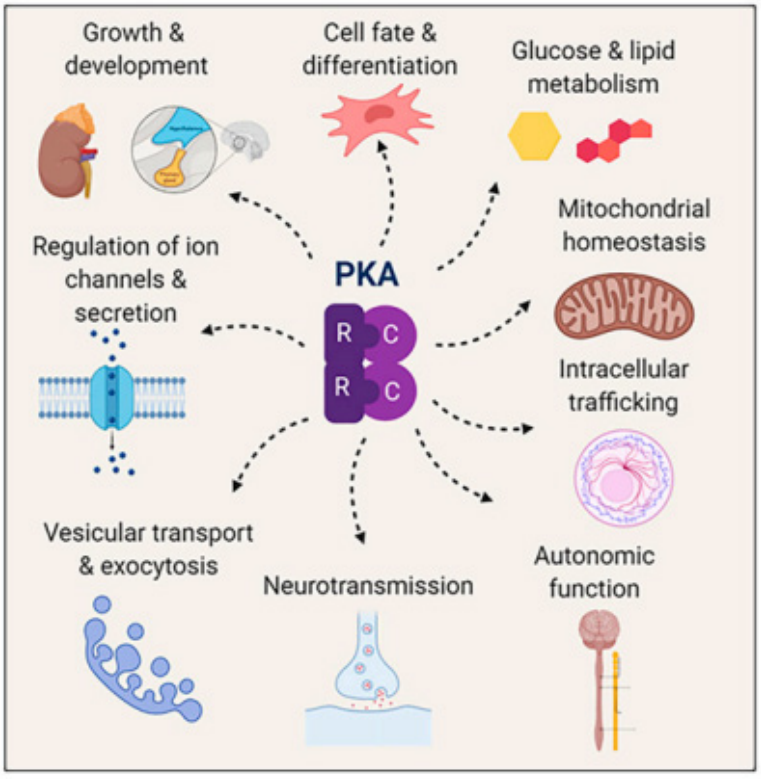

Figure 1. Protein kinase A is a central regulatory hub that mediates many physiologic processes, from hormonal growth and metabolism to transport and secretion [15].

Recurrent *USP6* gene rearrangements have been identified as a consistent genetic driving event in aneurysmal bone cyst (ABC) first described in 2004. Since then, it has been described in nodular fasciitis, myositis ossificans, fibro-osseous pseudotumour of digits, and cellular fibroma of tendon sheath [20]. USP6 (ubiquitin specific protease) is one of many deubiquinating enzymes involved in several cellular processes, such as intracellular trafficking, protein turnover, inflammatory signaling, and cell transformation. The *USP6* fusion gene causes transcriptional upregulation of the entire coding sequence of *USP6* due to promoter switch. This leads to tumorigenesis, osteoblastic maturation, osteolysis, inflammation and neovascularization through several pathways, including NF-κB, Wnt/β-catenin, Jak1-STAT3 and c-Jun, that can transform mesenchymal cells and affects multiple osteoblasts regulatory pathways [21-26]. Remarkably nodular fasciitis, myositis ossificans, fibro-osseous pseudotumor of digits (FOPD), and aneurysmal bone cyst all share clinicopathological characteristics. These disorders mainly occur in younger patients and show bland looking myofibroblastic tissue culture-like morphology, and variable production of bone (mainly in myositis ossificans and FOPD). The abnormalities appear sudden with rapid growth and secondary involution, and are therefore called transient neoplasms when occurring in soft tissue [2, 27]. In **chapter 4** and **5,** we reported on the frequency of *USP6* gene rearrangement in myositis ossificans and FOPD, respectively. Like nodular fasciitis and APC, both these conditions harbor *USP6* gene rearrangements, which show that these lesions form a spectrum of diseases rather than being separate entities, as is also discussed in **chapter 4** and **5**. In the present day these neoplasms are well-known and are collectively referred to as '*USP6*-associated neoplasms' [28]. Screening for *USP6* rearrangement is there for now an integral part of the diagnostic workup when dealing with (myo)fibroblastic lesions of soft tissue and bone [21, 27-32].

Another possible differential diagnosis in the myxoid fibroblastic/myofibroblastic group is soft tissue angiofibroma (STAF), especially the myxoid variant. STAF is a rare and recently defined benign soft tissue tumor entity and has characteristic histomorphological and genetic features, which includes recurrent chromosomal translocation t(5;8)(p15;q13), resulting in a consistent rearrangement of *NCOA2* in a large subset of cases [33, 34]. The majority of STAFs contain the *AHRR- NCOA2* fusion transcript [33, 35]. Other previously identified fusion genes include the reciprocal *NCOA2-AHRR*, *NCOA2-ETV4*, *ETV4-AHRR*, *P4HA2-TBCK*, *TBCK-P4HA2* and *GTF2I-NCOA2* [33, 35-37]. In our study, as described in **chapter 6**, we identified the novel *GAB1-ABL1* fusion transcript by RT-PCR as an alternative fusion gene in STAF that previously had not been described.

GAB1 (Grb2-associated binding protein 1) belongs to a family of scaffolding proteins and is involved in the integration of different signal transductions including the MAPK and PI3K cascades [38]. *ABL1* (Abelson tyrosin protein kinase 1) is a proto-oncogene with cell cycle function involved in a variety of cellular processes, including cell division, adhesion and differentiation. The *GAB1-ABL1* fusion places *ABL1* kinase expression under the control of the *GAB1* promotor. Since our first description three other studies also showed a *GAB1-ABL1* fusion in benign soft tissue tumors that were referred to as solitary fibrous tumor, soft tissue perineurioma and STAF [39-41]. Like the '*USP6*-associated neoplasms' mentioned before, there is now an incentive to reclassify these cases as '*GAB1::ABL1* fusion-positive spindle cell neoplasms' that have, similar to our described case, a predilection for children and young adults [39].

Recurrent fusion genes act as oncogenic drivers in a growing number of soft tissue tumors and molecular analysis is a valuable diagnostic adjunct, especially in biopsies of tumor types without a specific immunohistochemical profile. Moreover, fusion genes harbor important tumor-related therapeutic and prognostic consequences in malignant lesions. For example, myxoid liposarcoma (MLS), a potential mimic of STAF and other myxoid tumors [2, 34, 42, 43], is a malignant tumor where approximately one-third of cases show tendency to metastasize to other soft tissue sites, including mediastinum and retroperitoneum, but also to bone, lung and liver with a consecutive fatal outcome [44]. In **chapter 7**, we reported on MLS at distal sites of the extremities which is exceedingly rare [45-48]. MLS is the only translocation-associated liposarcoma subtype and the majority harbors the specific fusion gene *FUS-DDIT3* and, more rarely, *EWSR1-DDTI3*. These gene fusions were also detected in our study by using RT-PCR and FISH. The different isoforms of *FUS-DDIT3* fusion transcripts are not associated with distinct histology or clinical outcome [49, 50]. Atypical presentation of MLS is important to recognize, due to its ability to widespread metastasize. This is even more important when adequate surgical margins are difficult to reach, such as in the foot and ankle.

In **chapter 8** we characterized multifocal desmoid tumors. This is an exceedingly rare event and mostly seen in patients with a germline *APC* mutations with a subsequent second somatic hit. However, sporadic multifocal desmoid fibromatosis can also occur and their genetic and clinical characteristics are not well understood. Desmoid fibromatosis are derived from mesenchymal progenitor cells (MPC) harboring a recurrent *CTNNB1* mutation leading to nuclear accumulation of β-Catenin. Within the nucleus, it acts as a transcription factor subsequently

leading to activation of the Wnt signaling pathway resulting in cell proliferation of myofibroblastic cells [31, 51, 52].

The migrating capacity of mesenchymal progenitor cells, including the *CTNNB1* mutated MPCs, could explain multifocal development of this tumor type [52]. This is reflected by the occurrence of the same mutation in the different lesions tested per patient in our series as described in **chapter 8**. On the other hand, different *CTNNB1* mutations in multifocal desmoid tumors have also been reported, hypothesizing that these genetic events can take place in different developmental stages of MPC [53]. Clinical management is naturally more difficult in multifocal cases than in the commonly unilocular cases. Several studies have shown that specific *CTNNB1* hotspot mutations influence prognosis, with p.Ser45Phe (p.S45F) *CTNNB1* mutation being a risk factor for local recurrence after curative surgery [54-56]. Therefore, identification of reliable clinical or genetic biomarkers predicting behavior in (multi)focal desmoid fibromatosis is needed to facilitate a more patient tailored approach for successful clinical management.

All above-described molecular changes are stable genetic events and their detection can be used as a complementary diagnostic tool and help clinicians with treatment management. New insights in genomic alterations can also influence the well-known morphological soft tissue tumor classification leading to the recognition of new tumor subtypes. Each subtype will share common genetic features shaping a more nuanced and clinical relevant classification of soft tissue tumors, which will help to make therapeutic decisions.

References

1. Miettinen, M., Modern soft tissue pathology: tumors and non-neoplastic conditions. 2010: Cambridge University Press.
2. Fletcher CDM, B.J., Hogendoorn PCW, Mertens F, eds, World Health Organization Classification of Soft Tissue and Bone. 4th Edition, ed. B.J. Fletcher CDM, Hogendoorn PCW, Mertens F. 2013, Lyon: IARC Press.
3. Nielsen, G.P., J.X. O'Connell, and A.E. Rosenberg, Intramuscular myxoma: a clinicopathologic study of 51 cases with emphasis on hypercellular and hypervascular variants. Am J Surg Pathol, 1998. 22(10): p. 1222-7.
4. Bartuma, H., et al., Fusion of the FUS and CREB3L2 genes in a supernumerary ring chromosome in low-grade fibromyxoid sarcoma. Cancer Genet Cytogenet, 2010. 199(2): p. 143-6.
5. Mertens, F., et al., Clinicopathologic and molecular genetic characterization of low-grade fibromyxoid sarcoma, and cloning of a novel FUS/CREB3L1 fusion gene. Lab Invest, 2005. 85(3): p. 408-15.
6. Okamoto, S., et al., Activating Gs(alpha) mutation in intramuscular myxomas with and without fibrous dysplasia of bone. Virchows Arch, 2000. 437(2): p. 133-7.
7. Delaney, D., et al., GNAS1 mutations occur more commonly than previously thought in intramuscular myxoma. Mod Pathol, 2009. 22(5): p. 718-24.
8. Walther, I., et al., Analysis of GNAS1 mutations in myxoid soft tissue and bone tumors. Pathol Res Pract, 2014. 210(1): p. 1-4.
9. Eijkelenboom, A., et al., Reliable Next-Generation Sequencing of Formalin-Fixed, Paraffin-Embedded Tissue Using Single Molecule Tags. J Mol Diagn, 2016. 18(6): p. 851-863.
10. Hiatt, J.B., et al., Single molecule molecular inversion probes for targeted, high-accuracy detection of low-frequency variation. Genome Res, 2013. 23(5): p. 843-54.
11. Candeliere, G.A., P.J. Roughley, and F.H. Glorieux, Polymerase chain reaction-based technique for the selective enrichment and analysis of mosaic arg201 mutations in G alpha s from patients with fibrous dysplasia of bone. Bone, 1997. 21(2): p. 201-6.
12. Gorelov, V.N., et al., Overexpression of Gs alpha subunit in thyroid tumors bearing a mutated Gs alpha gene. J Cancer Res Clin Oncol, 1995. 121(4): p. 219-24.
13. Schwindinger, W.F., C.A. Francomano, and M.A. Levine, Identification of a mutation in the gene encoding the alpha subunit of the stimulatory G protein of adenylyl cyclase in McCune-Albright syndrome. Proc Natl Acad Sci U S A, 1992. 89(11): p. 5152-6.
14. Shenker, A., et al., Severe endocrine and nonendocrine manifestations of the McCune-Albright syndrome associated with activating mutations of stimulatory G protein GS. J Pediatr, 1993. 123(4): p. 509-18.
15. Ramms, D.J., et al., Galphas-Protein Kinase A (PKA) Pathway Signalopathies: The Emerging Genetic Landscape and Therapeutic Potential of Human Diseases Driven by Aberrant Galphas-PKA Signaling. Pharmacol Rev, 2021. 73(4): p. 155-197.
16. Sunitsch, S., et al., Detection of GNAS mutations in intramuscular / cellular myxomas as diagnostic tool in the classification of myxoid soft tissue tumors. Diagn Pathol, 2018. 13(1): p. 52.
17. Di Vito, A., C. Mignogna, and G. Donato, The mysterious pathways of cardiac myxomas: a review of histogenesis, pathogenesis and pathology. Histopathology, 2015. 66(3): p. 321-32.
18. Horvath, A., et al., Mutations and polymorphisms in the gene encoding regulatory subunit type 1-alpha of protein kinase A (PRKAR1A): an update. Hum Mutat, 2010. 31(4): p. 369-79.

19. Bertherat, J., et al., Mutations in regulatory subunit type 1A of cyclic adenosine 5'-monophosphate-dependent protein kinase (PRKAR1A): phenotype analysis in 353 patients and 80 different genotypes. J Clin Endocrinol Metab, 2009. 94(6): p. 2085-91.
20. Cordier, F. and D. Creytens, Unravelling the USP6 gene: an update. J Clin Pathol, 2023. 76(9): p. 573-577.
21. Oliveira, A.M. and M.M. Chou, USP6-induced neoplasms: the biologic spectrum of aneurysmal bone cyst and nodular fasciitis. Hum Pathol, 2014. 45(1): p. 1-11.
22. Legrand, M., M.L. Jourdan, and G. de Pinieux, Histopathogenesis of bone- and soft-tissue tumor spectrum with USP6 gene rearrangement: multiple partners involved in the tissue repair process. Histol Histopathol, 2023. 38(3): p. 247-260.
23. Li, L., et al., Ubiquitin-Specific Protease USP6 Regulates the Stability of the c-Jun Protein. Mol Cell Biol, 2018. 38(2).
24. Madan, B., et al., USP6 oncogene promotes Wnt signaling by deubiquitylating Frizzleds. Proc Natl Acad Sci U S A, 2016. 113(21): p. E2945-54.
25. Pringle, L.M., et al., Atypical mechanism of NF-kappaB activation by TRE17/ubiquitin-specific protease 6 (USP6) oncogene and its requirement in tumorigenesis. Oncogene, 2012. 31(30): p. 3525-35.
26. Quick, L., et al., Jak1-STAT3 Signals Are Essential Effectors of the USP6/TRE17 Oncogene in Tumorigenesis. Cancer Res, 2016. 76(18): p. 5337-47.
27. Erickson-Johnson, M.R., et al., Nodular fasciitis: a novel model of transient neoplasia induced by MYH9-USP6 gene fusion. Lab Invest, 2011. 91(10): p. 1427-33.
28. Hiemcke-Jiwa, L.S., et al., USP6-Associated Neoplasms: A Rapidly Expanding Family of Lesions. Int J Surg Pathol, 2020. 28(8): p. 816-825.
29. Amary, M.F., et al., Detection of USP6 gene rearrangement in nodular fasciitis: an important diagnostic tool. Virchows Arch, 2013. 463(1): p. 97-8.
30. Oliveira, A.M., et al., USP6 (Tre2) fusion oncogenes in aneurysmal bone cyst. Cancer Res, 2004. 64(6): p. 1920-3.
31. Patel, N.R., et al., USP6 activation in nodular fasciitis by promoter-swapping gene fusions. Mod Pathol, 2017. 30(11): p. 1577-1588.
32. Agaram, N.P., et al., USP6 gene rearrangements occur preferentially in giant cell reparative granulomas of the hands and feet but not in gnathic location. Hum Pathol, 2014. 45(6): p. 1147-52.
33. Jin, Y., et al., Fusion of the AHRR and NCOA2 genes through a recurrent translocation t(5;8)(p15;q13) in soft tissue angiofibroma results in upregulation of aryl hydrocarbon receptor target genes. Genes Chromosomes Cancer, 2012. 51(5): p. 510-20.
34. Marino-Enriquez, A. and C.D. Fletcher, Angiofibroma of soft tissue: clinicopathologic characterization of a distinctive benign fibrovascular neoplasm in a series of 37 cases. Am J Surg Pathol, 2012. 36(4): p. 500-8.
35. Yamada, Y., et al., Histological spectrum of angiofibroma of soft tissue: histological and genetic analysis of 13 cases. Histopathology, 2016. 69(3): p. 459-69.
36. Arbajian, E., et al., A novel GTF2I/NCOA2 fusion gene emphasizes the role of NCOA2 in soft tissue angiofibroma development. Genes Chromosomes Cancer, 2013. 52(3): p. 330-1.
37. Panagopoulos, I., et al., Gene fusions AHRR-NCOA2, NCOA2-ETV4, ETV4-AHRR, P4HA2-TBCK, and TBCK-P4HA2 resulting from the translocations t(5;8;17)(p15;q13;q21) and t(4;5)(q24;q31) in a soft tissue angiofibroma. Oncol Rep, 2016. 36(5): p. 2455-2462.

38. Chen, L., et al., Novel inhibitors induce large conformational changes of GAB1 pleckstrin homology domain and kill breast cancer cells. PLoS Comput Biol, 2015. 11(1): p. e1004021.
39. Agaimy, A., et al., GAB1::ABL1 fusions define a distinctive soft tissue neoplasm, with variable perineurial differentiation, and a predilection for children and young adults. Genes Chromosomes Cancer, 2023. 62(8): p. 449-459.
40. Choo, F., et al., GAB1-ABL1 fusions in tumors that have histologic overlap with NTRK-rearranged spindle cell tumors. Genes Chromosomes Cancer, 2021. 60(9): p. 623-630.
41. Panagopoulos, I., et al., Recurrent Fusion of the GRB2 Associated Binding Protein 1 (GAB1) Gene With ABL Proto-oncogene 1 (ABL1) in Benign Pediatric Soft Tissue Tumors. Cancer Genomics Proteomics, 2020. 17(5): p. 499-508.
42. Wortman, J.R., et al., Neoadjuvant radiation in primary extremity liposarcoma: correlation of MRI features with histopathology. Eur Radiol, 2016. 26(5): p. 1226-34.
43. Wang, W.L., et al., Extensive adipocytic maturation can be seen in myxoid liposarcomas treated with neoadjuvant doxorubicin and ifosfamide and pre-operative radiation therapy. Clin Sarcoma Res, 2012. 2(1): p. 25.
44. Antonescu, C.R., et al., Monoclonality of multifocal myxoid liposarcoma: confirmation by analysis of TLS-CHOP or EWS-CHOP rearrangements. Clin Cancer Res, 2000. 6(7): p. 2788-93.
45. Chang, H.R., et al., The prognostic value of histologic subtypes in primary extremity liposarcoma. Cancer, 1989. 64(7): p. 1514-20.
46. Buehler, D., T.B. Marburger, and S.D. Billings, Primary subcutaneous myxoid liposarcoma: a clinicopathologic review of three cases with molecular confirmation and discussion of the differential diagnosis. J Cutan Pathol, 2014. 41(12): p. 907-15.
47. Nishio, J., et al., Myxoid liposarcoma of the ankle: a case report. J Foot Ankle Surg, 2012. 51(1): p. 76-9.
48. Werd, M.B., et al., Myxoid liposarcoma of the ankle. J Foot Ankle Surg, 1995. 34(5): p. 465-74.
49. Antonescu, C.R., et al., Prognostic impact of P53 status, TLS-CHOP fusion transcript structure, and histological grade in myxoid liposarcoma: a molecular and clinicopathologic study of 82 cases. Clin Cancer Res, 2001. 7(12): p. 3977-87.
50. Bode-Lesniewska, B., et al., Relevance of translocation type in myxoid liposarcoma and identification of a novel EWSR1-DDIT3 fusion. Genes Chromosomes Cancer, 2007. 46(11): p. 961-71.
51. Salas, S., et al., Molecular characterization by array comparative genomic hybridization and DNA sequencing of 194 desmoid tumors. Genes Chromosomes Cancer, 2010. 49(6): p. 560-8.
52. Wu, C., et al., Aggressive fibromatosis (desmoid tumor) is derived from mesenchymal progenitor cells. Cancer Res, 2010. 70(19): p. 7690-8.
53. Doyen, J., et al., Spatio-temporal genetic heterogeneity of CTNNB1 mutations in sporadic desmoid type fibromatosis lesions. Virchows Arch, 2016. 468(3): p. 369-74.
54. Colombo, C., et al., CTNNB1 45F mutation is a molecular prognosticator of increased postoperative primary desmoid tumor recurrence: an independent, multicenter validation study. Cancer, 2013. 119(20): p. 3696-702.
55. Lazar, A.J., et al., Specific mutations in the beta-catenin gene (CTNNB1) correlate with local recurrence in sporadic desmoid tumors. Am J Pathol, 2008. 173(5): p. 1518-27.
56. van Broekhoven, D.L., et al., Prognostic value of CTNNB1 gene mutation in primary sporadic aggressive fibromatosis. Ann Surg Oncol, 2015. 22(5): p. 1464-70.

Chapter 10

Discussion and future perspectives

Soft tissue tumors are thought to originate during the process of mesenchymal stem cell (MSC) differentiation and transformation. This process is influenced by many different genetic changes occurring in oncogenes and tumor suppressor genes that affect many downstream signaling pathways crucial for neoplastic growth [1]. As far as we know up till now, three core molecular mechanisms drive soft tissue tumorigenesis: (i) dysregulation of gene expression by aberrant chimeric transcription factors generated by specific gene fusions in translocation-associated soft tissue tumors, (ii) somatic mutations in key genes involved in signaling pathways, (iii) and DNA copy number alterations, which also involve genes that play a role in proliferation, apoptosis and cell differentiation.

Major advances have been made in recent years in molecular technologies identifying recurrent chromosomal and genomic alterations in soft tissue tumors leading to enhanced knowledge of biological mechanisms associated with soft tissue tumor development. This has accelerated the discovery of novel diagnostic, prognostic and predictive molecular biomarkers [2-4]. At present, high-throughput genome-wide molecular methods, like massive parallel sequencing (MPS) also known as next-generation sequencing (NGS), are being used in daily diagnostic practice and will continue to be an important clinical tool in soft tissue tumor management [5-7].

MPS technologies can extract information from the genome (DNA), transcriptome (RNA), epigenome (methyl-Seq) and chromatin (ChIP-Seq) as described in more detail below. These sequencing platforms are much faster and more comprehensive methods than the traditional Sanger sequencing. However these techniques can be labor-intensive and generate much more data than required for diagnostics [6]. This has led to the development of more focused version of MPS, known as targeted sequencing. These platforms use a more selective profile of genes or regions that are already known to be associated with tumor pathogenesis [8]. Targeted MPS uses either hybridization capture or amplicon-based enrichment with multiplex PCR. Thereby a panel of specific target genomic regions can be sequenced more efficiently and at greater depth [5, 9, 10].

Hybridization capture technique can be applied with DNA or RNA (e.g. Illumina Trusight) and has the advantage of only needing as little as 10 ng input. In case of soft tissue tumors this is especially helpful considering often limited sampling in form of biopsies, hypocellularity of tumors and poor-quality FFPE samples [11-13]. In comparison to amplicon-based methods, hybridization capture requires more input DNA or RNA, takes longer and is more expensive [14].

Amplicon-based methods (e.g. Archer or Oncomine), like hybridization capture can be used with DNA or RNA and have a simpler and faster workflow, but are less robust with large panels, and may therefore miss more mutations [9, 15]. Both methods however are able to detect alternative unknown fusions partners unlike the traditional RT-PCR with Sanger. This is particularly useful given the promiscuity of soft tissue-associated genes like *EWSR1* and *FUS*. Both methods are primarily used with RNA sequencing, because it gives the technical advantage to pick up the breaking points of these genes, since these ends lie closer together in comparison to DNA sequencing where these breaking points are widely divided over the genome and therefore much more difficult to pick up. Continuing improvements are being made in both hybridization capture and amplicon-based techniques to reduce bias and errors as well as increasing multiplex capacity [16, 17]. This is attractive in soft tissue tumor diagnostics since it detects structural rearrangements defining translocation-associated entities, and is now the most popular mode for the discovery of novel fusion genes. Combining these outcomes with clinical data is required to define a clinical relevant picture leading to patient-tailored management. RNA sequencing is already incorporated in the pathological diagnostic work-up in most academic laboratories in the past few years and will spread to more laboratories in the near future.

In past few years, MPS sequencing techniques also have shown an important role for mutation detection in epigenetic regulatory complexes especially in soft tissue tumors. These proteins help to control the accessibility of genes and thus the transcriptional signature of a cell through interactions with, or direct modifications of chromatin. Dysfunction in these epigenetic regulators of chromatin can lead to activation of oncogenic pathways or silencing tumor suppressors by altering the expression of numerous downstream target genes [18, 19]. In some tumors these critical target genes are known, but in many others these remain to be characterized.

Especially in the past decade epigenetic dysregulation has shown to be an important factor in histogenesis of soft tissue tumors [2, 18, 19]. Mutations in epigenetic regulators that lead to this epigenetic dysregulation can have effects on DNA methylation and histone modification. Because these epigenetic mechanisms modify gene expression without changing DNA on a cellular level, new MPS techniques were developed; DNA methylation (methyl-Seq) extracts information of the epigenome and histone modification (ChIP-seq) extracts information of the chromatin. DNA methylation occurs by the addition of a methyl group to DNA, thereby often modifying the function of the genes and affecting gene expression. Multiple studies in recent years have shown beneficial use of methylation data for the diagnostic process, prognosis and potential therapeutic targets of soft tissue tumors [20-23].

Histones are proteins that condense and package DNA into chromosomes. Modifications to these proteins affect different cell processes such as transcriptional activation/inactivation, chromosome packaging, DNA damage and repair. The modification of histones is an important post-translational process that plays a key role in gene expression. The modifications impact gene expression by changing the structure of chromatin or through recruitment of histone modifiers. Thus, quantitative detection of various histone modifications using ChIP-seq provides useful information for a better understanding of epigenetic regulation of cellular processes and the development of histone modifying enzyme-targeted drugs [24-28].

In soft tissue tumors research in histone modification is relatively new. A well-known example where histone modification plays a role in differential diagnostics and even prognosis, is the loss of H3K27 tri-methylation in malignant peripheral nerve sheath tumor [29-31]. Both DNA methylation and histone modification are upcoming fields in soft tissue tumor research, which will help to increase our knowledge of soft tissue tumor development in the near future. Further investigations will lead to a better understanding of which alterations in epigenetic regulators affect gene accessibility and gene expression. The underlying mechanisms of tumor progression might be answered through these studies. Undoubtedly, this will lead to new diagnostic and prognostic biomarkers as well as potential novel targeted therapies [27, 28].

While the above mentioned targeted MPS can and has been used to discover novel gene mutations and fusion partners as shown in this thesis, at least one fusion partner has to be covered by the targeted panel. Therefore, techniques with a broader coverage than targeted MPS, such as whole exome and especially whole genome sequencing (WGS), may be advantageous in clinical settings for diagnostic and discovery purposes [32-35].

Whole exome sequencing (WES) is a technique that analyzes only the coding DNA (representative of the transcribed exons) of the whole genome, while non-transcribed DNA is left out [36]. Because this accounts for only 1.5% of the human genome the costs are lower than for WGS while there is also an increasing sequencing depth of these exomes. At first this method, like WGS, was only feasible using fresh-frozen material which is not always available. In recent years advances in sequencing technologies allowed the use of FFPE-extracted DNA for analysis, which unlike fresh-frozen tissue, is routinely available for tumor patients [37]. These factors make this method more attractive for laboratories to use WES in clinical practice compared to WGS [38].

On the other hand, WGS is a technology which analyses the entire genomic DNA sequence at a single time providing the most comprehensive characterization of the genome. This includes the detection of single nucleotide variants (point mutations), indels, structural variants (translocations/fusion genes), copy number variations (amplifications, losses and loss of heterozygosity), microsatellite instability, tumor mutational burden, germline mutations, SNP analysis for penetrance of germline mutations, integration of viral DNA and even pharmacogenetics. Another advantage of WGS is the ability to detect aberrations in non-coding DNA responsible for gene regulatory regions, such as promoter regions (as mentioned before). Massive amounts of bioinformatic data will become available from WGS and filtering all these datasets into clinically relevant genetic changes remains a big challenge that is only feasible by collaboration with an experienced bioinformatics support team. WGS has the potential to be a self-learning system where, with increasing input of tumor data, it can, for example, generate driver analyses and potentially find new drivers. Another feature of WGS is the mutational signature classifier. Mutational signatures are patterns of mutations that arise during tumorigenesis and provide insight into etiologies of each tumor [32-35, 39]. For example, in case of an undifferentiated tumor where conventional diagnostic work-up does not help to find the correct diagnosis, a mutational signature classifier used on WGS data can provide this information [35]. With increasing amount of tumor data these classifiers will help to create a more precise picture of tumor etiology, classification, prognosis and treatment.

Because WGS produces massive amounts of data, it requires abundant amount of storage capacity and intensive computational analysis, which makes this technique quite expensive and to date, it is not a wide-spread standard application in tumor diagnostics. The use of WGS in clinical practice at this moment, mainly in academic laboratories, is limited to biopsies of primary tumors of unknown origin and finding potentially drugable targets in metastasized patients, who have finished all possible regular treatments [35, 40]. However, it is widely applied in the field of biomedical research and it is expected that many more potential diagnostic and therapeutic targets will be discovered, which will fundamentally transform the field of personalized medicine. Especially, considering the ongoing advantages in reducing WGS costs and applicability of FFPE-extracted DNA [41].

Although immunohistochemistry has been around for many years and provides only limited information compared to many of the molecular techniques, all the above-mentioned molecular approaches made a remarkable impact on the development of useful derivative immunohistochemical markers. In recent years,

multiple markers emerged to serve as surrogates for underlying genetic alterations, for example STAT6 for solitary fibrous tumor, SS18-SSX for synovial sarcomas and MUC4 for low-grade fibromyxoid sarcoma; all three markers resulted from fusion genes [42-44]; MDM2 and CDK4 for liposarcoma, which were linked to MDM2 amplification [45] and H3K27me3 in malignant peripheral nerve sheath tumor reflecting changes in epigenetic histone modification [30]. Immunohistochemistry is a relatively cheap and simple test that can be used for mainly diagnostic and potentially prognostic purposes.

Pathologists are historically known for their work on histological characterization of tissues and tumors. The last decades, more and more additional techniques supplemented that primary process. The upcoming development of high-throughput molecular techniques like MPS and epigenetic profiling will transform the field of pathology. Accurate interpretation of all histological, immunohistochemical and genetic data will support the diagnostic process and provide clinicians with information they need for optimal patient management. To do so, interaction with with many different specialists is required, such as molecular biologists and bioinformaticians amongst others. Up till today, this mainly remains restricted to academic centers and oncology institutes where patient care and research activities are closely intertwined. With increasing accessibility and declining costs of molecular technologies, it is logical to assume that in the future some form of comprehensive genetic data will become available for most tumor samples.

Another very promising new 'technique' is the upcoming field of artificial intelligence (AI), that has been increasingly applied in the field of computational pathology [46, 47]. It can assist in diagnosis [48, 49], classification [50-52] and predicting outcome [53-55]. Deep learning algorithms can outperform the human eye and provide a more consistent analysis of pathology images therefore reduce the inter- and intraobserver variability in comparison to the pathologist alone. Such algorithms are even capable of screening for underlying molecular alterations in tumors using only hematoxylin and eosin-stained slides [55-58]. While MPS is the most used technique for detecting genomic alterations, it remains relatively time consuming, expensive and sometimes inaccessible to patients that don't have access to tertiary cancer centers. Therefore screening for genomic alterations using deep learning algorithms could provide a relatively inexpensive and rapid way to classify tumors not only for diagnostics, but also for possible targeted therapy strategy and predicting outcome.

Concluding remarks

In soft tissue tumor pathology, genetic information has been part of the diagnostic process for many years, and evidently pathologist plays an eminent and central role in future research in soft tissue tumor biology. The significant contributions of new molecular techniques will impact translational research, generating increasing knowledge and understanding of the pathogenetic basis of soft tissue tumors. Simultaneously, discovery of potentially new diagnostic, prognostic and predictive biomarkers will occur with subsequent incorporation into clinical practice. In upcoming years, most genetic and molecular data will be generated by high-throughput sequencing techniques (WGS amongst others) and will eventually replace older techniques like FISH. Recording useful genetic alterations will be part of the normal pathology report and will inform clinicians about therapeutic decisions for optimal patient management and ultimately lead to improved outcome of patients with soft tissue tumors.

References

1. Xiao, W., et al., Mesenchymal stem cell transformation and sarcoma genesis. Clin Sarcoma Res, 2013. 3(1): p. 10.
2. Schaefer, I.M., G.M. Cote, and J.L. Hornick, Contemporary Sarcoma Diagnosis, Genetics, and Genomics. J Clin Oncol, 2018. 36(2): p. 101-110.
3. Obeidin, F., What's new in bone and soft tissue pathology 2023: guidelines for molecular testing. J Pathol Transl Med, 2023. 57(3): p. 184-187.
4. Rottmann, D., E. Abdulfatah, and L. Pantanowitz, Molecular testing of soft tissue tumors. Diagn Cytopathol, 2023. 51(1): p. 12-25.
5. Wang, X.Q., et al., Advances in sarcoma molecular diagnostics. Genes Chromosomes Cancer, 2022. 61(6): p. 332-345.
6. Tucker, T., M. Marra, and J.M. Friedman, Massively parallel sequencing: the next big thing in genetic medicine. Am J Hum Genet, 2009. 85(2): p. 142-54.
7. Racanelli, D., et al., Next-Generation Sequencing Approaches for the Identification of Pathognomonic Fusion Transcripts in Sarcomas: The Experience of the Italian ACC Sarcoma Working Group. Front Oncol, 2020. 10: p. 489.
8. Dilliott, A.A., et al., Targeted Next-generation Sequencing and Bioinformatics Pipeline to Evaluate Genetic Determinants of Constitutional Disease. J Vis Exp, 2018(134).
9. Wong, S.Q., et al., Targeted-capture massively-parallel sequencing enables robust detection of clinically informative mutations from formalin-fixed tumours. Sci Rep, 2013. 3: p. 3494.
10. Zheng, Z., et al., Anchored multiplex PCR for targeted next-generation sequencing. Nat Med, 2014. 20(12): p. 1479-84.
11. Dickson, B.C. and D. Swanson, Targeted RNA sequencing: A routine ancillary technique in the diagnosis of bone and soft tissue neoplasms. Genes Chromosomes Cancer, 2019. 58(2): p. 75-87.
12. Heydt, C., et al., Detection of gene fusions using targeted next-generation sequencing: a comparative evaluation. BMC Med Genomics, 2021. 14(1): p. 62.
13. Pei, J., et al., Clinical application of RNA sequencing in sarcoma diagnosis: An institutional experience. Medicine (Baltimore), 2019. 98(25): p. e16031.
14. Samorodnitsky, E., et al., Evaluation of Hybridization Capture Versus Amplicon-Based Methods for Whole-Exome Sequencing. Hum Mutat, 2015. 36(9): p. 903-14.
15. Wang, J., et al., Capture-based high-coverage NGS: a powerful tool to uncover a wide spectrum of mutation types. Genet Med, 2016. 18(5): p. 513-21.
16. Peng, Q., et al., Reducing amplification artifacts in high multiplex amplicon sequencing by using molecular barcodes. BMC Genomics, 2015. 16(1): p. 589.
17. McConnell, L., et al., A novel next generation sequencing approach to improve sarcoma diagnosis. Mod Pathol, 2020. 33(7): p. 1350-1359.
18. Wojcik, J. and K. Cooper, Epigenetic Alterations in Bone and Soft Tissue Tumors. Adv Anat Pathol, 2017. 24(6): p. 362-371.
19. Nacev, B.A., et al., The epigenomics of sarcoma. Nat Rev Cancer, 2020. 20(10): p. 608-623.
20. Sun, W., et al., Distinct methylation profiles characterize fusion-positive and fusion-negative rhabdomyosarcoma. Mod Pathol, 2015. 28(9): p. 1214-24.
21. Koelsche, C., et al., Sarcoma classification by DNA methylation profiling. Nat Commun, 2021. 12(1): p. 498.

22. Lyskjaer, I., et al., DNA methylation-based profiling of bone and soft tissue tumours: a validation study of the 'DKFZ Sarcoma Classifier'. J Pathol Clin Res, 2021. 7(4): p. 350-360.
23. Roohani, S., et al., Sarcoma classification by DNA methylation profiling in clinical everyday life: the Charite experience. Clin Epigenetics, 2022. 14(1): p. 149.
24. Arimura, Y., et al., Cancer-associated mutations of histones H2B, H3.1 and H2A.Z.1 affect the structure and stability of the nucleosome. Nucleic Acids Res, 2018. 46(19): p. 10007-10018.
25. Bennett, R.L., et al., A Mutation in Histone H2B Represents a New Class of Oncogenic Driver. Cancer Discov, 2019. 9(10): p. 1438-1451.
26. Nacev, B.A., et al., The expanding landscape of 'oncohistone' mutations in human cancers. Nature, 2019. 567(7749): p. 473-478.
27. Cermakova, K. and H.C. Hodges, Next-Generation Drugs and Probes for Chromatin Biology: From Targeted Protein Degradation to Phase Separation. Molecules, 2018. 23(8).
28. Pfister, S.X. and A. Ashworth, Marked for death: targeting epigenetic changes in cancer. Nat Rev Drug Discov, 2017. 16(4): p. 241-263.
29. Cleven, A.H., et al., Loss of H3K27 tri-methylation is a diagnostic marker for malignant peripheral nerve sheath tumors and an indicator for an inferior survival. Mod Pathol, 2016. 29(9): p. 1113.
30. Schaefer, I.M., C.D. Fletcher, and J.L. Hornick, Loss of H3K27 trimethylation distinguishes malignant peripheral nerve sheath tumors from histologic mimics. Mod Pathol, 2016. 29(1): p. 4-13.
31. Marchione, D.M., et al., Histone H3K27 dimethyl loss is highly specific for malignant peripheral nerve sheath tumor and distinguishes true PRC2 loss from isolated H3K27 trimethyl loss. Mod Pathol, 2019. 32(10): p. 1434-1446.
32. Alexandrov, L.B., et al., Signatures of mutational processes in human cancer. Nature, 2013. 500(7463): p. 415-21.
33. Roepman, P., et al., Clinical Validation of Whole Genome Sequencing for Cancer Diagnostics. J Mol Diagn, 2021. 23(7): p. 816-833.
34. Samsom, K.G., et al., Feasibility of whole-genome sequencing-based tumor diagnostics in routine pathology practice. J Pathol, 2022. 258(2): p. 179-188.
35. Schipper, L.J., et al., Complete genomic characterization in patients with cancer of unknown primary origin in routine diagnostics. ESMO Open, 2022. 7(6): p. 100611.
36. Choi, M., et al., Genetic diagnosis by whole exome capture and massively parallel DNA sequencing. Proc Natl Acad Sci U S A, 2009. 106(45): p. 19096-101.
37. Astolfi, A., et al., Whole exome sequencing (WES) on formalin-fixed, paraffin-embedded (FFPE) tumor tissue in gastrointestinal stromal tumors (GIST). BMC Genomics, 2015. 16: p. 892.
38. Schwarze, K., et al., Are whole-exome and whole-genome sequencing approaches cost-effective? A systematic review of the literature. Genet Med, 2018. 20(10): p. 1122-1130.
39. Degasperi, A., et al., A practical framework and online tool for mutational signature analyses show inter-tissue variation and driver dependencies. Nat Cancer, 2020. 1(2): p. 249-263.
40. Schipper, L.J., et al., Clinical Impact of Prospective Whole Genome Sequencing in Sarcoma Patients. Cancers (Basel), 2022. 14(2).
41. Robbe, P., et al., Clinical whole-genome sequencing from routine formalin-fixed, paraffin-embedded specimens: pilot study for the 100,000 Genomes Project. Genet Med, 2018. 20(10): p. 1196-1205.

42. Doyle, L.A., et al., MUC4 is a highly sensitive and specific marker for low-grade fibromyxoid sarcoma. Am J Surg Pathol, 2011. 35(5): p. 733-41.
43. Doyle, L.A., et al., Nuclear expression of STAT6 distinguishes solitary fibrous tumor from histologic mimics. Mod Pathol, 2014. 27(3): p. 390-5.
44. Baranov, E., et al., A Novel SS18-SSX Fusion-specific Antibody for the Diagnosis of Synovial Sarcoma. Am J Surg Pathol, 2020. 44(7): p. 922-933.
45. Sirvent, N., et al., Detection of MDM2-CDK4 amplification by fluorescence in situ hybridization in 200 paraffin-embedded tumor samples: utility in diagnosing adipocytic lesions and comparison with immunohistochemistry and real-time PCR. Am J Surg Pathol, 2007. 31(10): p. 1476-89.
46. Cui, M. and D.Y. Zhang, Artificial intelligence and computational pathology. Lab Invest, 2021. 101(4): p. 412-422.
47. Rosenthal, J., et al., Building Tools for Machine Learning and Artificial Intelligence in Cancer Research: Best Practices and a Case Study with the PathML Toolkit for Computational Pathology. Mol Cancer Res, 2022. 20(2): p. 202-206.
48. Cruz-Roa, A.A., et al., A deep learning architecture for image representation, visual interpretability and automated basal-cell carcinoma cancer detection. Med Image Comput Comput Assist Interv, 2013. 16(Pt 2): p. 403-10.
49. Yeung, M.C.F. and I.S.Y. Cheng, Artificial intelligence significantly improves the diagnostic accuracy of deep myxoid soft tissue lesions in histology. Sci Rep, 2022. 12(1): p. 6965.
50. Korbar, B., et al., Deep Learning for Classification of Colorectal Polyps on Whole-slide Images. J Pathol Inform, 2017. 8: p. 30.
51. Polonia, A., et al., Artificial Intelligence Improves the Accuracy in Histologic Classification of Breast Lesions. Am J Clin Pathol, 2021. 155(4): p. 527-536.
52. Jin, L., et al., Artificial intelligence neuropathologist for glioma classification using deep learning on hematoxylin and eosin stained slide images and molecular markers. Neuro Oncol, 2021. 23(1): p. 44-52.
53. Bychkov, D., et al., Deep learning based tissue analysis predicts outcome in colorectal cancer. Sci Rep, 2018. 8(1): p. 3395.
54. Farahmand, S., et al., Deep learning trained on hematoxylin and eosin tumor region of Interest predicts HER2 status and trastuzumab treatment response in HER2+ breast cancer. Mod Pathol, 2022. 35(1): p. 44-51.
55. Yamashita, R., et al., Deep learning model for the prediction of microsatellite instability in colorectal cancer: a diagnostic study. Lancet Oncol, 2021. 22(1): p. 132-141.
56. Coudray, N., et al., Classification and mutation prediction from non-small cell lung cancer histopathology images using deep learning. Nat Med, 2018. 24(10): p. 1559-1567.
57. Kather, J.N., et al., Deep learning can predict microsatellite instability directly from histology in gastrointestinal cancer. Nat Med, 2019. 25(7): p. 1054-1056.
58. Erak, E., et al., Predicting Prostate Cancer Molecular Subtype With Deep Learning on Histopathologic Images. Mod Pathol, 2023. 36(10): p. 100247.

10

Chapter 11

Nederlandse samenvatting

Weke delen tumoren zijn relatief zeldzaam en bestaan uit een grote groep verschillende entiteiten. Het stellen van de juiste diagnose is vaak een hele uitdaging vanwege de overlappende karakteristieken. De afgelopen jaren zijn er substantiële vorderingen gemaakt in het identificeren van repeterende genetische veranderingen wat heeft het geleid tot verbreding van onze kennis van de biologische mechanismen van weke delen tumoren met als gevolg de ontwikkeling van nieuwe waardevolle diagnostische testen. Deze nieuwe inzichten hebben geleid en zullen blijven leiden tot belangrijke re- en/of sub classificatie van de verschillende entiteiten en een klinisch relevante weke delen tumorclassificatie.

In dit proefschrift richten wij ons op deze terugkerende genetische veranderingen in verschillende typen weke delen tumoren gebruik makend van verschillende moleculaire technieken, met als hoofdonderwerp myxoide tumoren zoals intramusculaire myxomen en cardiale myxomen. Daarnaast geven we aandacht aan het toenemende spectrum van tumoren met een USP6 herrangschikking. Als laatste hebben we de genfusies in soft tissue angiofibroom en myxoid liposarcoom en mutaties van het CTNNB1 gen in de zeldzame multifocale desmoid fibromatosis onderzocht en geëvalueerd.

Myxoide weke delen tumoren worden gekarakteriseerd door hun uitgebreide aanwezigheid van myxoide extracellulaire matrix. Ze bestaan uit een heterogene groep van tumoren variërend van benigne en zelflimiterende tumoren tot hooggradig maligne sarcomen. Doordat er een relevante klinische en morfologische overlap aanwezig is tussen deze tumoren kunnen er problemen ontstaan in de differentiaal diagnose. Immunohistochemie is vaak van ondergeschikt belang omdat ze geen specifiek profiel hebben. Aanvullende technieken zoals moleculaire diagnostiek kunnen een belangrijke bijdrage leveren aan het stellen van de juiste diagnose in de groep van myxoide tumoren.

Intramusculair myxoom (IM), zoals besproken in **hoofdstuk 2**, is meestal een hypocellulaire tumor afgewisseld met hypercellulaire gebieden. In kleine biopten kunnen deze tumoren makkelijk worden aangezien voor laaggradig fibromyxoid sarcoom of laaggradig myxofibrosarcoom. De gangbare zienswijze is dat driver mutaties van deze tumoren exclusief gelokaliseerd zijn in codon 201 van exon 8 van het GNAS gen (res. hotspot mutaties c.601C>T en c602G>A), die coderen voor de alfa subeenheid van het stimulerende G-eiwit dat op zijn beurt het enzym adenylaat cyclase activeert. Door de hypocellulariteit en het somatisch mozaicisme in het grootste deel van deze laesies is mutatie detectie een hele uitdaging en kan de aanwezigheid van een mutatie makkelijk gemist worden.

In ons onderzoek (**hoofdstuk 2**) hebben we gebruik gemaakt van de relatief nieuwe moleculaire techniek genaamd next generation sequencing (NGS) welke gebruik maakt van afzonderlijk getagde moleculaire inversie probes (single-molecule tagged molecular inversion probes, oftewel smMIP). De smMIP techniek combineert multiplex analyse met afzonderlijk getagde moleculen, ook wel bekend als Unique Molecule Identifiers (UMI). Doordat deze techniek het hele exon screent, hebben wij 4 additionele mutaties gedetecteerd die niet eerder beschreven zijn in intramusculair myxoom. We identificeerden een c.680A>G mutatie in exon 9, en drie nieuwe mutaties in exon 8. Een mutatie op positie c.601, namelijk c.601C>A, die eerder ook beschreven is in fibreuze dysplasie en twee mutaties op positie c.602, namelijk c.602G>C en c.602G>T welke tot nu toe alleen beschreven zijn in sporadische endocriene tumoren.

De cAMP-afhankelijke proteïnekinase, of proteïnekinase A (PKA), maakt deel uit van een signaaltransductie-cascade. PKA reguleert complexe netwerken van eiwitfosforylatie die uiteindelijk leiden tot een breed spectrum van fysiologische functies, variërend van steroïdogenese in de bijnierschors tot het behoud van stamcellen in de haarfollikel (Figuur 1). Er zijn verschillende bekende PKA-gebonden pathwys, zoals de Ras-pathway en de transforming growth factor-β pathway (TGF-β). De meest recent bestudeerde pathway is het Gαs-PKA-pathway, met mutaties die gezien zijn in *GNAS*, *PRKACA* en *PRKAR1A*.

Het mechanisme van tumorgenese in IM is niet volledig begrepen, maar de heersende opvatting is dat *GNAS*-mutaties in mesenchymale stamcellen van skeletspieren (MSC's) leiden tot een myxoïd fenotype. Een opmerkelijke gelijkenis is aanwezig in het geval van cardiale myxomen, waarbij mutaties in *PRKAR1A*, ook betrokken bij de eerder genoemde Gαs-PKA-pathway, die ontstaan in de endocardiale MSC's, ook leiden tot een myxoïd fenotype. Dit suggereert dat mutaties in het PKA-pathway verantwoordelijk kunnen zijn voor de myxoïde aard van deze tumoren.

In **hoofdstuk 3** bespreken we het onderwerp van cardiale myxomen, een goedaardige myxoïde tumor die een van de kenmerken is van het Carney Complex (CNC), een familiaal meervoudig neoplasie-syndroom, dat in ongeveer 80% van de gevallen wordt gekarakteriseerd door kiembaanmutaties in *PRKAR1A*, dat de RIα-regulerende subeenheid van de cAMP-afhankelijke proteïnekinase A (PKA) codeert. Mutaties binnen het *PRKAR1A*-gen leiden tot een gemuteerd eiwit of veroorzaken een non-sense mRNA, dat niet vertaald wordt naar RIα-eiwit, ook wel non-sense gemedieerde mRNA-degradatie genoemd. Dit verlies van RIα-functie resulteert

uiteindelijk in ongeremde activiteit van de PKA-katalytische subeenheden, wat leidt tot verhoogde celproliferatie en tumorvorming. Het is echter minder goed vastgesteld wat de rol van *PRKAR1A*-genmutaties is in de pathogenese van niet-CNC-geassocieerde sporadische cardiale myxomen.

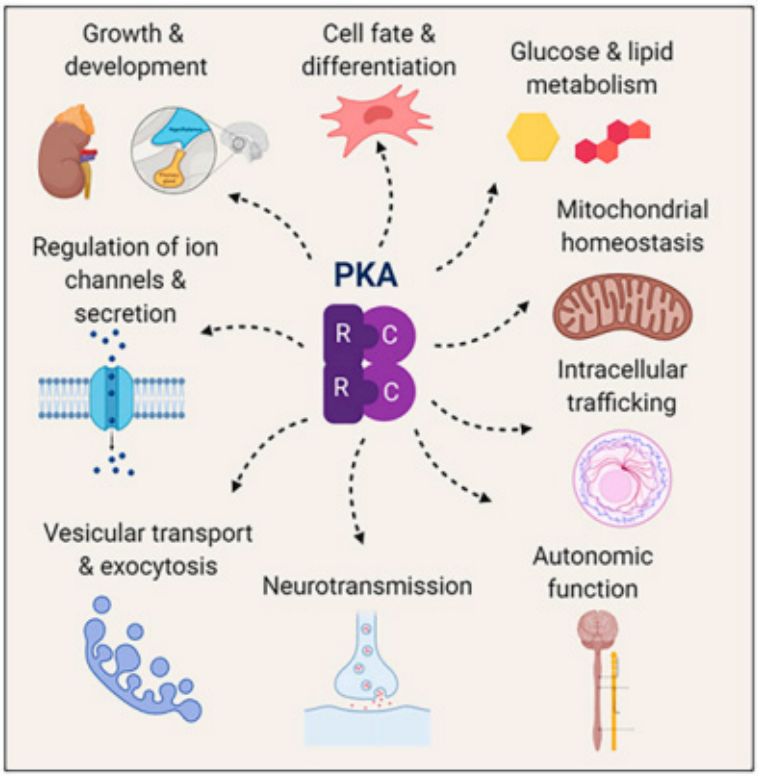

Figuur 1. Protein kinase A is een centraal regulatiepunt dat veel fysiologische processen bemiddelt, van hormonale groei en metabolisme tot transport en secretie.

Net als bij IM zal de relatieve hypocellulariteit van deze tumor en de daaruit voortvloeiende lage concentratie van geïsoleerd DNA profiteren van gevoelige technieken voor mutatiedetectie. We onderzochten de aanwezigheid van *PRKAR1A*-genmutaties met behulp van twee verschillende gerichte next-generation sequencing-technieken (Ion Torrent amplicon-NGS (Ion AmpliSeq) en de single molecule molecular inversion probe (smMIP)-techniek) in een cohort van 24 sporadische cardiale myxomen. Onze studies tonen aan dat 14 van de 24 sporadische cardiale myxomen *PRKAR1A*-genmutaties bevatten, die voornamelijk worden vertegenwoordigd door frameshift-, nonsense- en splice-site-mutaties (samen

84%), wat leidt tot een voortijdig stopcodon en waarschijnlijk wordt gedegradeerd via non-sense gemedieerde mRNA-degradatie. De andere 16% van de *PRKAR1A*-genetische veranderingen betroffen missense-mutaties, vaak gelegen in belangrijke functionele domeinen van de regulatorische subeenheid RIα. Opmerkelijk is dat 64% (n=9/14) van de gevallen van sporadisch cardiaal myxoom meer dan één *PRKAR1A*-genmutatie bevatte, wat wijst op bi-allelische inactivatie van *PRKAR1A*. Concluderend, *PRKAR1A*-genmutaties die geassocieerd zijn met verlies van RIα-functie en activatie van PKA-activiteit werden waargenomen in ~60% van de gevallen van sporadisch cardiaal myxoom, wat sterk wijst op een essentiële rol voor PKA in het bemiddelen van cardiale myocyt-proliferatie en myxoom-tumorgenese, zoals waargenomen door Di Vito et al.

Repeterende *USP6* herrangschikking was geïdentificeerd als een consistent driver mechanisme en was voor het eerst beschreven in aneurysmatische bot cyste (ABC) en later ook in nodulaire fasciitis. *USP6* (ubiquitine specifiek protease) is een van de deubiquiniserende enzymen betrokken bij verschillende cellulaire processen zoals intracellulair verkeer, eiwit transitie, inflammatoire singnalering en celtransformatie. Het *USP6* fusiegen resulteert in *USP6* overexpressie door promotorswitch wat leidt tot tumorgenese, osteoblastische maturatie, osteolyse, inflammatie en neovascularisatie.

Nodulaire fasciitis, myositis ossificans, fibro-osseous pseudotumor van digits (FOPD) en aneurysmatische botcyste delen allemaal dezelfde klinisch-pathologische karakteristieken. Ze komen voornamelijk voor in jongvolwassenen en laten een uniform rustig beeld zien van myofibroblastair weefselkweek-achtige morfologie en variabele hoeveelheid bot (voornamelijk in myositis ossificans en FOPD). Deze tumoren hebben een korte levensduur, groeien snel en gaan in regressie waardoor de tumoren in de weke delen ook wel voorbijgaande gezwellen worden genoemd.

Al deze tumoren hebben een *USP6* herrangschikking waardoor je deze groep als een continu spectrum van een ziekte kan beschouwen in plaats van separate entiteiten zoals beschreven in **hoofdstuk 4** en **5**. Screenen voor *USP* herrangschikking is een integraal onderdeel van het diagnostisch proces van (myo)fibroblastaire laesies van bot en weke delen.

Een andere potentiële differentiaal diagnose in de groep van myxoide fibroblastaire/myofibroblastaire tumoren is het soft tissue angiofibroom (STAF), met name de myxoide variant. STAF is een zeldzame en recent gedefinieerde weke delen tumor en heeft karakteristieke histomorfologische en genetische kenmerken met een chromosomale translocatie t(5;8)(p15;q13) die resulteert in een consistente herrangschikking van

NCOA2 in het grootste deel van de gevallen. De meerderheid daarvan heeft een *AHRR-NCOA2* fusiegen. Andere eerder beschreven fusiegenen zijn de omgekeerde *NCOA2-AHRR*, *NCOA2-ETV4*, *ETV4-AHRR*, *P4HA2-TBCK*, *TBCK-P4HA2* en *GTF2I-NCOA2*.

Met RT-PCR vonden wij in onze studie (**hoofdstuk 6**) *GAB1-ABL* als alternatief fusiegen in STAF die niet eerder is beschreven. *GAB1* (Grb2-geassocieerd bindingseiwit 1) behoort tot de familie van scaffolding eiwitten en is betrokken bij de integratie van verschillende signaal transducties zoals de MAPK en PI3K cascades. *ABL1* (Abselon tyrosine kinase eiwit 1) is een proto-oncogen met een functie in de celcyclus die betrokken is bij verschillende cellulaire processen zoals celdeling, adhesie en differentiatie.

Repeterende fusiegenen zijn drivermutaties in een toenemende hoeveelheid weke delen tumoren aanwezig zijn en moleculaire analyse is daarom een waardevolle diagnostische aanvulling. Vooral in biopten van tumoren zonder een specifiek immunohistochemisch profiel. Bovendien hebben fusiegenen belangrijke tumorgerelateerde therapeutische en prognostische consequenties in maligne laesies. Bijvoorbeeld myxoid liposarcoom (MLS), een potentiele differentiaal diagnose van STAF en andere myxoide weke delen tumoren, heeft in ongeveer een derde van de gevallen de neiging om te metastaseren naar andere weke delen lokalisaties zoals het mediastinum en retroperitoneum, maar ook naar bot, long en lever met een eventuele fatale uitkomst.

In **hoofdstuk 7** besteden we aandacht aan de extreem zeldzame lokalisatie van MLS in distale extremiteiten. MLS is het enige translocatie-geassocieerde liposarcoom-subtype en de meerderheid bevat specifieke fusiegenen *FUS-DDIT3* en, meer zeldzaam, *EWSR1-DDTI3*. In onze studie zijn deze fusiegenen ook gevonden door middel van RT-PCR en FISH. De verschillende isovormen van *FUS-DDIT3* fusiegenen zijn niet geassocieerd met histologische kenmerken of klinische uitkomsten. Het is belangrijk om de atypische presentatie van MLS te herkennen gezien de metastaserende potentie van dit sarcoom. Dit is nog belangrijker op het moment dat chirurgische vrije marges moeilijk haalbaar zijn, zoals in de voet en enkel. Onze studie liet zien dat MLS in distale extremiteiten zich ook agressief kunnen gedragen.

In **hoofdstuk 8** karakteriseren we multifocaal desmoid fibromatose. Dit is een zeer zeldzaam fenomeen dat meestal gezien wordt in patiënten met een kiembaanmutatie in het *APC* gen met een daaropvolgende tweede somatische mutatie. Echter sporadisch ontstaan multifocaal desmoid komt ook voor en de genetische en klinische karakteristieken zijn nog onduidelijk.

Desmoid fibromatose ontstaat vanuit mesenchymale voorloper cellen (MPC) met een *CTNNB1* mutatie leidend tot stapeling van β-catenine in de kern. Het eiwit transporteert naar de kern waar het werkt als transcriptiefactor leidend tot activatie van de Wnt signaal pathway. Dit resulteert vervolgens in cel proliferatie van myofibroblastaire cellen.

De circulerende capaciteit van mesenchymale voorloper cellen, inclusief de *CTNNB1* gemuteerde voorloper cellen, zouden de multifocale ontwikkeling van deze tumor goed kunnen verklaren. Dit wordt ondersteunt door de aanwezigheid van dezelfde mutaties in meerdere laesies in de geteste patiënten in onze serie in hoofdstuk 8. Echter er zijn ook verschillende *CTNNB1* mutaties in multifocaal desmoid beschreven die leiden tot de hypothese dat genetische afwijkingen plaats vinden in de verschillende ontwikkelingsstadia van mesenchymale voorloper cellen.

Klinisch management is uiteraard moelijker in multifocale casus dan in de klassieke unifocale casus. Meerdere studies hebben laten zien dat specifieke *CTNNB1* hotspot mutaties de prognose beïnvloeden, zoals bijvoorbeeld p.Ser45Phe (p.S45F) *CTNNB1* mutatie die een risicofactor voor lokaal recidief na radicale chirurgie lijkt te zijn. Daarom is de identificatie van betrouwbare klinische of genetische biomarkers die het gedrag voorspellen in (multi)focaal desmoid fibromatose erg gewenst om zo een meer patiëntgerichte succesvolle therapie te faciliteren.

Alle hierboven beschreven moleculaire veranderingen zijn consistente genetische afwijkingen en de detectie hiervan kan gebruikt worden als aanvullende diagnostische test om clinici te helpen met therapiemanagement. Nieuwe inzichten in genomische veranderingen kunnen ook de bekende morfologische weke delen tumor classificatie beïnvloeden leidend tot re- of subclassificatie zodat er nieuwe tumorfamilies ontstaan met dezelfde genetische achtergrond, die een meer genuanceerd en klinisch relevante classificatie vormen en kunnen helpen met het maken van therapeutische keuzes.

Discussie en toekomstperspectief

In het algemeen wordt aangenomen dat weke delen tumoren ontstaan tijdens het proces van differentiatie en transformatie van mesenchymale stamcellen (MSC). Dit proces wordt beïnvloed door verschillende genetische veranderingen in oncogenen en tumor suppressor genen, die veel downstream signaalroutes beïnvloeden die cruciaal zijn voor neoplastische groei. Tot nu toe weten we dat drie

moleculaire kern mechanismen de tumorgenese van weke delen tumoren sturen: i) dysregulatie van genexpressie door aberrante chimere transcriptiefactoren die worden gegenereerd door specifieke genfusies in translocatie-positieve weke delen tumoren, ii) somatische mutaties in sleutelgenen die betrokken zijn bij signaalroutes, en iii) veranderingen in DNA-kopie aantallen van genen die een rol spelen bij proliferatie, apoptose en cel differentiatie.

In de afgelopen jaren zijn er belangrijke vorderingen gemaakt in moleculaire technologieën die terugkerende chromosomale en genomische veranderingen in weke delen tumoren kunnen identificeren, wat heeft geleid tot een verbeterd inzicht in de biologische mechanismen die geassocieerd zijn met de ontwikkeling van weke delen tumoren. Dit heeft de ontdekking van nieuwe diagnostische, prognostische en predictieve moleculaire biomarkers versneld. High-throughput genomische moleculaire technieken, zoals massive parallel sequencing (MPS), ook wel bekend als next-generation sequencing (NGS), worden al dagelijks gebruikt in de diagnostische praktijk en zullen een belangrijk klinisch hulpmiddel blijven in het managen van weke delen tumoren.

MPS-technologieën kunnen informatie extraheren uit het genoom (DNA), transcriptoom (RNA), epigenoom (methyl-Seq) en chromatine (ChIP-Seq) zoals hieronder uitgebreider is beschreven. Deze sequencing platforms zijn veel sneller en geven een volledigere beeld dan de traditionele Sanger sequencing. Echter, deze technieken kunnen arbeidsintensief zijn en genereren veel meer data dan nodig voor diagnostiek. Dit heeft geleid tot de ontwikkeling van een meer gerichte versie van MPS, bekend als targeted sequencing. Deze platforms gebruiken een meer selectief profiel van genen of gebieden die al bekend zijn als geassocieerd met tumoren. Targeted MPS gebruikt ofwel hybridisatie capture of amplicon-gebaseerde verrijking met multiplex PCR. Op deze manier kun je een panel van specifieke genomische gebieden efficiënter en dieper sequencen.

De hybridisatie capture techniek kan worden toegepast met DNA of RNA (bijvoorbeeld Illumina Trusight) en heeft het voordeel dat maar een lage hoeveelheid input DNA (10 ng) is vereist. In het geval van weke delen tumoren is dit bijzonder nuttig gezien de vaak beperkte hoeveelheid weefsel in de vorm van biopsieën, de hypocellulariteit van tumoren en de slechte kwaliteit van de fomaline-gefixeerde (FFPE) biopten. In vergelijking met amplicon-gebaseerde methoden, heeft hybridisatie capture meer input DNA of RNA nodig, duurt het langer en is het duurder.

Amplicon-gebaseerde methoden, zoals Archer of Oncomine, kunnen ook worden gebruikt met DNA of RNA en hebben een eenvoudigere en snellere workflow, maar

zijn minder robuust bij grote panels, waardoor meer mutaties gemist worden. Beide methoden zijn echter in staat om alternatieve onbekende fusiepartners te detecteren, in tegenstelling tot de traditionele RT-PCR met Sanger. Dit is vooral nuttig gezien de promiscuïteit van weke delen tumor-geassocieerde genen, zoals EWSR1 en FUS. Beide methoden worden voornamelijk gebruikt met RNA sequencing, omdat dit de technische voordelen biedt om de breekpunten van deze genen te detecteren, omdat ze als fusie op RNA niveau dicht bij elkaar liggen in vergelijking met DNA sequencing, waar deze breekpunten wijd verspreid over het genoom liggen en daarom veel moeilijker te detecteren zijn. Voortdurende verbeteringen worden aangebracht in zowel hybridisatie capture als amplicon-gebaseerde technieken om bias en fouten te verminderen, evenals om de multiplexcapaciteit te vergroten. Dit is aantrekkelijk in de diagnostiek van weke delen tumoren, aangezien het structurele herschikkingen detecteert die translocatie-geassocieerde entiteiten definiëren en is tegenwoordig de meest populaire manier voor de ontdekking van nieuwe fusiegenen. Het combineren van deze uitkomsten met klinische gegevens is vereist om een klinisch relevant beeld te definiëren dat leidt tot patiëntgerichte behandeling. RNA sequencing is in de afgelopen jaren al opgenomen in de pathologische diagnostische werkwijze in de meeste academische laboratoria en zal zich in de nabije toekomst verspreiden naar meer laboratoria.

In de afgelopen jaren hebben MPS sequencing technieken ook een belangrijke rol gespeeld bij de detectie van mutaties in epigenetische regulatoren, vooral in weke delen tumoren. Deze eiwitten helpen de toegankelijkheid van genen te controleren en daardoor het transcriptieprofiel van een cel door interacties met, of directe modificaties van chromatine. Dysfunctie in deze epigenetische regulatoren van chromatine kan leiden tot activatie van oncogenen pathways, of het stilleggen van tumor suppressors door de expressie van talrijke downstream target genen te veranderen. In sommige tumoren zijn deze kritische target genen bekend, maar in veel andere moeten deze nog worden gekarakteriseerd.

In het afgelopen decennium heeft epigenetische dysregulatie met name aangetoond een belangrijke factor te zijn in de histogenese van weke delen tumoren. Mutaties in epigenetische regulatoren die leiden tot deze epigenetische dysregulatie kunnen effecten hebben op DNA-methylatie en histonmodificatie. Aangezien deze epigenetische mechanismen genexpressie wijzigen zonder het DNA op cellulair niveau te veranderen, zijn er nieuwe MPS-technieken ontwikkeld; DNA-methylatie (methyl-Seq) haalt informatie uit het epigenoom en histonmodificatie (ChIP-seq) haalt informatie uit chromatine.

DNA-methylatie vindt plaats door de toevoeging van een methylgroep aan DNA, waardoor vaak de functie van de genen wordt gewijzigd en de genexpressie wordt beïnvloed. Meerdere studies in de afgelopen jaren hebben het nuttige gebruik van methylatiedata aangetoond voor het diagnostische proces, prognose en potentiële therapeutische doelen van weke delen tumoren.

Histonen zijn eiwitten die DNA condenseren en verpakken in chromosomen. Modificaties aan deze eiwitten beïnvloeden verschillende cellulaire processen, zoals transcriptieactivatie/-inactivatie, chromosoom verpakking, DNA-schade en -herstel. De modificatie van histonen is een belangrijk post-translationeel proces dat een sleutelrol speelt in genexpressie. De modificaties beïnvloeden genexpressie door de structuur van chromatine te veranderen of door histonmodificeerders aan te trekken. Daarom biedt kwantitatieve detectie van verschillende histonmodificaties met behulp van ChIP-seq nuttige informatie voor een beter begrip van de epigenetische regulatie van cellulaire processen en de ontwikkeling van op histonmodificerende enzym gerichte geneesmiddelen.

In het onderzoek naar weke delen tumoren is onderzoek naar histonmodificatie relatief nieuw. Een bekend voorbeeld waarbij histonmodificatie een rol speelt in differentiaal diagnostiek en zelfs prognose, is het verlies van H3K27-tri-methylatie in maligne perifere zenuwschede tumor. Zowel DNA-methylatie als histonmodificatie zijn opkomende gebieden in het onderzoek naar weke delen tumoren en zullen helpen om onze kennis van de ontwikkeling van weke delen tumoren in de nabije toekomst te vergroten, en verder onderzoek zal leiden tot een beter begrip over welke veranderingen in epigenetische regulatoren de gen toegankelijkheid en genexpressie beïnvloeden. De onderliggende mechanismen van tumorprogressie zouden door deze studies kunnen worden beantwoord. Dit zal ongetwijfeld leiden tot nieuwe diagnostische en prognostische biomarkers, evenals potentiële nieuwe gerichte therapieën.

Hoewel de eerdergenoemde targeted MPS al wordt gebruikt om nieuwe genmutaties en fusiepartners te ontdekken, moet minstens één fusiepartner worden gedekt door het gerichte panel. Daarom kunnen technieken met een bredere dekking dan targeted MPS, zoals whole exome sequencing (WES) en vooral whole genome sequencing (WGS), voordelig zijn in klinische setting voor diagnostische en ontdekkingsdoeleinden.

Whole exome sequencing is een techniek dat alleen het coderende DNA (representatief voor de getranscribeerde exonen) van het gehele genoom analyseert, terwijl niet-

getranscribeerd DNA wordt weggelaten. Omdat dit slechts 1,5% van het menselijk genoom vertegenwoordigt, zijn de kosten lager dan voor WGS, terwijl er ook een toenemende sequencing diepte van deze exomen kan worden bereikt. Aanvankelijk was deze methode, net als WGS, alleen haalbaar met vers-ingevroren tumor materiaal, dat niet altijd beschikbaar is. In de afgelopen jaren heeft vooruitgang in sequencing technologieën het gebruik van FFPE-geëxtraheerd DNA voor analyse mogelijk gemaakt, wat in tegenstelling tot vers-ingevroren weefsel routinematig beschikbaar is voor tumorpatiënten. Deze factoren maken deze methode aantrekkelijker om te gebruiken voor laboratoria in de klinische praktijk dan WGS.

WGS is een technologie die de gehele genomische DNA-sequentie in één keer analyseert en de meest uitgebreide karakterisering van het genoom biedt. Dit omvat de detectie van enkelvoudige nucleotidemutaties (puntmutaties), indels, structurele varianten (translocaties/fusiegenen), copy number variaties (amplificaties, verliezen en verlies van heterozygotie), microsatelliet instabiliteit (MSI), tumor mutational burden (TMB), germline mutaties, SNP-analyse voor penetrantie van germline mutaties, integratie van viraal DNA en zelfs farmacogenetica. Een ander voordeel van WGS is de mogelijkheid om afwijkingen in niet-coderend DNA te detecteren die verantwoordelijk zijn voor genregulerende gebieden, zoals promotor gebieden. Massale hoeveelheden data zullen beschikbaar komen van WGS en het filteren van al deze datasets naar klinisch relevante genetische veranderingen blijft een grote uitdaging die alleen haalbaar is door samenwerking met een ervaren bioinformatica team. WGS heeft het potentieel om een zelflerend systeem te zijn waar, met toenemende invoer van tumordata, het bijvoorbeeld driveranalyses kan genereren en mogelijk nieuwe drivers kan vinden. Een ander kenmerk van WGS is de mutational signature classifier. Mutational signatures zijn patronen van mutaties die ontstaan tijdens tumorgenese en inzicht geven in de etiologie van elke tumor. Bijvoorbeeld, in het geval van een ongedifferentieerde tumor waarbij de conventionele diagnostische werkwijze niet helpt om de juiste diagnose te vinden, kan een mutational signature classifier die op WGS-gegevens wordt gebruikt deze informatie bieden. Met de toenemende hoeveelheid tumordata zullen deze classifiers helpen om een preciezer beeld van tumor etiologie, classificatie, prognose en behandeling te creëren.

Omdat WGS enorme hoeveelheden data produceert, een overvloed aan opslag-capaciteit nodig heeft en intensieve computationele analyse vereist, is deze techniek vrij duur en is het tot nu toe geen wijdverspreide standaardtoepassing in tumordiagnostiek. Het gebruik van WGS in de klinische praktijk op dit moment, wat voornamelijk plaatsvindt in academische laboratoria, is beperkt tot biopsieën

van primaire tumoren van onbekende oorsprong en het vinden van potentiële behandel targets bij gemetastaseerde patiënten die alle mogelijke reguliere behandelingen hebben ondergaan. Het wordt echter veel gebruikt op het gebied van onderzoek en het wordt verwacht dat er veel meer potentiële diagnostische en therapeutische targets zullen worden ontdekt die het veld van gepersonaliseerde geneeskunde fundamenteel zullen transformeren, vooral gezien de voortdurende voordelen in het verlagen van de WGS-kosten en de toepasbaarheid van FFPE-geëxtraheerd DNA.

Hoewel immunohistochemie al vele jaren bestaat en slechts beperkte informatie biedt vergeleken met veel van de moleculaire technieken, hebben al deze bovengenoemde moleculaire benaderingen een opmerkelijke impact gehad op de ontwikkeling van nuttige afgeleide immunohistochemische markers. In de afgelopen jaren zijn meerdere markers ontstaan als surrogaten voor onderliggende genetische veranderingen, bijvoorbeeld STAT6 voor solitaire fibreuze tumor, SS18-SSX voor synoviaal sarcoom en MUC4 voor laaggradig fibromyxoid sarcoom; alle drie de markers zijn het resultaat van fusiegenen; MDM2 en CDK4 voor liposarcoom, die zijn gekoppeld aan MDM2-amplificatie en H3K27me3 in maligne perifere zenuwschede tumor die veranderingen in epigenetische histonmodificatie weerspiegelt. Immunohistochemie is een relatief goedkope en eenvoudige test die voornamelijk kan worden gebruikt voor diagnostische en mogelijk prognostische doeleinden.

Pathologen zijn historisch bekend om hun werk aan histologische karakterisering van weefsels en tumoren. In de afgelopen decennia zijn steeds meer aanvullende technieken aan dat primaire proces toegevoegd. De opkomende ontwikkeling van high-throughput moleculaire technieken zoals MPS en epigenetische profilering zal het veld van de pathologie transformeren. Nauwkeurige interpretatie van alle histologische, immunohistochemische en genetische gegevens zal het diagnostische proces ondersteunen en clinici voorzien van de informatie die ze nodig hebben voor optimale patiëntenzorg. Om dit te doen, moeten ze interactie hebben met veel verschillende specialisten, zoals moleculair biologen en bio-informatici onder andere. Tot op heden blijft dit voornamelijk beperkt tot academische centra en oncologie-instituten waar patiëntenzorg en onderzoeksactiviteiten nauw met elkaar zijn verweven. Met de toenemende toegankelijkheid en dalende kosten van moleculaire technologieën is het logisch om aan te nemen dat in de toekomst enige vorm van uitgebreide genetische data beschikbaar zal komen voor de meeste tumorsamples.

Een andere veelbelovende nieuwe 'techniek' is het opkomende veld van kunstmatige intelligentie (AI), dat steeds vaker wordt toegepast in het veld van computationele pathologie. Het kan helpen bij diagnose, classificatie en het voorspellen van uitkomsten. Deep learning algoritmen kunnen het menselijke oog overtreffen en een consistentere analyse van pathologie-afbeeldingen bieden, waardoor de inter- en intra-observer variabiliteit in vergelijking met de patholoog alleen maar worden gereduceerd. Dergelijke algoritmen zijn zelfs in staat om te screenen op onderliggende moleculaire veranderingen in tumoren met alleen hematoxylin- en eosine-gekleurde preparaten. Terwijl MPS de meest gebruikte techniek is voor het detecteren van genomische veranderingen, blijft het relatief tijdrovend, duur en soms ontoegankelijk voor patiënten die geen toegang hebben tot tertiaire kankercentra. Daarom kan screening op genomische veranderingen met behulp van deep learning algoritmen een relatief goedkope en snelle manier bieden om tumoren te classificeren, niet alleen voor diagnostiek maar ook voor mogelijke targeted therapieën en het voorspellen van uitkomsten.

Conclusie

In de pathologie van weke delen tumoren is genetische informatie al vele jaren onderdeel van het diagnostische proces en het is duidelijk dat de patholoog een eminente en centrale rol speelt in toekomstig onderzoek naar de biologie van weke delen tumoren. De significante bijdragen van nieuwe moleculaire technieken zullen dit onderzoek beïnvloeden, wat leidt tot een toenemende kennis en begrip van de pathogenetische basis van weke delen tumoren. Tegelijkertijd zal de ontdekking van mogelijk nieuwe diagnostische, prognostische en voorspellende biomarkers toenemen met daaropvolgende integratie in de klinische praktijk. In de komende jaren zullen de meeste genetische en moleculaire gegevens worden gegenereerd door high-throughput sequencing technieken (onder andere WGS) en zullen uiteindelijk oudere technieken zoals FISH vervangen. Het vastleggen van nuttige genetische veranderingen zal deel uitmaken van het normale pathologie-rapport en zal clinici informeren over therapeutische beslissingen voor optimale patiëntenzorg, wat uiteindelijk zal leiden tot verbeterde uitkomsten voor patiënten met weke delen tumoren.

Appendices

Research Data Management

List of publications

Curriculum Vitae

Dankwoord

Research Data Management

Ethics and privacy

This thesis is based on the results of research involving human participants, which were conducted in accordance with relevant national and international legislation and regulations, guidelines, codes of conduct and Radboudumc policy. All chapters had statements that the study was not subject to the Dutch Medical Research Involving Human Subjects Act (WMO), and were obtained from the recognized Medical Ethics Review Committee 'METC Oost-Nederland'.

The privacy of the participants in these studies was warranted by the use of pseudonymization. The pseudonymization key was stored on a secured network drive that was only accessible to members of the project who needed access to it because of their role within the project. The pseudonymization key was stored separately from the research data.

For all chapters data was used that was previously collected in the context of healthcare.

Data collection, storage and sharing

All clinical data was collected from care data from the Electronic Health Records (EPD and UDPS) and laboratory experiments from patient material. Chapter 2-7 are published open access. Chapter 2 and 4-8 were published before 2021, at which point the current Radboud RDM policy was not yet effective. Therefore, the data underlying these chapters has not been made available. Chapter 3 has been published after 2021. The data underlying chapter 3 is not suitable for reuse and will be archived for 10 years on the department server after termination of the study.

List of Publications

1. Detection of PRKAR1A gene mutations in sporadic cardiac myxomas: a study of 24 cases.
Elise Bekers, Diede A G van Bladel, Madeleine R Berendsen, Astrid Eijkelenboom, J Han J M van Krieken, Marc Ooft, Emiel Ruijter, Ad Verhagen, Uta E Flucke, Blanca Scheijen
Virchows Arch. 2025 Feb 18. doi: 10.1007/s00428-025-04049-x. Online ahead of print.
PMID: 39966109

2. Prognostic Value of Cribriform and Intraductal Carcinoma in Grade Group 2 Prostate Cancer with and without Synchronous Nodal Metastases at Radical Prostatectomy: Results from a Case-Control Matched, Multicenter Study.
Hilda A de Barros, Michelle R Downes, Matteo Droghetti, **Elise M Bekers**, Francesca Giunchi, Eugenio Brunocilla, Riccardo Schiavina, Theodorus H van der Kwast, Pim J van Leeuwen, Henk G van der Poel
Urology. 2025 Feb 6:S0090-4295(25)00109-8. doi: 10.1016/j.urology.2025.01.061. Online ahead of print.
PMID: 39922236

3. Heterogeneity in response to neoadjuvant radiotherapy between soft tissue sarcoma histotypes: associations between radiology and pathology findings.
Nicolò Gennaro, Iris van der Loo, Sophie J M Reijers, Hester van Boven, Petur Snaebjornsson, **Elise M Bekers**, Zuhir Bodalal, Stefano Trebeschi, Yvonne M Schrage, Winette T A van der Graaf, Winan J van Houdt, Rick L M Haas, Yury S Velichko, Regina G H Beets-Tan, Annemarie Bruining
Eur Radiol. 2025 Mar;35(3):1337-1350. doi: 10.1007/s00330-024-11258-6. Epub 2024 Dec 19.
PMID: 39699680

4. Correction: Multispectral Fluorescence Imaging as a Tool to Distinguish Pelvic Lymphatic Drainage Patterns During Robot-assisted Lymph Node Dissection in Prostate Cancer.
Anne-Claire Berrens, Tessa Buckle, Matthias N van Oosterom, Leon J Slof, Pim J van Leeuwen, Esther M K Wit, Hilda A de Barros, Jakko A Nieuwenhuijzen, **Elise M Bekers**, Maarten L Donswijk, Fijs W B van Leeuwen, Henk G van der Poel
Ann Surg Oncol. 2025 Mar;32(3):2250. doi: 10.1245/s10434-024-16629-3.
PMID: 39673025

5. Multispectral Fluorescence Imaging as a Tool to Distinguish Pelvic Lymphatic Drainage Patterns During Robot-assisted Lymph Node Dissection in Prostate Cancer.
Berrens AC, Buckle T, van Oosterom MN, Slof LJ, van Leeuwen PJ, Wit EMK, de Barros HA, Nieuwenhuijzen JA, **Bekers EM**, Donswijk ML, van Leeuwen FWB, van der Poel HG.
Ann Surg Oncol. 2025 Feb;32(2):1372-1381.
PMID: 39562421

6. A DWI-based hypoxia model shows robustness in an external prostatectomy cohort.
Fernandez Salamanca M, Hompland T, Deręgowska-Cylke M, Van der Poel H, **Bekers E**, Guimaraes MAS, Lyng H, Van der Heide UA, Schoots IG, Van Houdt PJ.
Front Oncol. 2024 Jul 23;14:1433197. doi: 10.3389/fonc.2024.1433197. eCollection 2024.
PMID: 39109282 Free PMC article.

7. Low tristetraprolin expression activates phenotypic plasticity and primes transition to lethal prostate cancer in mice.
Morel KL, Germán B, Hamid AA, Nanda JS, Linder S, Bergman AM, van der Poel H, Hofland I, **Bekers EM**, Trostel SY, Burkhart DL, Wilkinson S, Ku AT, Kim M, Kim J, Ma D, Plummer JT, You S, Su XA, Zwart W, Sowalsky AG, Sweeney CJ, Ellis L.
J Clin Invest. 2024 Nov 19:e175680. doi: 10.1172/JCI175680. Online ahead of print.
PMID: 39560993

*

8. Penile intraepithelial neoplasia incidence, clinical classification, microenvironment and implications for imiquimod treatment.
Avitan O, Rafael T, Vreeburg M, Elst L, **Bekers EM**, Albersen M, Jordanova ES, Brouwer O.
BJU Int. 2024 Dec;134(6):881-889. doi: 10.1111/bju.16473. Epub 2024 Jul 19.
PMID: 39030899 Review.

9. Location-Based Oncological Outcomes of Sentinel Node Dissection in Radical Prostatectomy.
Droghetti M, Ozman O, Berrens AC, Piazza P, Paccapelo A, van Vliet R, Schiavina R, Brunocilla E, **Bekers E**, Donswijk M, van Leeuwen FWB, van der Poel H.
J Urol. 2024 Sep;212(3):409-419. doi: 10.1097/JU.0000000000004051. Epub 2024 May 24.
PMID: 38787799

10. Strong Correlation Between SUV_{max} on PSMA PET/CT and Numeric Drop-In γ-Probe Signal for Intraoperative Identification of Prostate Cancer Lesions.
Berrens AC, Sorbi MA, Donswijk ML, de Barros HA, Azargoshasb S, van Oosterom MN, Rietbergen DDD, **Bekers EM**, van der Poel HG, van Leeuwen FWB, van Leeuwen PJ.
J Nucl Med. 2024 Apr 1;65(4):548-554. doi: 10.2967/jnumed.123.267075.
PMID: 38485277

11. Agent-based modeling of the prostate tumor microenvironment uncovers spatial tumor growth constraints and immunomodulatory properties.
van Genderen MNG, Kneppers J, Zaalberg A, **Bekers EM**, Bergman AM, Zwart W, Eduati F.
NPJ Syst Biol Appl. 2024 Feb 21;10(1):20. doi: 10.1038/s41540-024-00344-6.
PMID: 38383542

12. Real-world data on malignant and borderline phyllodes tumors of the breast: A population-based study of all 921 cases in the Netherlands (1989 -2020).
Bartels SAL, van Olmen JP, Scholten AN, **Bekers EM**, Drukker CA, Vrancken Peeters MTFD, van Duijnhoven FH.
Eur J Cancer. 2024 Apr;201:113924. doi: 10.1016/j.ejca.2024.113924. Epub 2024 Feb 10.
PMID: 38364628

13. ^{99m}TcPSMA-radioguided surgery in oligorecurrent prostate cancer: the randomised TRACE-II trial.
Zuur LG, de Barros HA, van Oosterom MN, Berrens AC, Donswijk ML, Hendrikx JJMA, **Bekers EM**, Vis AN, Wit EM, van Leeuwen FB, van der Poel HG, van Leeuwen PJ.
BJU Int. 2024 Jul;134(1):81-88. doi: 10.1111/bju.16297. Epub 2024 Feb 12.
PMID: 38346924 Clinical Trial.

14. The accuracy and intra- and interobserver variability of PSMA PET/CT for the local staging of primary prostate cancer.
Donswijk ML, Ettema RH, Meijer D, Wondergem M, Cheung Z, **Bekers EM**, van Leeuwen PJ, van den Bergh RCN, van der Poel HG, Vis AN, Oprea-Lager DE.
Eur J Nucl Med Mol Imaging. 2024 May;51(6):1741-1752. doi: 10.1007/s00259-024-06594-0. Epub 2024 Jan 26.
PMID: 38273003

15. Histopathological concordance between prostate biopsies and radical prostatectomy specimens-implications of transrectal and transperineal biopsy approaches.
Hagens MJ, Ribbert LLA, Jager A, Veerman H, Barwari K, Boodt B, de Bruijn RE, Claessen A, Leter MR, van der Noort V, Smeenge M, Roeleveld TA, Rynja SP, Schaaf M, Weltings S, Vis AN, **Bekers E**, van Leeuwen PJ, van der Poel HG.
Prostate Cancer Prostatic Dis. 2024 Jun;27(2):312-317. doi: 10.1038/s41391-023-00714-x. Epub 2023 Sep 2.
PMID: 37660218

16. ASO Visual Abstract: Management of Benign Phyllodes Tumors: A Dutch Population-Based Retrospective Cohort Between 1989 and 2022. 7van Olmen JP, Beerthuizen AWJ, **Bekers EM**, Viegen I, Drukker CA, Peeters MTFDV, Bartels SAL, van Duijnhoven FH.
Ann Surg Oncol. 2023 Dec;30(13):8486. doi: 10.1245/s10434-023-14283-9.
PMID: 37728823

17. Management of Benign Phyllodes Tumors: A Dutch Population-Based Retrospective Cohort Between 1989 and 2022.
van Olmen JP, Beerthuizen AWJ, **Bekers EM**, Viegen I, Drukker CA, Vrancken Peeters MTFD, Bartels SAL, van Duijnhoven FH.
Ann Surg Oncol. 2023 Dec;30(13):8344-8352. doi: 10.1245/s10434-023-14128-5. Epub 2023 Aug 28.
PMID: 37639031

18. Atezolizumab With or Without Radiotherapy for Advanced Squamous Cell Carcinoma of the Penis (The PERICLES Study): A Phase II Trial.
de Vries HM, Rafael TS, Gil-Jimenez A, de Feijter JM, **Bekers E**, van der Laan E, Lopez-Yurda M, Hooijberg E, Broeks A, Peters D, Seignette IM, Pos FJ, Horenblas S, van Rhijn BWG, Jordanova ES, Brouwer OR, Schaake E, van der Heijden MS.
J Clin Oncol. 2023 Nov 1;41(31):4872-4880. doi: 10.1200/JCO.22.02894. Epub 2023 Jul 24.
PMID: 37487169

19. Histopathological concordance between prostate biopsies and radical prostatectomy specimens-implications of transrectal and transperineal biopsy approaches.
Hagens MJ, Ribbert LLA, Jager A, Veerman H, Barwari K, Boodt B, de Bruijn RE, Claessen A, Leter MR, van der Noort V, Smeenge M, Roeleveld TA, Rynja SP, Schaaf M, Weltings S, Vis AN, **Bekers E**, van Leeuwen PJ, van der Poel HG.
Prostate Cancer Prostatic Dis. 2023 Sep 2. doi: 10.1038/s41391-023-00714-x. Online ahead of print.
PMID: 37660218

20. Exploring the Onset and Progression of Prostate Cancer through a Multicellular Agent-based Model.
Passier M, van Genderen MNG, Zaalberg A, Kneppers J, **Bekers EM**, Bergman AM, Zwart W, Eduati F.
Cancer Res Commun. 2023 Aug 7;3(8):1473-1485. doi: 10.1158/2767-9764.CRC-23-0097. eCollection 2023 Aug.
PMID: 37554550

21. Reliable Visualization of the Treatment Effect of Transperineal Focal Laser Ablation in Prostate Cancer Patients by Magnetic Resonance Imaging and Contrast-enhanced Ultrasound Imaging.
van Riel LAMJG, van Kollenburg RAA, Freund JE, Almasian M, Jager A, Engelbrecht MRW, Smit RS, **Bekers E**, Nieuwenhuijzen JA, van Leeuwen PJ, van der Poel H, de Reijke TM, Beerlage HP, Oddens JR, de Bruin DM.
Eur Urol Open Sci. 2023 Jun 29;54:72-79. doi: 10.1016/j.euros.2023.06.002. eCollection 2023 Aug.
PMID: 37545846

22. Reliability of whole mount radical prostatectomy histopathology as the ground truth for artificial intelligence assisted prostate imaging.
Jager A, Postema AW, van der Linden H, Nooijen PTGA, **Bekers E**, Kweldam CF, Daures G, Zwart W, Mischi M, Beerlage HP, Oddens JR.
Virchows Arch. 2023 Aug;483(2):197-206. doi: 10.1007/s00428-023-03589-4. Epub 2023 Jul 6.
PMID: 37407736

23. A hybrid radioactive and fluorescence approach is more than the sum of its parts; outcome of a phase II randomized sentinel node trial in prostate cancer patients.
Wit EMK, KleinJan GH, Berrens AC, van Vliet R, van Leeuwen PJ, Buckle T, Donswijk ML, **Bekers EM**, van Leeuwen FWB, van der Poel HG.
Eur J Nucl Med Mol Imaging. 2023 Jul;50(9):2861-2871. doi: 10.1007/s00259-023-06191-7. Epub 2023 Apr 10.
PMID: 37036490

*

24. Clinical value of preoperative serum tumor markers CEA, CA19-9, CA125, and CA15-3 in surgically treated urachal cancer.
Stokkel LE, van Rossum HH, van de Kamp MW, Boellaard TN, **Bekers EM**, Kok NFM, van Rhijn BWG, Mertens LS.
Urol Oncol. 2023 Jul;41(7):326.e17-326.e24. doi: 10.1016/j.urolonc.2023.01.018. Epub 2023 Feb 21.
PMID: 36813613

25. Radiogenomics Analysis Linking Multiparametric MRI and Transcriptomics in Prostate Cancer.
Dinis Fernandes C, Schaap A, Kant J, van Houdt P, Wijkstra H, **Bekers E**, Linder S, Bergman AM, van der Heide U, Mischi M, Zwart W, Eduati F, Turco S.
Cancers (Basel). 2023 Jun 6;15(12):3074. doi: 10.3390/cancers15123074.
PMID: 37370685

26. First-in-patient study of OTL78 for intraoperative fluorescence imaging of prostate-specific membrane antigen-positive prostate cancer: a single-arm, phase 2a, feasibility trial.
Stibbe JA, de Barros HA, Linders DGJ, Bhairosingh SS, **Bekers EM**, van Leeuwen PJ, Low PS, Kularatne SA, Vahrmeijer AL, Burggraaf J, van der Poel HG.
Lancet Oncol. 2023 May;24(5):457-467. doi: 10.1016/S1470-2045(23)00102-X. Epub 2023 Apr 14.
PMID: 37062295

27. Genetic Aspects and Molecular Testing in Prostate Cancer: A Report from a Dutch Multidisciplinary Consensus Meeting.
Mehra N, Kloots I, Vlaming M, Aluwini S, Dewulf E, Oprea-Lager DE, van der Poel H, Stoevelaar H, Yakar D, Bangma CH, **Bekers E**, van den Bergh R, Bergman AM, van den Berkmortel F, Boudewijns S, Dinjens WNM, Fütterer J, van der Hulle T, Jenster G, Kroeze LI, van Kruchten M, van Leenders G, van Leeuwen PJ, de Leng WWJ, van Moorselaar RJA, Noordzij W, Oldenburg RA, van Oort IM, Oving I, Schalken JA, Schoots IG, Schuuring E, Smeenk RJ, Vanneste BGL, Vegt E, Vis AN, de Vries K, Willemse PM, Wondergem M, Ausems M.
Eur Urol Open Sci. 2023 Jan 25;49:23-31. doi: 10.1016/j.euros.2022.11.011. eCollection 2023 Mar.
PMID: 36874601

28. The prognostic value of lymph node staging with prostate-specific membrane antigen (PSMA) positron emission tomography/computed tomography (PET/CT) and extended pelvic lymph node dissection in node-positive patients with prostate cancer.
Meijer D, Ettema RH, van Leeuwen PJ, van der Kwast TH, van der Poel HG, Donswijk ML, Oprea-Lager DE, **Bekers EM**, Vis AN.
BJU Int. 2023 Mar;131(3):330-338. doi: 10.1111/bju.15881. Epub 2022 Sep 17.
PMID: 36069585

29. Correlation of radiological and histopathological response after neoadjuvant radiotherapy in soft tissue sarcoma.
Reijers SJM, Gennaro N, Bruining A, van Boven H, Snaebjornsson P, **Bekers EM**, van Coevorden F, Scholten AN, Schrage Y, van der Graaf WTA, Haas RLM, van Houdt WJ.
Acta Oncol. 2023 Jan;62(1):25-32. doi: 10.1080/0284186X.2023.2166427. Epub 2023 Jan 13.
PMID: 36637511

30. The oncological characteristics of non-prostate-specific membrane antigen (PSMA)-expressing primary prostate cancer on preoperative PSMA positron emission tomography/computed tomography.
Veerman H, Donswijk M, **Bekers E**, Bodar YJL, Meijer D, van Moorselaar RJA, Oprea-Lager DE, van der Noort V, van Leeuwen PJ, Vis AN, van der Poel HG.
BJU Int. 2022 Dec;130(6):750-753. doi: 10.1111/bju.15896. Epub 2022 Sep 30.
PMID: 36117468. No abstract available.

31. Predictive Value of Cribriform and Intraductal Carcinoma for the Nomogram-based Selection of Prostate Cancer Patients for Pelvic Lymph Node Dissection.
de Barros HA, Remmers S, Luiting HB, van Leenders GJLH, Roobol MJ, **Bekers EM**, Amin A, Haynes AM, Delprado W, Stricker PD, van der Poel HG, van der Kwast TH, van Leeuwen PJ.
Urology. 2022 Oct;168:156-164. doi: 10.1016/j.urology.2022.04.043. Epub 2022 Jul 5.
PMID: 35803346

32. The detection rate of apical tumour involvement on preoperative MRI and its impact on clinical outcomes in patients with localized prostate cancer.
Veerman H, Boellaard TN, van Leeuwen PJ, Vis AN, **Bekers E**, Hoeks C, Schoots IG, van der Poel HG.
J Robot Surg. 2022 Oct;16(5):1047-1056. doi: 10.1007/s11701-021-01333-1. Epub 2021 Nov 16.
PMID: 34783953

33. Drug-Induced Epigenomic Plasticity Reprograms Circadian Rhythm Regulation to Drive Prostate Cancer toward Androgen Independence.
Linder S, Hoogstraat M, Stelloo S, Eickhoff N, Schuurman K, de Barros H, Alkemade M**, Bekers EM**, Severson TM, Sanders J, Huang CF, Morova T, Altintas UB, Hoekman L, Kim Y, Baca SC, Sjöström M, Zaalberg A, Hintzen DC, de Jong J, Kluin RJC, de Rink I, Giambartolomei C, Seo JH, Pasaniuc B, Altelaar M, Medema RH, Feng FY, Zoubeidi A, Freedman ML, Wessels LFA, Butler LM, Lack NA, van der Poel H, Bergman AM, Zwart W.
Cancer Discov. 2022 Sep 2;12(9):2074-2097. doi: 10.1158/2159-8290.CD-21-0576.
PMID: 35754340

34. Alternative prostate cancer grading systems incorporating percent pattern 4/5 (IQ-Gleason) and cribriform architecture (cGrade) improve prediction of outcome after radical prostatectomy.
Seyrek N, Hollemans E, Andrinopoulou ER, Osanto S, Pelger RCM, van der Poel HG, **Bekers E**, Remmers S, Schoots IG, van Leenders GJLH.
Virchows Arch. 2022 Jun;480(6):1149-1157. doi: 10.1007/s00428-022-03301-y. Epub 2022 Feb 14.
PMID: 35157140

35. The impact of drainage pathways on the detection of nodal metastases in prostate cancer: a phase II randomized comparison of intratumoral vs intraprostatic tracer injection for sentinel node detection.
Wit EMK, van Beurden F, Kleinjan GH, Grivas N, de Korne CM, Buckle T, Donswijk ML, **Bekers EM**, van Leeuwen FWB, van der Poel HG.
Eur J Nucl Med Mol Imaging. 2022 Apr;49(5):1743-1753. doi: 10.1007/s00259-021-05580-0. Epub 2021 Nov 8.
PMID: 34748059

36. Feasibility of fluorescence imaging at microdosing using a hybrid PSMA tracer during robot-assisted radical prostatectomy in a large animal model.
Dell'Oglio P, van Willigen DM, van Oosterom MN, Bauwens K, Hensbergen F, Welling MM, van der Stadt H, **Bekers E**, Pool M, van Leeuwen P, Maurer T, van Leeuwen FWB, Buckle T.
EJNMMI Res. 2022 Mar 7;12(1):14. doi: 10.1186/s13550-022-00886-y.
PMID: 35254544

37. The clinical characteristics of patients with primary non-prostate-specific membrane antigen-expressing prostate cancer on preoperative positron emission tomography/computed tomography.
Veerman H, Donswijk M, **Bekers E**, Olde Heuvel J, Bodar YJL, Boellaard TN, van Montfoort ML, van Moorselaar RJA, Oprea-Lager DE, van Leeuwen PJ, Vis AN, van der Poel HG.
BJU Int. 2022 Mar;129(3):314-317. doi: 10.1111/bju.15664. Epub 2021 Dec 13.
PMID: 34854204

38. Cribriform architecture outperforms Gleason pattern 4 percentage and tertiary Gleason pattern 5 in predicting the outcome of Grade Group 2 prostate cancer patients.
Seyrek N, Hollemans E, Osanto S, Pelger RCM, van der Poel HG, **Bekers E**, Bangma CH, Rietbergen J, Roobol MJ, Schoots IG, van Leenders GJLH.
Histopathology. 2022 Feb;80(3):558-565. doi: 10.1111/his.14590. Epub 2021 Dec 14.
PMID: 34706119

39. c-MET Receptor-Targeted Fluorescence on the Road to Image-Guided Surgery in Penile Squamous Cell Carcinoma Patients.
Vries HM, **Bekers E**, van Oosterom MN, Karakullukcu MB, van HG, Poel D, van Leeuwen FWB, Buckle T, Brouwer OR.
J Nucl Med. 2022 Jan;63(1):51-56. doi: 10.2967/jnumed.120.261864. Epub 2021 May 14.
PMID: 33990404

40. Cerenkov Luminescence Imaging in Prostate Cancer: Not the Only Light That Shines.
Heuvel JO, de Wit-van der Veen BJ, van der Poel HG, van Leeuwen PJ, **Bekers EM**, Grootendorst MR, Vyas KN, Slump CH, Stokkel MPM.
J Nucl Med. 2022 Jan;63(1):29-35. doi: 10.2967/jnumed.120.260034. Epub 2021 Apr 30.
PMID: 33931467

41. Comedonecrosis Gleason pattern 5 is associated with worse clinical outcome in operated prostate cancer patients.
Hansum T, Hollemans E, Verhoef EI, Bangma CH, Rietbergen J, Osanto S, Pelger RCM, van Wezel T, van der Poel H, **Bekers E**, Helleman J, Remmers S, van Leenders GJLH.
Mod Pathol. 2021 Nov;34(11):2064-2070. doi: 10.1038/s41379-021-00860-4. Epub 2021 Jun 26.
PMID: 34175896

42. The Prognostic Potential of Human Prostate Cancer-Associated Macrophage Subtypes as Revealed by Single-Cell Transcriptomics.
Siefert JC, Cioni B, Muraro MJ, Alshalalfa M, Vivié J, van der Poel HG, Schoots IG, **Bekers E**, Feng FY, Wessels LFA, Zwart W, Bergman AM.
Mol Cancer Res. 2021 Oct;19(10):1778-1791. doi: 10.1158/1541-7786.MCR-20-0740. Epub 2021 Jun 15.
PMID: 34131070

43. The Diagnostic Value of FDG-PET/CT for Urachal Cancer.
Stokkel LE, Stokkel MPM, Donswijk ML, Lahaye MJ, **Bekers EM**, van Rhijn BWG, Mertens LS.
Clin Genitourin Cancer. 2021 Oct;19(5):373-380. doi: 10.1016/j.clgc.2021.03.002. Epub 2021 Mar 17.
PMID: 33858788

44. Distinct Patterns of Myeloid Cell Infiltration in Patients With hrHPV-Positive and hrHPV-Negative Penile Squamous Cell Carcinoma: The Importance of Assessing Myeloid Cell Densities Within the Spatial Context of the Tumor.
Rafael TS, de Vries HM, Ottenhof SR, Hofland I, Broeks A, de Jong J, **Bekers E**, Horenblas S, de Menezes RX, Jordanova ES, Brouwer OR.
Front Immunol. 2021 Jun 14;12:682030. doi: 10.3389/fimmu.2021.682030. eCollection 2021.
PMID: 34194435

45. Cribriform architecture in radical prostatectomies predicts oncological outcome in Gleason score 8 prostate cancer patients.
Hollemans E, Verhoef EI, Bangma CH, Rietbergen J, Osanto S, Pelger RCM, van Wezel T, van der Poel H, **Bekers E**, Helleman J, Roobol MJ, van Leenders GJLH.
Mod Pathol. 2021 Jan;34(1):184-193. doi: 10.1038/s41379-020-0625-x. Epub 2020 Jul 20.
PMID: 32686748

46. H3K27me3 expression and methylation status in histological variants of malignant peripheral nerve sheath tumours.
Lyskjaer I, Lindsay D, Tirabosco R, Steele CD, Lombard P, Strobl AC, Rocha AM, Davies C, Ye H, **Bekers E**, Ingruber J, Lechner M, Amary F, Pillay N, Flanagan AM.
J Pathol. 2020 Oct;252(2):151-164. doi: 10.1002/path.5507. Epub 2020 Sep 1.
PMID: 32666581 Free PMC article.

47. ^{68}Ga-PSMA Cerenkov luminescence imaging in primary prostate cancer: first-in-man series.
Olde Heuvel J, de Wit-van der Veen BJ, van der Poel HG, **Bekers EM**, Grootendorst MR, Vyas KN, Slump CH, Stokkel MPM.
Eur J Nucl Med Mol Imaging. 2020 Oct;47(11):2624-2632. doi: 10.1007/s00259-020-04783-1. Epub 2020 Apr 2.
PMID: 32242253

48. Case of the month from the Netherlands Cancer Institute, Amsterdam: how to differentiate between benign and malignant prostatic cysts.
Veerman H, van Leeuwen PJ, **Bekers E**, van der Poel HG.
BJU Int. 2020 Aug;126(2):240-244. doi: 10.1111/bju.15156.
PMID: 32776450

49. Clinicopathological characteristics of glomeruloid architecture in prostate cancer.
Hollemans E, Verhoef EI, Bangma CH, Rietbergen J, Osanto S, Pelger RCM, van Wezel T, van der Poel H, **Bekers E**, Helleman J, Roobol MJ, van Leenders GJLH.
Mod Pathol. 2020 Aug;33(8):1618-1625. doi: 10.1038/s41379-020-0507-2. Epub 2020 Feb 20.
PMID: 32080350

50. Diagnostic Laparoscopy and Abdominal Cytology Reliably Detect Peritoneal Metastases in Patients with Urachal Adenocarcinoma.
Stokkel LE, Mehta AM, Behrendt MA, de Jong J, **Bekers EM**, Hendricksen K, Aalbers AGJ, Kok NFM, Meinhardt W, Mertens LS, van Rhijn BWG.
Ann Surg Oncol. 2020 Jul;27(7):2468-2475. doi: 10.1245/s10434-020-08206-1. Epub 2020 Feb 12.
PMID: 32052302

51. TLE3 loss confers AR inhibitor resistance by facilitating GR-mediated human prostate cancer cell growth.
Palit SA, Vis D, Stelloo S, Lieftink C, Prekovic S, **Bekers E**, Hofland I, Šuštić T, Wolters L, Beijersbergen R, Bergman AM, Győrffy B, Wessels LF, Zwart W, van der Heijden MS.
Elife. 2019 Dec 19;8:e47430. doi: 10.7554/eLife.47430.
PMID: 31855178

52. Prognostic significance of NAB2-STAT6 fusion variants and TERT promotor mutations in solitary fibrous tumors/hemangiopericytomas of the CNS: not (yet) clear.
Vogels R, Macagno N, Griewank K, Groenen P, Verdijk M, Fonville J, Kusters B; French CNS SFT/HPC Consortium; Dutch CNS SFT/HPC Consortium; Figarella-Branger D, Wesseling P, Bouvier C, Flucke U.
Acta Neuropathol. 2019 Apr;137(4):679-682. doi: 10.1007/s00401-019-01968-3. Epub 2019 Feb 2.
PMID: 30761420

53. Identification of novel GNAS mutations in intramuscular myxoma using next-generation sequencing with single-molecule tagged molecular inversion probes.
Bekers EM, Eijkelenboom A, Rombout P, van Zwam P, Mol S, Ruijter E, Scheijen B, Flucke U.
Diagn Pathol. 2019 Feb 8;14(1):15. doi: 10.1186/s13000-019-0787-3.
PMID: 30736805

*

54. MRI as a tool to assess surgical margins and pseudocapsule features directly following partial nephrectomy for small renal masses.
van Oostenbrugge TJ, Runneboom W, **Bekers E**, Heidkamp J, Langenhuijsen JF, Veltien A, Maat A, Mulders PFA, Hulsbergen-van de Kaa CA, Fütterer JJ.
Eur Radiol. 2019 Feb;29(2):509-516. doi: 10.1007/s00330-018-5630-9. Epub 2018 Jul 24.
PMID: 30043161

55. Frequent clonal relations between metastases and non-index prostate cancer lesions.
Kneppers J, Krijgsman O, Melis M, de Jong J, Peeper DS, **Bekers E**, van der Poel HG, Zwart W, Bergman AM.
JCI Insight. 2019 Jan 24;4(2):e124756. doi: 10.1172/jci.insight.124756.
PMID: 30674724

56. COL1A1 is a fusionpartner of USP6 in myositis ossificans - FISH analysis of six cases.
Flucke U, **Bekers EM**, Creytens D, van Gorp JM.
Ann Diagn Pathol. 2018 Oct;36:61-62. doi: 10.1016/j.anndiagpath.2018.06.009. Epub 2018 Jun 30.
PMID: 29980413

57. Risk Factors and Clinical Outcomes of Head and Neck Cancer in Inflammatory Bowel Disease: A Nationwide Cohort Study.
Nissen LHC, Derikx LAAP, Jacobs AME, van Herpen CM, Kievit W, Verhoeven R, van den Broek E, **Bekers E**, van den Heuvel T, Pierik M, Rahamat-Langendoen J, Takes RP, Melchers WJG, Nagtegaal ID, Hoentjen F; Dutch Initiative on Crohn and Colitis (ICC); Dutch Head and Neck Society, PALGA group; IBD/HNC group.
Inflamm Bowel Dis. 2018 Aug 16;24(9):2015-2026. doi: 10.1093/ibd/izy096.
PMID: 30759216

58. Fibro-osseous pseudotumor of digits - Expanding the spectrum of clonal transient neoplasms harboring USP6 rearrangement.
Flucke U, Shepard SJ, **Bekers EM**, Tirabosco R, van Diest PJ, Creytens D, van Gorp JM.
Ann Diagn Pathol. 2018 Aug;35:53-55. doi: 10.1016/j.anndiagpath.2018.05.003. Epub 2018 May 12.
PMID: 29787930

59. Multifocal occurrence of extra-abdominal desmoid type fibromatosis - A rare manifestation. A clinicopathological study of 6 sporadic cases and 1 hereditary case.
Bekers EM, van Broekhoven DLM, van Dalen T, Bonenkamp JJ, van der Geest ICM, de Rooy JWJ, van Gorp JM, Creytens DH, de Leng WWJ, Scheijen B, Eijkelenboom A, Flucke U.
Ann Diagn Pathol. 2018 Aug;35:38-41. doi: 10.1016/j.anndiagpath.2018.04.001. Epub 2018 Apr 21.
PMID: 29705714

60. Myositis ossificans - Another condition with USP6 rearrangement, providing evidence of a relationship with nodular fasciitis and aneurysmal bone cyst.
Bekers EM, Eijkelenboom A, Grünberg K, Roverts RC, de Rooy JWJ, van der Geest ICM, van Gorp JM, Creytens D, Flucke U.
Ann Diagn Pathol. 2018 Jun;34:56-59. doi: 10.1016/j.anndiagpath.2018.01.006. Epub 2018 Jan 12.
PMID: 29661729

61. Mutational analysis using Sanger and next generation sequencing in sporadic spindle cell hemangiomas: A study of 19 cases.
Ten Broek RW, **Bekers EM**, de Leng WWJ, Strengman E, Tops BBJ, Kutzner H, Leeuwis JW, van Gorp JM, Creytens DH, Mentzel T, van Diest PJ, Eijkelenboom A, Flucke U.
Genes Chromosomes Cancer. 2017 Dec;56(12):855-860. doi: 10.1002/gcc.22501. Epub 2017 Sep 23.
PMID: 28845532

62. Soft tissue angiofibroma: Clinicopathologic, immunohistochemical and molecular analysis of 14 cases.
Bekers EM, Groenen PJTA, Verdijk MAJ, Raaijmakers-van Geloof WL, Roepman P, Vink R, Gilhuijs NDB, van Gorp JM, Bovée JVMG, Creytens DH, Flanagan AM, Suurmeijer AJH, Mentzel T, Arbajian E, Flucke U.
Genes Chromosomes Cancer. 2017 Oct;56(10):750-757. doi: 10.1002/gcc.22478. Epub 2017 Jul 25.
PMID: 28639284

63. Chronic temporomandibular joint pain: two cases of osteoid osteoma and a review of the literature.
Deferm JT, Steens SCA, Vriens D, **Bekers EM**, Kalaykova SI, Borstlap WA.
Int J Oral Maxillofac Surg. 2017 Sep;46(9):1130-1137. doi: 10.1016/j.ijom.2017.03.036. Epub 2017 May 8.
PMID: 28495394

64. Evaluation of tongue squamous cell carcinoma resection margins using ex-vivo MR.
Steens SCA, **Bekers EM**, Weijs WLJ, Litjens GJS, Veltien A, Maat A, van den Broek GB, van der Laak JAWM, Fütterer JJ, van der Kaa CAH, Merkx MAW, Takes RP.
Int J Comput Assist Radiol Surg. 2017 May;12(5):821-828. doi: 10.1007/s11548-017-1524-6. Epub 2017 Jan 27.
PMID: 28130702

65. Myxoid liposarcoma of the foot: a study of 8 cases.
Bekers EM, Song W, Suurmeijer AJ, Bonenkamp JJ, van der Geest IC, Braam PM, Ploegmakers MJ, Desar IM, Tops BB, van Gorp JM, Creytens DH, Mentzel T, Flucke U.
Ann Diagn Pathol. 2016 Dec;25:37-41. doi: 10.1016/j.anndiagpath.2016.09.003. Epub 2016 Sep 17.
PMID: 27806844

66. Solitary fibrous tumor - clinicopathologic, immunohistochemical and molecular analysis of 28 cases.
Vogels RJ, Vlenterie M, Versleijen-Jonkers YM, Ruijter E, **Bekers EM**, Verdijk MA, Link MM, Bonenkamp JJ, van der Graaf WT, Slootweg PJ, Suurmeijer AJ, Groenen PJ, Flucke U.
Diagn Pathol. 2014 Nov 29;9:224. doi: 10.1186/s13000-014-0224-6.
PMID: 25432794

67. Metastatic melanoma mimicking solitary fibrous tumor: report of two cases.
Bekers EM, van Engen-van Grunsven AC, Groenen PJ, Westdorp H, Koornstra RH, Bonenkamp JJ, Flucke U, Blokx WA.
Virchows Arch. 2014 Feb;464(2):247-51. doi: 10.1007/s00428-014-1542-5. Epub 2014 Jan 24.
PMID: 24458518

*

Curriculum Vitae

Elise Bekers was born on 15th of April 1985 in Tilburg, the Netherlands and grew up in the nearby town Oisterwijk. From already an early age (11 years old), Elise wanted to become a pathologist. After graduating from 2College high school in Oisterwijk in 2003, she therefore started her medical school at the Erasmus University in Rotterdam. She chose pathology for her final rotations and completed them at Elisabeth-TweeSteden Hospital in Tilburg and Queen Elizabeth Hospital Blantyre in Malawi. She completed her medical school in 2013 and consecutively started with her residency in pathology at Radboud University Medical Centre and also did rotations at Jeroen Bosch Hospital in 's-Hertogenbosch and at Stichting PAMM at Catharina Hospital in Eindhoven. During a rotation in soft tissue and bone pathology Elise noticed her growing interest in the field and raised her interest in research and to follow a PhD program. This led to the current thesis in the field of soft tissue pathology under the supervision of Prof. Dr. Han van Krieken, Dr. Uta Flucke and Dr. Blanca Scheijen. In the last year of her residency she did a specialized rotation in soft tissue and bone pathology in the Royal National Orthopaedic Hospital in London under the supervision of Prof. Dr. A. Flanagan. She graduated her residency in 2016 and started working as a pathologist at Jeroen Bosch Hospital in 's-Hertogenbosch for 2 years followed by almost 6 years at the Netherlands Cancer Institute, Antoni van Leeuwenhoek in Amsterdam. Here she was also involved in research, mainly in the field of prostate and penile cancer as well as in soft tissue pathology. Currently she operates as a medical manager and pathologist at PAMM at the Catharina Hospital in Eindhoven. Her fields include soft tissue pathology, uropathology, thoracic pathology and gastro-intestinal pathology.

Dankwoord

Eindelijk, na al die jaren sinds ik begonnen ben aan deze reis, met tussenkomst van allerlei onverwachte omstandigheden zoals o.a. een COVID-pandemie, is het nu toch echt zover. Het is af. Het is klaar en uiteindelijk ben ik blij met het resultaat.

Dit resultaat had er absoluut nooit geweest zonder de allesomvattende hulp en motivatie van met name **Dr. Uta Flucke**, **Dr. G.P.H. (Blanca) Scheijen** en **Prof. dr. J.H.J.M. (Han) van Krieken**. Ik kan deze 3 mensen niet genoeg bedanken voor hun hulp in soms bange tijden. Ik ga het niet verder uitweiden in dit dankwoord, ik kan alleen zeggen: deze lieve mensen krijgen een persoonlijke boodschap.

Ik wil wel graag speciaal stilstaan bij de toppers van analisten en KMBPers die al die moleculaire analyses (en dat zijn er nog al wat geweest) hebben uitgevoerd, zeer kundig en zo snel als het kon. Zonder jullie was dit allemaal niet gelukt, dus **Astrid Eijkelenboom, Paul Rombout, Diede van Bladel, Madeleine Berendsen, Patricia Groenen, Paul Roepman, Bastiaan Tops, Danique van Broekhoven, Wendy de Leng, Winny Raaijmakers-van Geloof** en **Marian Verdijk**. Ontzettend bedankt voor al jullie harde werk en hulp! Jullie zijn absolute toppers.

Uiteraard wil ik ook alle andere mensen en medeauteurs die hebben meegeholpen niet verstek laten gaan en bedank ik uit de grond van mijn hart voor alle medewerking.

Het heeft allemaal heel lang geduurd, maar er rest mij maar 1 ding om te zeggen (des Elises):

HOUDOE en BEDANKT!

*

9 789465 151403 >

Radboudumc university medical center

IN·DEI·NOMINE·FELICITER

Radboud University